Paclitaxel induces micronucleation and activates pro-inflammatory cGAS/STING signaling in triple negative breast cancer.

by

Yang Hu

A dissertation submitted in partial fulfillment of

the requirements for the degree of

Doctor of Philosophy

(Cellular and Molecular Biology)

at the

UNIVERSITY OF WISCONSIN-MADISON

2021

Date of final oral examination: June 7th, 2021

The dissertation is approved by the following members of the Final Oral Committee

Mark E. Burkard, Professor, Medicine

Beth A. Weaver, Associate Professor, Cell and Regenerative Biology

Christian M. Capitini, Associate Professor, Pediatrics

Shigeki Miyamoto, Professor, Oncology

Zachary S. Morris, Assistant Professor, Human Oncology

TABLE OF CONTENTS

ABSTRACT ..... **v**

ACKNOWLEDGEMENTS ..... **vii**

ABBREVIATIONS ..... **ix**

CHAPTER 1: INTRODUCTION **1**

1.1 Mitosis and its regulatory checkpoints in animal cells 1

1.2 Aneuploidy and chromosomal instability in cancer 6

1.3 The role of aneuploidy and CIN in immunogenicity 10

1.4 Therapeutic targeting of cGAS/STING for immune checkpoint blockade 12

1.5 Amplifying immunity using conventional therapies in breast cancer 16

1.51 Immunogenic Cell Death *18*

1.52 Increased surface immune markers *19*

1.53 Immune Cell Cytotoxicity *20*

1.54 Immune Cell Modulation *21*

1.55 T-cell Activation and Recruitment *22*

1.6 Potential roles of specific therapies 24

1.61 Chemotherapies *24*

1.62 Targeted therapies *26*

1.63 HER2-directed therapies in immune modulation *30*

1.64 Potential anti-synergistic effects of standard therapies *32*

1.7 Gaps in knowledge 33

Fig. 1.1: Proteins comprising the kinetochore 35

Fig. 1.2: Mechanisms of immune activation by breast cancer therapies 37

Table 1.1: Summary of conventional therapies effects on the immune system 39

CHAPTER 2: PACLITAXEL INDUCES MICRONUCLEATION AND ACTIVATES PRO-INFLAMMATORY CGAS/STING SIGNALING IN TRIPLE NEGATIVE BREAST CANCER 40

2.1 Abstract 41

2.2 Introduction 42

2.3 Results 44

2.31 Paclitaxel increased tumor-infiltrating lymphocytes in some but not all clinical patient samples 44

2.32 Paclitaxel induces cGAS-positive micronuclei following mitosis on multipolar spindles 46

2.33 Paclitaxel activates cGAS signaling in triple-negative breast cancer cell lines. 49

2.34 Paclitaxel induces cGAS-dependent soluble factors that induce M1 polarization. 51

2.35 Microtubule-targeting agents increase surface PD-L1 expression in TNBC. .. 54

2.36 Some triple negative breast cancer patients with high levels of tumor cGAS have durable responses on combination therapy. 56

2.4 Discussion 57

2.5 Materials and Methods: 64

Cell lines and culture conditions 64

Reagents and antibodies 64

Clinical samples 65

Quantification criteria for tumor-infiltrating lymphocytes *66*

Immunohistochemistry *67*

Time-lapse video microscopy *68*

Immunofluorescence microscopy *68*

Micronuclei quantification criteria *70*

ELISAs for 2'3'-cGAMP and IFN-β *72*

CRISPR-cas9 knockout of cGAS *72*

RNA interference *73*

THP-1 differentiation *73*

Digitonin permeabilization *74*

Real-time quantitative PCR *74*

Immunoblot *76*

Flow cytometry *77*

2.6 Acknowledgements 79

Cover Figure: Putative Mechanism 81

Fig. 1. Some but not all triple-negative breast cancer patients develop tumor-infiltrating lymphocytes following neoadjuvant paclitaxel. 83

Fig. 2. Paclitaxel causes cGAS-positive micronuclei to form in interphase following delayed mitosis on multipolar spindles. 85

Fig. 3. Paclitaxel activates cGAS signaling in triple-negative breast cancer cell lines. .. 87

Fig. 4. Paclitaxel causes secretion of cGAS-dependent soluble factors in breast cancer that induce M1 polarization in human macrophages. 90

Fig. 5. Nanomolar paclitaxel and other microtubule-targeting agents can increase surface PD-L1 expression in TNBC cell line MDA-MB-436 dependent on cGAS expression. 91

Fig. 6. Patients expressing higher levels of cGAS have increased disease control after combined microtubule-targeting agents and PD-1/PD-L1 inhibitors. 94

Fig. S1. cGAS-positive micronuclei are present in patient samples after paclitaxel. 95

Fig. S2. Nanomolar microtubule-targeting agents such as paclitaxel cause cGAS-positive micronuclei predominantly in multinucleated TNBC cell lines. 98

Fig. S3. cGAS is concentrated in interphase micronuclei with envelope defects after paclitaxel. 99

Fig. S4. Paclitaxel activates STING pathway in MDA-MB-231 but not in interphase. . 101

Fig. S5. THP-1 macrophages exhibit M1 polarization after exposure to conditioned media from or co-culture with MDA-MB-231 after paclitaxel. 104

Fig. S6. Expression of PD-L1 is not modulated by nanomolar paclitaxel at the protein level. 105

Fig. S7. cGAS expression positively correlates with progression-free survival in patients treated with chemotherapy. 108

CHAPTER 3: CONCLUSIONS AND FUTURE DIRECTIONS 109

APPENDIX 114

Chromosomal instability positively correlates to increased immune cell infiltration in cancer 114

Chromosomal instability upregulates interferon in acute myeloid leukemia 121

REFERENCES 122

ABSTRACT

Breast cancer is the most common type of cancer affecting women worldwide with an increasing annual incidence (Sung et al., 2020). While therapies for treating localized breast cancer will frequently result in cure, mortality for metastatic breast cancer is still high due to few effective targeted treatments (Chen et al., 2017). Conventional chemotherapies are a mainstay for metastatic breast cancers, though durable responses are rare (Dent et al., 2007). Immunotherapies promise long-term responses through immune activation but have been underwhelming in breast cancer relative to other cancer types (Emens, 2018).

In chapter one, I will review the mechanisms of existing therapeutic strategies that can recruit an immune response in breast cancers. From the mechanistic overview, I suggest biomarkers for combinations of conventional chemo- and immunotherapies. Since some conventional non-immunogenic therapies cause chromosomal instability, this chapter will begin with a review of mitosis, aneuploidy, chromosomal instability and the various mechanisms by which chemotherapy, targeted therapies, and endocrine therapy could stimulate an immune response. In doing so, I hope to provide a mechanistic basis for future investigations of treatment combinations in the clinical setting. By reviewing the major mechanisms of conventional therapies, I hope to convey the importance that understanding mechanism may help us to select the proper biomarker for therapies, in particular in combination with immunotherapies.

Chapter two will focus on how paclitaxel chemotherapy can activate the cGAS/STING pathway to induce polarization of macrophages to a pro-inflammatory M1 phenotype. This chapter explores one of the most widely used chemotherapies in breast

cancer and extends work completed in the Weaver lab investigating the mechanism of multipolar spindle formation by low dose paclitaxel. Specifically, this chapter will explore cGAS/STING as a proxy for how paclitaxel can exert cell extrinsic effects through activation of this pathway and stimulate an innate immune response. Through this work, we suggest that cGAS expression should be explored as a candidate biomarker for selecting patients for combination therapy with immune checkpoint inhibitors.

ACKNOWLEDGEMENTS

Since beginning graduate school, I had encountered many challenges; however, I have been able to overcome many of them with the support of many generous and kind individuals, most of all my mentor, Mark Burkard, and the Medical Scientist Training Program. Thank you, Mark, for believing in me that I can become a good scientist and be successful. Thank you for giving me the freedom to explore ideas in your lab and for communicating with me at the level of a colleague rather than as an employee or technician. Even though I joined your lab with little confidence in myself, your sensitive mentorship helped me to grow into an open-minded scientist with more confidence in my abilities and work. My thesis committee made up of Drs. Beth Weaver, Christian Capitini, Shigeki Miyamoto, Zach Morris and previously, Fotis Asimakouplous has been instrumental to my success. Without your guidance throughout my training, I would not have been able to accomplish what I have today. Thank you for challenging me every step along the way. Although it was not an easy path and I still have much to learn, I feel grateful to get a tremendous start on how to be a better scientist.

I would also like to offer my sincerest gratitude to lab mates past and present, who have welcome and helped me since day one. Thank you, Rob, Ryan, Ning, James, Alka and Dave for welcoming me into the lab and for accepting me despite having joined with little notice. Thank you all for your mentorship and guidance. The lessons you have all taught me on how to be a better colleague and team player have been invaluable. Graduate school can also be an isolating experience, and I am so grateful for all the times we spent together during our journey at work and at play. I will forever remember those moments and I believe they will have a positive impact on me going forward.

Thank you to Rob, Rachel, Rebeca, Roshan and Andrew for continuing to be a positive influence in my life as our lab transitioned members over the years. I would also like to thank my undergraduate student, Baraa, for sticking it out with me for all these years. We might have not accomplished all we set out to do, but we have accomplished a lot. I am so grateful and honored to have been your mentor throughout your undergraduate career. I am also grateful to interact with the many other undergraduate students who have worked in our group.

Most of all, I am grateful for the unconditional support of my family. Thank you to my parents, Jianzhi and Mary, for always being there for me during difficult times and for my sister, Rebecca, for being an inspiration. I would also like to thank all of my other friends whom I have not mentioned here for their steadfast positive support. Without you, I would not be here today.

ABBREVIATIONS

APC/C – Anaphase Promoting Complex/Cyclosome

Bub1 – Budding Uninhibited by Benzimidazole 1

Bub3 – Budding Uninhibited by Benzimidazole 3

BubR1 - Budding Uninhibited by Benzimidazole-Related 1

CDC20 – Cell Division Cycle 20

cGAS – Cyclic GMP-AMP Synthase

CCN – Constitutive Centromere-Associated Network

CENP – Centromere Protein

CIN – Chromosomal Instability

DAPI – 4’,6-diamidino-2-phenylindole

DNA – Deoxyribonucleic Acid

ER – Estrogen Receptor

ERBB2 (HER2) – Human Epidermal Growth Factor Receptor 2

FDA – Food and Drug Administration

KMN – Kinetochore Microtubule Network

Knl1 – Kinetochore scaffold 1

Mad1 – Mitotic Arrest Deficient 1

Mad2 – Mitotic Arrest Deficient 2

Mis12 – Minichromosome Instability 12

MPS1 – Multipolar Spindle 1

mRNA – Messenger Ribonucleic Acid

NCI – National Cancer Institute

NSCLC – Non-Small Cell Lung Cancer

PARP – Poly (ADP-ribose) Polymerase

PD-1 – Programmed Cell Death Protein 1

PD-L1 – Programmed Death-Ligand 1

RNA – Ribonucleic Acid

SAC – Spindle Assembly Checkpoint

STING – Stimulator of Interferon Genes

TCGA – The Cancer Genome Atlas

TNBC – Triple negative breast cancer

Tp53 – Tumor protein P53 (the Guardian of the Genome)

CHAPTER 1: INTRODUCTION

1.1 Mitosis and its regulatory checkpoints in animal cells

Mitosis is the critical process of cell division by which replicated DNA is segregated equally into two daughter cells (McIntosh, 2016). Mitosis is fundamental for continued propagation and development at the cellular and organismal levels. In literature, mitosis is known as M phase and is one of four stages of the cell cycle, which also include G1 (gap 1), G2 (gap 2), and S (DNA synthesis) phases (Israels & Israels, 2000). G_o is another phase referring to a reversible state of quiescence that can be induced by external stressors or the programming of rarely dividing cells. Collectively, G_o, G1, G2 and S phases comprise interphase. Despite the complexity of mitosis, M phase is the shortest of the four cell stages and only lasts from minutes to hours (Cooper, 2000). Following mitosis, cells can undergo cytokinesis to physically separate DNA and cytoplasmic components into their own membrane-bound cells.

Mitosis can be separated into distinct sequential phases known as prophase, prometaphase, metaphase, anaphase, and telophase (McIntosh, 2016). Prior to mitosis, cells undergo S phase, which is characterized by duplication of DNA, centrosomes and organelles (Fischer et al., 2018). During prophase, the replicated chromatin condenses into sister chromatids attached at the centromere (Hartwell et al., 2008). A process known as compaction occurs, where DNA becomes increasingly coiled and packed into chromosomes (Martínez-Balbás et al., 1995). This results in increased chromatid thickness and decreased chromatin length, allowing visualization of these structures under low or high magnification under a brightfield or fluorescence microscopy (Hartwell et al., 2008). When the DNA becomes tightly wound, most transcription processes are

silenced as factors become displaced and lose access to the formerly loose chromatin (Martínez-Balbás et al., 1995). In addition, the nucleolus begins dissolving, which results in fewer ribosomes being produced and decreased translation (Cooper, 2000). In the cytoplasm, the two centrosomes begin moving apart as microtubules originate, grow, and radiate from these centrosomes to form the mitotic spindle. Weakening of the lamin network occurs and causes the nuclear membrane to become porous, initiating nuclear envelope breakdown (Beaudouin et al., 2002). This process ultimately allows the cytoplasm and nucleoplasm to mix, a phenotype that marks the end of prophase.

The transition to prometaphase begins with nuclear envelope breakdown, allowing microtubules originating from the two centrosomes to grow and attach to the kinetochores of sister chromatids (Lian & Chircop, 2016). The kinetochore is comprised of multiple proteins located at the centromere of sister chromatids (Figure 1.1). The kinetochore forms the bridge between microtubules and chromatids (Cheeseman, 2014). Key proteins of the inner kinetochore include the constitutive centromere-associated network (CCAN) found at the centromere. These inner kinetochore proteins directly bind centromeric nucleosomes through CENPA (Hori et al., 2008, 2013). The outer kinetochore contains a complex of core proteins KNL1, Mis12 and NDC80, the latter of which is directly linked to the microtubule (Varma & Salmon, 2012). The kinetochore also binds motor proteins such as dyneins and kinesins that help regulate proper attachment to the microtubules and assist in the pulling of the kinetochores towards the equator of the cell to form the metaphase plate (Howell et al., 2001; Mayr et al., 2007). The role of prometaphase is to ensure that all kinetochores are able to properly attach to microtubules from opposing centrosomes, such that each sister

chromatid pair is attached to microtubules and achieves biorientation (Kapoor et al., 2006). To prevent mitotic errors, chromosomes must have amphitelic attachments such that each kinetochore of the sister chromatid pair is attached to microtubules from the nearest facing pole (Godek et al., 2015). Once kinetochores have proper attachments to microtubules, the spindle assembly checkpoint is satisfied, and anaphase can begin (May & Hardwick, 2006). Proper attachments also lead to chromosome alignment at the equator of the cell called the metaphase plate, which is important for proper cell division (Tan et al., 2015).

Before sister chromatids can separate to their respective poles, the spindle assembly checkpoint (SAC), which ensures proper attachment of microtubules to the kinetochore, must be silenced (Bokros & Wang, 2016). This is important because separation prior to proper attachments of chromatids to microtubules will result in missegregation of chromosomes and in turn, aneuploid daughter cells in the subsequent interphase (Bharadwaj & Yu, 2004). Aneuploidy, which is a hallmark of cancer, is detrimental to both the fidelity of DNA content and cellular functions and can contribute towards tumorigenesis. The SAC helps to prevent aneuploidy by delaying anaphase onset until all unattached kinetochores have a microtubule attachment.

The SAC is comprised of mitotic checkpoint complex proteins including BUBR1, BUB1, BUB3, MAD1, MAD2, MPS1 and CDC20 (Musacchio & Salmon, 2007). Kinases such as Aurora B are also involved in the SAC. In an unattached kinetochore, the MCC inhibits the anaphase-promoting complex or cyclosome (APC/C) (Izawa & Pines, 2015). Mechanistically, Mps1 phosphorylates the Knl1 MELT repeats on unattached kinetochores where Bub3 is recruited (Yamagishi et al., 2012). Bub1 is subsequently

recruited to Bub3 through the Bub1 GLEBS motif and forms the scaffold for recruiting Cdc20 through the ABBA motif (Ji et al., 2017). Mad1 is assembled on the Conserved Domain 1 (CD1) motif of Bub1 through a phosphorylation on Thr 461 (G. Zhang et al., 2017). Mad1 on the unattached kinetochore recruits Mad2, which converts the protein from an open to closed conformation (Maldonado & Kapoor, 2011). This allows the formation of a heterotetramer Mad1-Mad2 complex, which can further catalyze the formation of more closed Mad2. These closed Mad2 will then bind to CDC20 to form a complex that will inhibit the APC/C and prevent anaphase onset. Silencing of the SAC through MCC inhibition occurs when microtubules attach to the kinetochore (Foley & Kapoor, 2013). Once the microtubule is attached, p31-comet can be recruited to the kinetochore and inhibit the MCC from converting the form of Mad2 from open to closed (Westhorpe et al., 2011). In addition, MPS1 can also be released from the kinetochore, which helps in MCC inhibition. The motor proteins of the attached microtubule such as dynein also remove proteins such as Mad1, Mad2 and MPS1 from the kinetochore (Howell et al., 2001). These events result in activation of the APC/C. CDC20 forms an active complex with APC/C because it is no longer inhibited by the closed form of Mad2 (Qiao et al., 2016). APC/C then ubiquitinates securin, leading to its degradation, which frees separase from inhibition (Hornig et al., 2002). This allows separase to degrade cohesin at the centromere of the sister chromatids, breaking the physical linkage between the two chromatids allowing them to separate to opposite poles by microtubule forces.

During Anaphase A, one copy of the sister chromatid, one for each chromosome, migrates to opposite poles, where the centrosomes forming the spindle poles are

located (Asbury, 2017). The kinetochore fibers shorten during this stage of anaphase. Anaphase A ends once the sister chromatids reach their respective spindle poles. During Anaphase B, centrosomes forming the spindle poles move outward (Scholey et al., 2016). These movements are accomplished by the growing and shrinking of microtubules (kinetochore, interpolar and astral) and by forces exerted via motor proteins. During telophase, the nuclear envelope reforms around chromosomes at the poles and the spindle disassembles. This is also accompanied by the decondensation of chromosomes and reappearance of the nucleoli. After the end of mitosis, cytokinesis occurs, which physically separates the two newly formed daughter cells (Pollard & O'Shaughnessy, 2019). This final step of mitosis is characterized by the formation of a cleavage furrow and actin-myosin contractile ring between the two connected cells. Once the contractile ring tightens, abscission occurs, ending mitosis.

1.2 Aneuploidy and chromosomal instability in cancer

According to the National Cancer Institute, aneuploidy is defined as “the occurrence of one or more extra or missing chromosomes leading to an unbalanced chromosome complement, or any chromosome number that is not an exact multiple of the haploid number (23 in human beings).” At the end of the 19th century, von Hansemann observed abnormal mitotic phenotypes such as multipolar spindles at the cellular level, which can lead to subsequent aneuploidy during interphase. Since cells have multiple checks and balances to ensure proper chromosome segregation, aneuploidy only occurs at low levels in normal human cells and tissues (Knouse et al., 2014). Uncorrected errors at any step of mitosis, either due to random occurrence or insults such as radiation, can generate aneuploidy. In normal cells, aneuploidy can be lethal and will typically cause proliferation defects (Compton, 2011). Interestingly, some trisomic aneuploidies are viable in human beings. This is seen most commonly for Trisomy 21 (Down Syndrome). Other viable trisomies include those of chromosomes 8 (Warkany Syndrome), 13 (Patau Syndrome), 18 (Edwards Syndrome) and sex chromosome trisomies. Unlike trisomies, monosomies are lethal in human beings except for X-chromosome monosomy (45XO genotype), which results in Turner syndrome. For cancer cells, aneuploidy is not only common but remarkably well-tolerated. Under pressures of selection, the presence of aneuploidy may confer a growth advantage, where upregulation of oncogenes can enhance fitness over euploid karyotypes (Ben-David & Amon, 2020).

In 1902, Boveri was the first scientist to postulate that cancers can be caused by abnormal mitoses resulting from different mechanisms in experiments conducted in sea

urchins. Indeed, aneuploidy is very common in cancer, comprising around 90% of solid and 75% of hematopoietic cancers (Weaver & Cleveland, 2006, 2008). A concept related to aneuploidy is chromosomal instability (CIN), which is defined as “the recurrent gain and loss of chromosomes over multiple cell divisions” (Burkard & Weaver, 2017). While aneuploidy is typically thought of as the state of an abnormal number of chromosomes, CIN is seen as an increased rate of structural and/or numerical chromosome abnormalities. Whole chromosome analyses have shown that CIN exists in 44% of solid and 14% of hematopoietic cancers (Zasadil et al., 2014a). CIN and aneuploidy are often found together, and it is generally accepted that recurrent gains and losses of chromosomes due to CIN can cause aneuploidy. The causative factors of CIN are malfunctioning biological processes that result in mitotic errors including defects in the SAC, microtubule dynamics and attachments, centrosome duplication resulting in amplification, telomere maintenance, DNA replication and sister chromatid cohesion (Bakhoum & Swanton, 2014). Interestingly, certain aneuploid phenotypes may result in increased or decreased synthesis of proteins involved in mitosis that can consequently induce error-prone mitotic phenotypes and cause CIN. For example, both decreased and increased levels of Mad1 weakens the mitotic checkpoint and induce chromosomal instability (Ryan et al., 2012). In addition, aneuploid yeast strains exhibited genetic alterations characteristics of genomic instability (Sheltzer et al., 2011). These findings suggest that under certain conditions, aneuploidy can also cause CIN.

Since CIN generates a diversity of aneuploid karyotypes, it predisposes cancer cells to faster adaptations (Sansregret et al., 2018). This is because aneuploid cells can confer proliferation advantages under extreme stress, whereas euploid karyotypes are

hindered, despite otherwise decreased overall fitness. This was observed when comparing aneuploid to euploid yeast strains and also when yeast exposed to high heat acquired chromosome duplications (Pavelka et al., 2010; Yona et al., 2012). In addition, trisomy 7 and 13 HCT116 cell lines tend to be more resistant to cisplatin and paclitaxel when compared to the euploid wild type (Replogle et al., 2020).

In one study, partial inhibition of Mps1, which is required for proper mitotic checkpoint signaling, was used to titrate CIN, resulting in different levels of chromosome missegregation events (Burkard & Weaver, 2017; Sansregret et al., 2017). Chemical inhibition of Mps1 resulted in survival for clones that had mutations in APC/C, which decreased CIN, suggesting that one mechanism by which cancer cells can tolerate selective pressures such as higher rates of CIN is to upregulate pathways that result in lower CIN under those selective pressures. Surprisingly, while low CIN was tolerated and even conferred some increase in proliferation with loss of p53, these effects were abolished for high rates of CIN, which severely decreased proliferation even in the absence of p53.

While CIN is associated with poor prognosis in solid tumors, excessive CIN has been shown to be lethal in cell line models where levels of mitotic checkpoint proteins BubR1 and Mad2 are absent, resulting in massive chromosome loss (citation). Indeed, excessive CIN has been shown to correlate to better survival for a large clinical dataset including ER-/ERBB2, ovarian, squamous NSCLC and gastric tumors (citation). In this study, a gene signature score, which measured total functional aneuploidy, CIN70 was used as surrogate measure of chromosomal instability to measure survival in 2125 patients. When categorized by quartile, CIN was predictive of worse prognosis in the

third highest quartile but was predictive of better prognosis in the highest quartile (Birkbak et al., 2011). While the surrogate measure for CIN70 as a marker for CIN has limitations, results from this study suggest that high CIN can potentially be used as a therapeutic strategy.

Work done previously in the Weaver lab, suggests that low dose paclitaxel can induce extreme CIN by causing the formation of multipolar spindles in primary breast cancers. As the dosage of paclitaxel was increased, cell lines exhibited a greater degree of CIN as observed by multipolar spindles and misaligned chromosomes as well as increased aneuploidy. Critically, these phenotypes were also accompanied by increased cell death (Zasadil et al., 2014a). In addition, mitotic arrest and interphase cytotoxicity of paclitaxel were ruled out as potential explanations for these effects.

1.3 The role of aneuploidy and CIN in immunogenicity

Most studies to date have focused on the effects of CIN on cell intrinsic processes involving tumorigenesis and proliferation. Recently, the consequences of CIN on the tumor immune microenvironment are being explored and add to the growing literature of how CIN can exert tumor-extrinsic effects. For example, G1-arrested senescent aneuploid cells generated from MPS1 inhibitor are able to be cleared in co-culture by natural killer cell line, NK92, significantly more efficiently than euploid cells (Santaguida et al., 2017). In addition, tetraploid colorectal cancer cell line CT26 expressed increased immunogenic markers such as cell surface calreticulin compared to wild type due to increased endoplasmic reticulum stress (Senovilla et al., 2012). Another study examined tetraploid CT26 cells forming tumors at a similar rate as wild type when injected into immunodeficient Rag γ BALB/c mice. However, in immunocompetent BALB/c mice, the tetraploid CT26 cells were noticeably delayed in tumor formation, suggesting tetraploidy inducing immune surveillance. This was further verified when growth of hyperploid cell tumors in C57Bl/6 mice was inhibited but rescued when these cells were grown in mice deficient of interferon-gamma and interferon-alpha receptor 1, which is involved in immune recognition of cancer cells. Similarly, colon organoids generated from tetraploid Tp53 deficient colonocytes grew in immunodeficient but not immunocompetent mice (Boilève et al., 2013). On the other hand, one study suggests that CIN may contribute towards downregulation of genes associated with antigen presentation and increased immune evasion due to selection of tumors with suppression of the STING pathway (Tripathi et al., 2019).

These studies suggest that aneuploidy and CIN can upregulate an immune response at least in the short term. CIN can result in lagging chromosomes and chromatin bridges, which can form micronuclei. Micronuclei rupture has been associated with cGAS/STING activation, which upregulates type 1 interferons to induce an immune response (Mackenzie et al., 2017b). Given the connection of CIN to immunogenicity, therapeutic targeting of CIN has recently been of great interest in the field. For example, radiation, which induces chromosomal instability, increases prognosis of both animals and patients in combination with immunotherapies in melanoma. The mechanistic pathway has been hypothesized to be radiation activating cGAS/STING via DNA damage and micronuclei formation to sensitize tumors to immunotherapies.

1.4 Therapeutic targeting of cGAS/STING for immune checkpoint blockade

Historically, cytosolic DNA sensing is recognized as a protective mechanism that host cells employ against dsDNA viruses to alert the immune system of their presence (Margolis et al., 2017). When foreign dsDNA is detected in the cytosol, affected cells can activate cGAS to synthesize Type-I interferons and pro-inflammatory products that can attract immune cells such as macrophages, T-cells and dendritic cells to initiate a targeted immune response. More recent studies have shown that cytosolic DNA sensors are non-discriminant to self-DNA, which presents an exploitable pathway by which cancer cells can be forced to alert the immune system for detection and destruction (L. Sun et al., 2013a).

While many DNA sensors have been discovered, cGAS has been shown to be the chief cytosolic DNA sensor and therapeutic target of interest (Vance, 2016). Mechanistically, cGAS binds to double stranded DNA, resulting in synthesis of 2’3’-cGAMP, a cyclic dinucleotide that functions as a major substrate of stimulator of interferon genes in human beings. 2’3’-cGAMP can activate downstream STING signaling to increase the production of type-I interferons such as interferon-beta and interferon-stimulated genes, which can both activate and attract innate immune cells to the cancer cell secreting these products to promote an adaptive immune response, ultimately resulting in the recruitment of stromal tumor-infiltrating lymphocytes to the tumor (X.-D. Li et al., 2013; S. Liu et al., 2015; L. Sun et al., 2013a; J. Wu et al., 2013). To complicate matters, cells have counter-regulatory mechanisms in place to prevent overt activation of recruited lymphocytes resulting from STING activation. This includes the upregulation of immune checkpoint signals from interferon-beta (Garcia-Diaz et al.,

2017; Morimoto et al., 2018). Not surprisingly, pre-clinical STING agonists have typically been combined with immune checkpoint blockade in animal models to boost the effects of both therapies and have been described as a sensitizer for immunotherapy (Fu et al., 2015).

Strategies have been developed to target STING signaling, but so far, these efforts have not resulted in commercially available drugs (Naour et al., 2020). Fortunately, several conventional therapies have been recently shown to activate the cGAS-STING pathway by causing treated cancer cells to expose their self-DNA to the cGAS sensor (Yum et al., 2020). Mechanistically, conventional therapies that impair mitosis such as microtubule inhibitors can promote chromosome missegregation, which causes the formation of micronuclei (Lohard et al., 2020; Zierhut et al., 2019a). These micronuclei often have weak nuclear membranes and can rupture to expose dsDNA to cytosolic cGAS. In addition, therapies that result in DNA breakages such as PARP inhibitors, radiation and anthracyclines have also been hypothesized to cause DNA fragments to leak into the cytosol from the nucleus, further amplifying cGAS activation in the cancer cell (Harding et al., 2017b; Mackenzie et al., 2017b; Shen et al., 2019; Z. Wang, Chen, et al., 2019b). In some instances, DNA and 2’3’-cGAMP can be transferred from dying cancer cells to innate immune cells, where cGAS activation can occur (Carozza et al., 2020).

When dsDNA is exposed to cGAS in either the cancer or immune cell, this can result in production of 2’3’-cGAMP and downstream STING signaling using the cell’s own machinery to activate pro-inflammatory signaling (Harding et al., 2017b; Mackenzie et al., 2017b). These therapies when combined with immune checkpoint blockade are

hypothesized to result in potentially synergistic immune activation in patients (Yum et al., 2020). Several clinical trials have already started looking into the effects of microtubule inhibitors, PARP inhibitors and radiation in combination with immune checkpoint blockade in reducing cancer in patients with positive outcomes (Hu et al., 2017; Peyraud & Italiano, 2020).

Since cGAS is required to produce 2'3'-cGAMP, we hypothesize that expression of this protein in tumor biopsies may be predictive for patients, who can benefit from combination therapy with immune checkpoint blockade therapies. Concordantly, cGAS expression in pan-cancer by RNA sequencing of TCGA cohorts suggest increased T-cell infiltration (An et al., 2019). Furthermore, in 7 patients treated with microtubule inhibitor (nab-paclitaxel or eribulin) and immune checkpoint blockade (PD-1 or PD-L1), we found a statistically significant correlation between cGAS expression and tumor control (see Chapter 2, Figure 6). These data suggest that cGAS may have predictive value as a biomarker and is a candidate biomarker for evaluation in animal studies and clinical trials.

These efforts have been especially relevant for triple negative breast cancers because recent efforts to improve prognosis for metastatic and other difficult-to-treat populations have focused on immunotherapies which promise durable responses responses (Emens, 2018). However, immune checkpoint inhibitors have limited efficacy as single agents. For example, KEYNOTE-086 tested pembrolizumab in a small cohort of metastatic, triple-negative breast cancer patients, yielding an objective response rate of 21.4% and 5.7% for treatment-naïve and previously treated PD-L1 positive patients,

respectively (Adams et al., 2019; Tokumaru et al., 2020). Such trials suggest that it is not enough to relieve an immunosuppressive tumor microenvironment in breast cancer.

In contrast to single-agent immune checkpoint inhibitors, combinations with chemotherapy have yielded better results in breast cancer (Heinhuis et al., 2019). In neoadjuvant therapy with paclitaxel, the I-SPY2 trial found pembrolizumab improved complete response (pCR) rate nearly threefold in patients with TNBC (60% vs 22%) (Nanda et al., 2020). Atezolizumab received accelerated approval for PD-L1 positive TNBC in combination with nab-paclitaxel due to an improved progression-free survival of 1.7 months in IMpassion-130 (Schmid et al., 2018). Accelerated approval of pembrolizumab with chemotherapy was granted after KEYNOTE-355, though multiple chemotherapies were selected (Cortes et al., 2020). In short, combinations of immune checkpoint inhibitor have shown more promise when combined with existing chemotherapies. It is not yet known whether combinations are synergistic due to immune activation by chemotherapy, or if the effects are merely additive—combining two treatments with non-overlapping toxicities will generally improve response rate and progression-free survival (Emens & Middleton, 2015). If there is synergy, then specific combinations of chemotherapy or targeted drugs with immune checkpoint inhibition may be privileged and offer the best response.

1.5 Amplifying immunity using conventional therapies in breast cancer

It is well known that some breast cancers respond better than others to conventional therapies (Houssami et al., 2012). A further complicating factor is that some tumor or immune system characteristics might be necessary to enable the immunogenic response to standard chemotherapy. If so, it would be important to select the right patients and tumors, in which a particular chemotherapy and immunotherapy could interact to make outcomes more favorable. In short, there are potentially complex interactions between the mechanism of a standard drug, tumor biology, immune checkpoint inhibitor, and the host immune system. Due to this complexity, it will not be likely possible to empirically define patient subsets from disparate trials. Instead, it is optimal to identify and test potential mechanisms of interactions in future trials that could mediate a chemotherapy-checkpoint inhibitor interaction in specific patient subsets. Since the immune-modulating mechanisms of conventional therapies may be different, different biomarkers may be appropriate depending on the combination therapy used, even for conventional therapies that are very similar. For example, IMpassion-131, which tested paclitaxel in place of nab-paclitaxel demonstrated no improvement in survival when PD-L1 expression on immune cells was used as a biomarker to select for patients despite both therapies being quite similar (Miles, 2020). While other factors such as pre-medication steroids may influence these results, we cannot rule out the differences in how both therapies may activate the immune system, which places importance on the potential impact of mechanism on combination therapy efficacy. In particular, the combination of paclitaxel and PD-L1 inhibitor therapy offers marginally

longer PFS compared to paclitaxel monotherapy, suggesting that some immune response may still be present, although this trend is not statistically significant.

To better understand if chemotherapies can exert synergistic effects on an immune response, we must understand their mechanistic processes. Therefore, I will review the mechanisms of existing therapies and their role in immune activation based on current literature. Next, I review the effects that each conventional therapy has on the immune system and the potential mechanisms by which these immune effects are mediated. Finally, I will discuss tumor and host-specific factors that could be required for synergy in individual patients. I divided the effects of conventional therapies into six categories, which are immunogenic cell death, increased surface immune markers, cGAS-STING activation, T-cell activation and recruitment, immune cell modulation and immune cell cytoxicity (Figure 2). I summarize the immune responses activated by conventional therapies in Table 1.

Conventional therapies for breast cancer such as chemotherapies are cytotoxic because they prevent proliferation by indirectly or directly disrupting DNA synthesis, repair, and segregation during cell division (Bracci et al., 2014). Some also target kinases that are central to proliferation pathways (Table 1). Conventional therapies elicit an immune response by indirect paracrine signaling originating from cancer cells or by directly modulating immune cell activity and viability (Opzoomer et al., 2019). Newer therapies such as vaccines and adoptive cell transfer directly target immune activation by promoting the expression of tumor antigens on the surface of host cells or by engineering cytotoxic T-cells to attack cancer cells, respectively.

Mechanisms for immune activation can indirectly be due to changes in copies of chromosomes in cancer cells, resulting in potentially increased expression of existing tumor antigens, secretion of pro-inflammatory cytokines and cell death in a manner that recruits a host immune response (Figure 2). Similarly, many of these pathways are functional in host immune cells and can boost an immune response by altering expression of immunogenic ligands or by selectively depleting immunosuppressive cells. Here, I systematically review the immunomodulatory mechanisms exhibited by conventional breast cancer therapies.

1.51 Immunogenic Cell Death

Immunogenic cell death (ICD) is a unique cellular response to microbial infection and exogenous stimuli including chemotherapy and radiation (Fucikova et al., 2020). This response results in major stress on the endoplasmic reticulum and other organelles, resulting in cell death that is typically associated with release of damage-associated molecular patterns (DAMPs) and exposure of calreticulin on the cell membrane (Galluzzi et al., 2020). Cell death caused by certain chemotherapies such as DNA crosslinkers and damaging agents are particularly effective at inducing ICD (Hato et al., 2014). ICD releases DAMPs that can bind to pattern recognition receptors (PRRs) on innate immune cells such as dendritic cells to facilitate maturation and antigen presentation resulting in differentiation and proliferation of antitumoral T-cells. ICD-inducing treatments may potentially synergize with immune checkpoint inhibitors since the latter can further boost the antitumoral adaptive immune response activated by ICD (Emens & Middleton, 2015). In addition, expression of some DAMPs have been shown

to have prognostic and predictive significance in both animal models and patients (Pol et al., 2015).

In breast cancer, biomarkers of ICD including HMG-B1, LC3B+, STQSM1/p62 have been evaluated histologically on biopsies from 1798 patients in a breast cancer study showing that poor prognosis is significantly associated with loss of HMGB1 expression and active autophagy (Ladoire et al., 2016; Rapoport & Anderson, 2019). In another study involving 52 patients with breast cancer and 8 patients with esophageal squamous cell carcinoma, pre-treatment biopsies and resected surgical specimens were both evaluated for calreticulin and HMGB1, which were both found to be significantly elevated after neoadjuvant chemotherapy relative to pretreatment samples (Aoto et al., 2018). Of note, the expression of these markers did not predict monotherapy efficacy and survival. However, the mechanism of ICD in inducing an immune response suggests that when used in combination with immunotherapies such as immune checkpoint inhibitors, ICD-inducing therapies may potentially work best in patients expressing ICD markers such as those described.

1.52 Increased surface immune markers

Conventional cancer therapies such as HER2-targeted, mTOR inhibitors, anthracyclines, PARP inhibitors, microtubule inhibitors and radiation can increase immune markers on the surface of cancer cells (Amiel et al., 2012; Garcia-Diaz et al., 2017; Goel et al., 2017; Griguolo et al., 2019; O'Donnell et al., 2018; S.-Y. Sun, 2020; Walle et al., 2018). These surface markers can modulate an immune response in both positive and negative ways. For example, for HER2-targeted therapies, exogenous

antibodies bound to the surface of cancer cells are able to direct natural killer cells to the tumor for targeted lysis in a process known as antibody-dependent cellular cytotoxicity (Griguolo et al., 2019). Other therapies such as anthracyclines, PARP inhibitors and radiation may induce immune evasion by increasing expression of immune checkpoint ligands such as PD-L1 and CTLA-4 on the surface of cancer cells, resulting in T-cell exhaustion. Mechanistically, this is thought to occur due to the production of Type I and Type II interferons from these therapies, which can involve activation of cGAS-STING and JAK-STAT pathways (Garcia-Diaz et al., 2017).

1.53 Immune Cell Cytotoxicity

Chemotherapy and radiation are non-discriminately toxic to all cell types, particularly those that are actively proliferating (Baskar et al., 2014; Stover et al., 2016). Due to this cytotoxicity, a well-known side effect is immunosuppression due to depletion of proliferating immune cells. Fortunately, doses are given over time rather than continuously, allowing for immune cell populations to recover in between treatments, and there is longitudinal evidence suggesting that after treatment, T-cells experience at least partial recovery (Gustafson et al., n.d.; Rotstein et al., 1985). However, incomplete elimination of cancer stem cells by chemotherapy or radiation coupled by elimination of immune cells may allow the cancer to return in an immunosuppressive environment and become therapeutically resistant (Jiang et al., 2020; Morrison et al., 2010).

At the same time, some types of immunosuppressive immune cell populations such as myeloid-derived suppressor cells and regulatory T-cells (Tregs) are more easily depleted by chemotherapy and radiation than other types of white blood cells, allowing

for potential synergy with immunotherapy (Sánchez-Margalet et al., 2019; Z. Wang et al., 2017). Depletion of immunosuppressive cell populations occurs to some extent with most conventional therapies excluding HER2-targeted therapies. Fortunately, T-cells are typically resistant to these therapies as evidenced by the increased efficacy of combined conventional therapy and immunotherapy in eliciting an effective T-cell mediated antitumoral response (Heinhuis et al., 2019). Therefore, the presence of immunosuppressive cell populations may serve as potential biomarkers for efficacy of conventional therapies and potentially may also result in synergy with immunotherapies.

1.54 Immune Cell Modulation

Conventional therapies can modulate immune cell responses. The presentation of tumor antigens on MHC-I molecules allows professional antigen presenting cells to interface with the adaptive immune system to activate and recruit cytotoxic T-cells directed against the tumor (McDonnell et al., 2015). MHC-I can be upregulated by radiation and other chemotherapies that induce interferons, which can increase cell surface expression of MHC-I molecules (Zhou, 2009). Conventional DNA-damaging agents such as radiation can also promote the expression of neo-antigens, which can bind to MHC I molecules to promote a targeted immune response (Lhuillier et al., 2021). Potential biomarkers of interest include expression of functional cGAS and STING proteins as well as a functioning interferon secretion pathway. In addition, conventional therapies such as taxanes can mediate M1 macrophage polarization to reverse the immunosuppressive effects of tumor-associated macrophages, resulting in a more robust immune response (Wanderley et al., 2018).

The M1/M2 nomenclature was used to highlight differences between macrophages in mice that had either a Th1- or Th2- dominant adaptive immune response (Orecchioni et al., 2019). Macrophages from Th1-dominant C57BL/6 can produce nitric oxide with IFN-γ or LPS stimulation in contrast to macrophages from Th2-dominant BALB/c mice, which increase arginine metabolism to ornithine instead (Mills et al., 2000). Later studies showed that M1 macrophages were pro-inflammatory and played a role in the elimination of cancer cells and pathogens compared to M2 macrophages, which could promote tumor growth and stimulate an anti-inflammatory reaction (Italiani & Boraschi, 2014). Numerous molecular signatures distinguish the two types of macrophage phenotypes. For example, M1 macrophages have been shown to upregulate a pro-inflammatory genes and chemotactic genes including CXCL10 and CXCL11 (Orecchioni et al., 2019). M2 macrophages can upregulate anti-inflammatory cytokines and chemokines such as IL10 and CCL18, among others (Orecchioni et al., 2019). In addition, M2 macrophage have higher mRNA expression of matrix metalloproteinases such as MMP9 compared to M1 macrophages (Jager et al., 2016).

1.55 T-cell Activation and Recruitment

The expression of T-cell exhaustion markers on both tumor and immune cells can hamper T-cell mediated antitumoral immunity by creating an immunosuppressive environment (Anderson et al., 2017). Blockade of immune checkpoints can overcome T-cell exhaustion by antibodies against PD-1/PD-L1 and CTLA-4 (Grywalska et al., 2018). Furthermore, therapies such as adoptive cell transfer can be used to re-engineer T-cells

and other immune cells obtained from the patient to selectively target tumors, which can be combined with immunotherapies to potentially increase treatment efficacy (Kalos & June, 2013).

1.6 Potential roles of specific therapies

1.61 Chemotherapies

Fluouracil (5-FU) is an inhibitor of thymidylate synthase, which is a key enzyme that synthesizes pyrimidine thymidylate for DNA synthesis to prevent cell proliferation (Ghiringhelli et al., 2013). While effective in killing some types of cancer cells, 5-FU also exerts its effects on immune cells by selectively depleting myeloid-derived suppressor cells (MDSCs) in a colon cancer model. MSDCs are immunosuppressive and generally increase in number with progressing disease to suppress antitumoral T-cell activation (Vincent et al., 2010). Strikingly, other immune cell populations, including T-cells, NK cells, dendritic cells and B cells, are not adversely affected by 5-FU. As a consequence of MSDC depletion, 5-FU indirectly increases IFN-gamma production by tumor-infiltrating CD8+ T-cells to recruit an antitumoral immune response. However, subsequent studies examined repeated cycles of 5-FU to impair the anti-tumor functions of cytotoxic T-cells in a CT26 tumor-bearing mouse model (Y. Wu et al., 2016). These effects suggest that combination immunotherapy may be more effective when limiting the amount of chemotherapy used. While these treatments focus on targeting MDSCs rather than cancer cells themselves, we cannot eliminate the possibility that the type of cancer may affect results.

Gemcitabine is a pyrimidine nucleoside antimetabolite that prevents proliferation in breast cancer by impairing DNA replication (Heinemann, 2005). Similar to 5-FU, gemcitabine has indirect effects on immune cell populations and has been reported in one study to inhibit MDSCs while augmenting expansion of T-cells in the 4T1 tumor-bearing BALB/c mice (Heinemann, 2005). In a syngeneic thymoma model, gemcitabine

was reported to have less efficacy over 5-FU at inducing MDSC apoptotic cell death (Vincent et al., 2010).

Cyclophosphamide is a highly toxic alkylating agent with an active metabolite, phosphoramide mustard, that reacts with either cytidine or guanine from DNA to form inter-strand cross-links in a cell cycle independent manner (Ahlmann & Hempel, 2016). Due to its non-specific effects on all types of cells, cyclophosphamide is recognized as an immunosuppressant. Despite its generally immunosuppressive effects, cyclophosphamide can counteract immunosuppression in cancer by selectively depleting Tregs after a single dose in multiple cancer models and patients (Awwad & North, 1988; Hong et al., 2010; Hughes et al., 2018; P. Liu et al., 2010; Moschella et al., 2013; Noguchi et al., 2016; Takeuchi et al., 2012).

Platinum agents such as oxaliplatin function by forming DNA-platinum adducts that interfere with DNA replication and transcription, ultimately inducing an apoptotic response (Hato et al., 2014). Cell death due to oxaliplatin can be immunogenic in that dying cells release three key signals, ATP, calreticulin and HMGB1 to recruit and activate dendritic cells for more effective antigen cross-presentation, presumably resulting in better T-cell mediated antitumoral immunity. In a cohort of 338 colorectal cancer patients comparing oxaliplatin-based combination chemotherapy versus sequential chemotherapy, patients with a loss-of-function allele for TLR4, which is the receptor for HMGB1, had worse progression-free and overall survival, suggesting that oxaliplatin may induce clinically meaningful immunogenic cell death (Tesniere et al., 2010).

Anthracyclines such as doxorubicin primarily function by interacting with topoisomerase-II to prevent ligation of dsDNA breakages, resulting in growth arrest and apoptotic cell death (Venkatesh & Kasi, 2020). Anthracyclines appear to induce immunogenic cell death in that ATP, calreticulin and HMGB1 are released by the apoptotic cell (Fucikova et al., 2011). It has also been long known that anthracyclines can result in release of Type-I interferons (Z. Zhang et al., 2015), and this has been linked to the cGAS-STING pathway (Imai et al., 2018). Apart from tumor cell-specific effects, anthracyclines have also been shown to eliminate MDSCs in mouse models of cancer (Alizadeh et al., 2014; X.-D. Li et al., 2013).

1.62 Targeted therapies

CDK4/6 inhibitors such as palbociclib, ribociclib and abemaciclib are classically thought to cause cell cycle arrest in G1 due to phosphorylation of retinoblastoma protein (Rb), resulting in activation of this tumor suppressor protein, resulting in apoptosis in some types of breast cancers. Critically, CDK4/6 inhibitors are relatively well-tolerated by patients, resulting in fewer side effects compared to chemotherapies (Sherr & Bartek, 2017; Thill & Schmidt, 2018). In cancer cell lines, CDK4/6 inhibitors can increase the capacity for antigen presentation through upregulation of MHC class I proteins on the cancer cell surface (Goel et al., 2017). Mechanistically, CDK4/6 activation of Rb leads to E2F transcription, which is a critical component for controlling transcription DNA methyltransferases (DNMTs), specifically *DNMT1*. Transcription of *DNMT1* prevents synthesis of type III interferons, which can directly upregulate MHC class I proteins. Therefore, CDK4/6 inhibitors can upregulate MHC class I proteins on the cell surface by

increasing type III interferon synthesis by inducing viral mimicry through inhibition of DNA methyltransferases (Goel et al., 2017). Unfortunately, these potentially therapeutic effects are circumvented in cancers where Rb protein is not expressed or non-functional, which is seen more in triple negative breast cancers compared to other subtypes. In the tumor microenvironment, CDK4/6 inhibitors can downregulate DNMT1 transcription in regulatory T-cells (Tregs), which results in hypomethylation of CDK1a promoter and increased expression of p21. p21 is a cell cycle inhibitor that prevents proliferation of Tregs, which are immunosuppressive.

Alpesilib is used to treat breast cancer and is an inhibitor of the phosphoinositide 3-kinase (PI3K), a key signaling protein that affects growth and proliferation. In breast cancer, the PI3K pathway can be hyper activated by gain-of-function mutations in oncogene *PIK3CA* and loss-of-function mutations in tumor suppressor gene *PTEN* (Okkenhaug et al., 2016), allowing cells to grow unimpeded. Rather than killing the cells outright, PI3K inhibition causes cancer cells to become dormant and mimic a nutrient-deprived state, owing to the pathway's role in nutrient sensing. Since this pathway is ubiquitously expressed, alpesilib and other PI3K inhibitors have off-target effects on host cells such as immune cells, specifically leukocytes that tend to express more PI3K compared to other cell types. These effects can be immunostimulatory through selective depletion of immunosuppressive regulatory T-cell populations via inhibition of isoforms PI3Kα/δ in mouse syngeneic tumor models (Carnevalli et al., 2018). In addition, selective inhibition of PI3Kα/δ can potentiate CD8+ T-cell activation without decreasing the rate of proliferation by enhancing IL-2 secretion, which serves as a survival signal for effector T-cells.

Rapalogues such as everolimus inhibit the function of a protein known as mechanistic target of rapamycin (mTOR), which is a constitutively expressed and evolutionarily conserved serine/threonine kinase from the family of PI3K-related kinases (Powell et al., 2012). Mechanistically, mTOR, which comprises two complexes mTORC1 and mTORC2, is inhibited when bound to a complex formed by the rapalogue and FK506 binding protein 12kDa (FKBP12) that acts as an allosteric inhibitor and changes the conformation of mTOR to prevent downstream signaling (H. Yang et al., 2013). mTOR is important for controlling cell growth and proliferation. Early mouse studies showed that rapamycin prevents T-cell proliferation, leading to the long-held belief that mTOR inhibition induces immunosuppression (Dumont et al., 1990). However, one preclinical cell line study suggested that mTOR inhibition can be immunostimulatory in certain contexts by studying dual mTORC1/2 kinase inhibitor, vistusertib (Langdon et al., 2018). This and other studies found that mTOR inhibition can upregulate production of the pro-inflammatory cytokine IL-12 in activated dendritic cells while simultaneously reducing the anti-inflammatory cytokine IL-10 (Amiel et al., 2012; Langdon et al., 2018; Ohtani et al., 2008; Weichhart et al., 2008).

mTOR inhibition can also increase expression of immune checkpoint protein, PD-L1, on cancer cell lines, including breast cancer, which may explain the observed decrease in T-cells seen in mouse studies with rapamycin (Amiel et al., 2012; O'Donnell et al., 2018; S.-Y. Sun, 2020). Mechanistically, this is thought to be due to decreased proteasomal degradation of PD-L1, which is facilitated by mTORC1. Therefore, rapalogues in combination with PD-1/PDL-1 inhibitors may reverse the immunosuppressive effects of rapologue monotherapy and is potential treatment

combination for difficult-to-treat cancers such as triple negative breast cancer (Vikas et al., 2018). Given the dose-dependent immunosuppressive nature of rapalogues, appropriately scheduling and titrating these combination therapies may determine their effectiveness in the clinical setting.

PolyADP-ribose polymerase (PARP) is an enzyme that repairs single stranded DNA breakages, which is more commonly upregulated in triple negative breast cancers (Ossovskaya et al., 2010). For cancers with BRCA1/2 mutations, small molecule PARP inhibitors (PARPi) have been developed to exert a synthetic lethal effect by disrupting homologous recombination, resulting in effective cell death (Han et al., 2020). PARP trapping, which is a mechanism for PARPi that tightly links PARP complexes to DNA has been shown to activate the cGAS-STING pathway (Kim et al., 2020; Murai et al., 2012). This finding connects PARPi to innate immunity.

Radiation induces ssDNA and dsDNA breakages at high doses, resulting in cell death and a myriad of immune responses. While at high doses, radiation can be immunosuppressive, radiation therapy targeted to the tumor can result in more efficient T-cell priming due to causing immunogenic cell death of the tumor and from activation of the cGAS-STING pathway of cells that survive the initial treatment (Walle et al., 2018). Type-I interferons are released by tumor cells with cGAS-STING activation and can attract antitumoral lymphocytes to the microenvironment. Finally, radiation therapy can increase tumor cell surface markers such as MHC-I, NK cell ligands and costimulatory receptors on to enhance activation of these associated cell types.

Microtubule targeting agents (MTAs) such as taxanes, vinorelbine and eribulin modify microtubule stability, resulting in chromosome missegregation and aneuploid daughter cells that undergo apoptosis (Weaver, 2014; Zasadil et al., 2014a). Mechanistically, MTAs induce multipolar mitoses in both cell culture and patients at clinically relevant concentrations, resulting in rupture-prone micronuclei in daughter cells (Lohard et al., 2020; Mitchison et al., 2017a). Multiple studies have indicated that micronuclei rupture can result in cGAS activation (Harding et al., 2017b; Mackenzie et al., 2017b). Both 2'3'-cGAMP and Type I interferons are synthesized downstream of cGAS activation, which have a variety of effects including polarization of macrophages to an M1 phenotype and activation of immune cells such as NK cells, T-cells and dendritic cells. (Carozza et al., 2020; Cordova et al., 2020; Hervas-Stubbs et al., 2011).

1.63 HER2-directed therapies in immune modulation

HER2+ BC patients have tumors that overexpress the *HER2* oncogene, which forms a protein tyrosine kinase receptor (RTK) that drives tumor growth and progression in about 15 to 20% of breast cancers (Krishnamurti & Silverman, 2014). Currently, therapies targeted against the extracellular domain of the HER2 receptor are most effective at treating this subtype of BC. These therapies include monoclonal antibodies such as trastuzumab and small molecule RTK inhibitors such as lapatinib. Both prevent the formation of heterodimers between the HER2 receptor and other related RTKs, which are an integral component of intracellular growth signaling pathways such as phosphatidylinositol 3 kinase (PI3K)/Akt and Ras/mitogen-activated protein kinase.

HER2 targeted treatments can impact the immune system by promoting antibody-dependent cellular cytoxicity (ADCC) (Griguolo et al., 2019). The Fc fragment of the bound antibody of trastuzumab can interact with receptors on natural killer (NK) cells, gamma-delta-T-cells and neutrophils of the innate immune system, thereby promoting ADCC (Baselga & Albanell, 2001; Molina et al., 2001). By increasing ADCC, more antigens are present in the tumor microenvironment, which can be taken up by professional antigen presenting cells. Activated NK cells can also facilitate dendritic cell priming and promote recruitment of T-cells by releasing pro-inflammatory cytokines and chemokines such as IFN-γ and TNF-α (Muntasell et al., 2017). As a small molecule, lapatinib also enhances STAT1 activation and recruitment of IFN-gamma secreting T-cells to the tumor (Hannesdóttir et al., 2013).

Outside of conventional chemotherapy and radiation are cancer vaccines, which are distinct tumor antigens that can be detected by host immune cells to orchestrate a specific adaptive immune response (Benedetti et al., 2017). NeuVax is composed of a HER2-derived peptide E75 (nelipepimut-S) combined with the immune-adjuvant granulocyte macrophage colony-stimulating factor (GM-CSF) that mechanistically can activate CD8+ CTLs and CD8+ memory cells against the E75 breast cancer MHC class I epitope, resulting in selective depletion of HER2+ breast cancer cells. AVX901 is an attenuated strain of Venezuelan equine encephalitis virus that highly expresses HER2 RNA to sensitize immune cells against HER2 as an antigen. INO-1400 is a DNA vaccine that is directed against human telomerase reverse transcriptase, which is commonly expressed in breast cancers.

1.64 Potential anti-synergistic effects of standard therapies

It has been long known that conventional therapies can be immunosuppressive given their nonspecific cytotoxicity, particularly at high concentrations (Penn & Starzl, 1973). In addition to potential mechanisms of synergy, it is possible that the certain drugs could antagonize immune checkpoint therapy by making the tumor less immunogenic, or by suppressing immunity systemically. It has long been a concern that corticosteroids, for example, can suppress the immune system and make immunotherapy less effective. While steroids have not impacted efficacy of immune checkpoint therapy in melanoma, when used for immune-mediated toxicities, corticosteroids could have an impact in breast cancer (Horvat et al., 2015). Indeed the effect of steroids could explain, in part, the differences observed in IMpassion 130 and IMpassion 131, only the latter of which involved routine steroid premedications (Miles, 2020; Schmid et al., 2018). In short, it is not assured that standard of care therapies will synergize or simply have additive effects with immunotherapy.

1.7 Gaps in knowledge

Many conventional therapies could potentially modulate tumor cell susceptibility to immune monitoring and response, activate the immune system to recognize and destroy tumor cells and deplete immunosuppressive populations in the tumor immune microenvironment. Given this, new strategies that rely on combining chemotherapies with immunotherapies might produce more effective treatments than either therapy alone. There already exists a wide body of literature that suggest combinations to test (Bailly et al., 2020). At the same time, adverse effects can be expected from combining treatments and care must be made to schedule and titrate combination therapies carefully to avoid toxicity in pre-clinical models before proceeding to patient treatment.

Moving forward, it will be important to consider these potential mechanisms of interactions in clinical investigations, and the biomarkers that may predict response. For example, it is well known that MHC-I interactions depend on HLA genotype. Further, cGAS expression can vary among breast cancers, so its mechanism of action may be limited specifically to cancers that express this innate immune sensor. In order to identify the mechanisms and biomarkers that predict interactions, it will be critical to design future studies that will identify the specific mechanisms of interaction.

In addition, there is substantial evidence to suggest that mechanisms for conventional therapies will result in acquired resistance and tumorigenesis (Holland & Cleveland, 2009; Lee et al., 2011). Furthermore, CIN can result in lagging chromosomes, which can result in micronuclei. Micronuclei can rupture and activate cGAS/STING. Chronic activation of cGAS/STING has been thought to result in metastasis by selectively activating NF-κB pathway, which can drive inflammation in the

absence of a Type-I interferon response (Bakhoum et al., 2018). Therefore, mechanisms of conventional therapies should be investigated in further detail to determine potential long term negative effects from therapeutic targeting of these pathways.

In Chapter 2, I will investigate a potential hypothesis for how clinically relevant concentrations of paclitaxel may activate an immune response in triple negative breast cancer. We hypothesize cGAS/STING pathway as a potential mechanism for how paclitaxel may activate innate immune signaling by polarizing M2 to M1 macrophages through paracrine signaling via either 2’3’-cGAMP or IFN-β. In the discussion, I will also review other cytosolic signaling pathways and why we decided to focus on the cGAS/STING pathway in particular.

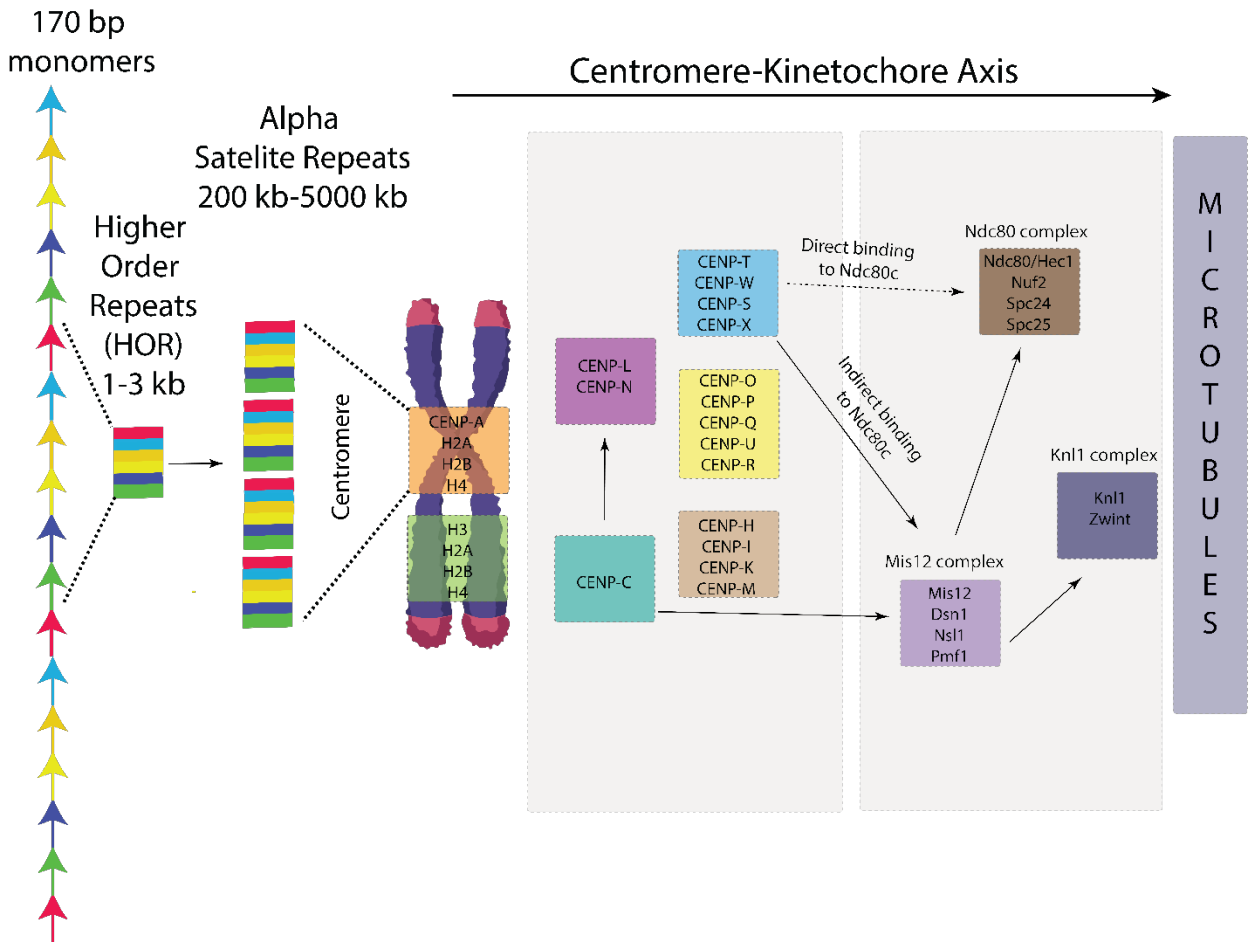

Fig. 1.1: Proteins comprising the kinetochore

Kinetochore is a proteinaceous complex that acts as a scaffold for microtubule binding. Kinetochores assemble on centromeres on each chromosome. Centromeres are composed of alpha satellite DNA, formed by the repetition of a 170 bp monomer sequence. The composition of the alpha satellite DNA is unique to individual chromosomes. In addition to the alpha satellite repeats, the location of the centromere in a chromosome is specified by the presence of CENPA, which is an alternate Histone 3 (H3) that forms octameric nucleosomes similar to H3. The kinetochore which assembles on the CENPA nucleosomes at the centromeres is composed of two protein-complexes: Constitutive Centromere Associated Network (CCAN) or inner-kinetochore and the KMN network or the outer-kinetochore. CCAN complex is composed of

subcomplexes such as CENP-C-H/I/K/M, CENP-L/N, CENP-O/P/Q/U/R and CENP-T/W/S/X. KMN network is composed of three subcomplexes: Knl1 complex, Mis12 complex and Ndc80 complex and is assembled on CCAN through CENP-C and CENP-T during mitosis. Once assembled, the kinetochores bind microtubules from opposite poles through the Ndc80 complex at the outer kinetochore. This figure contributed by Roshan X. Norman of the Mark Burkard Research Group.

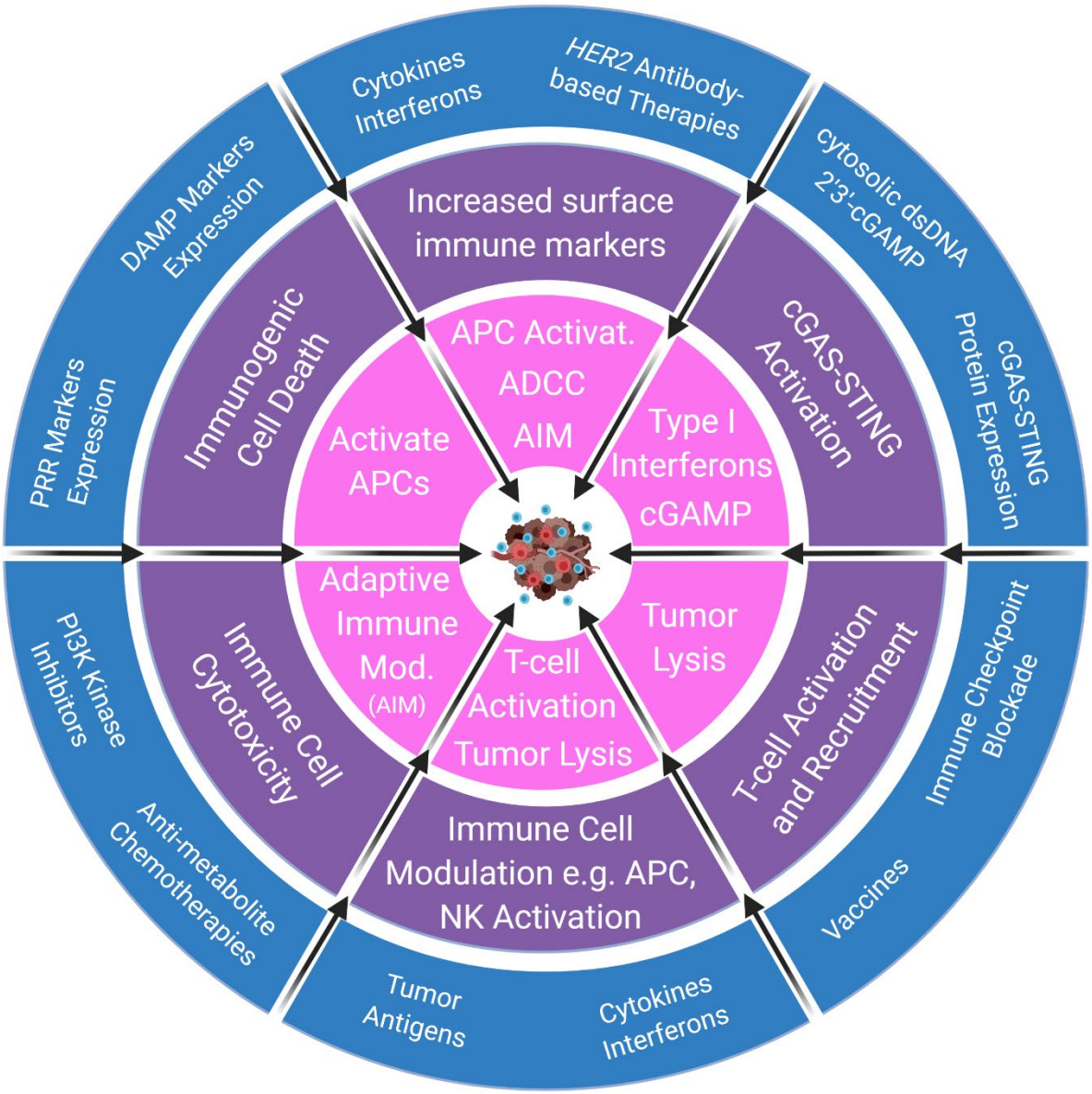

Fig. 1.2: Mechanisms of immune activation by breast cancer therapies

General schema of immune activation mechanisms. The outer ring (blue) represents potential biomarkers and types of therapies that can result in six immune-activating effects shown in the middle ring (purple), which are the increase of surface immune markers, induction of immunogenic cell death, activation of cGAS-STING, promotion of immune cytotoxicity, modulation of innate immune cells, and recruitment of T-cells.

Furthermore, these immune-activating effects in the middle ring (purple) can result in downstream activation of other immune processes shown in the inner ring (pink). Ultimately, these downstream effects can feedback into the other immune-activating processes shown in the middle (purple) and outer (blue) rings, resulting in multiple immune-activating effects from one type of therapy or mechanism.

			Immunity-enhancing Mechanisms
Therapies	**Drug Class**	**Cytotoxic Mechanism**	**Biomarkers**
Her2 inhibitor (trastuzumab pertuzumab)	Receptor tyrosine kinase inhibitor	Prevents proliferation	*HER2* protein expression
EGFR tyrosine kinase inhibitor (lapatinib)	Epidermal growth factor receptor kinase inhibitor	Prevents proliferation	*HER2* protein expression
CDK4/6 inhibitor (palbociclib, ribociclib, abemaciclib)	Cyclin-dependent kinase inhibitor	Prevents proliferation	*Rb* protein expression, *DNMT1* wild type DNA expression
mTOR inhibitor (everolimus)	mTOR kinase inhibitor	Prevents proliferation	*PIK3CA* gene signature
PI3K inhibitor (alpelisib)	PI3K kinase inhibitor	Prevents proliferation	*PIK3CA* gene signature
PARP inhibitor (olaparib, talozoparib, rucaparib)	PARP protein inhibitor	Prevents DNA repair	cGAS protein expression and *BRCA1/2* deletion
Anthracyclines (doxorubicin, epirubicin)	DNA intercalator, TOPOII inhibitor	DNA damage	cGAS protein expression
Microtubule Inhibitors (paclitaxel, docetaxel, vinorelbine, eribulin)	Antimitotics	Prevents proper mitosis	cGAS protein expression
Antimetabolites (5-Fluorouracil, Gemcitabine)	Antimetabolite	Prevents DNA synthesis	Presence MDSCs
Alkylating/platinum agents (cyclophosphamide, cisplatin, carboplatin)	DNA crosslinking compound	Prevents DNA repair/synthesis	Immunogenic Cell Death Markers
Radiation	DNA-damaging agent	Prevents proper mitosis, prevents repair/synthesis, DNA damage	cGAS protein expression
Vaccines	Tumor antigens	Expression of antigens on host cells to promote targeted immune response	High tumor mutation burden

	Tumor cell			Immune Cell		
Therapies	**Immunogenic Cell Death**	**Increased surface immune markers**	**cGAS-STING Activation**	**Immune Cell Cytotoxicity**	**Immune Cell Modulation**	**T-cell Activation and Recruitment**
Her2 inhibitor (trastuzumab pertuzumab)		x			x	
EGFR tyrosine kinase inhibitor (lapatinib)		x			x	
CDK4/6 inhibitor (palbociclib, ribociclib, abemaciclib)				x		x
mTOR inhibitor (everolimus)		x	x	x		
PI3K inhibitor (alpelisib)		x	x	x		
PARP inhibitor (olaparib, talozoparib, rucaparib)		x	x		x	
Anthracyclines (doxorubicin, epirubicin)		x	x	x	x	
Microtubule Inhibitors (paclitaxel, docetaxel, vinorelbine, eribulin)	x	x	x		x	
Antimetabolites (5-Fluorouracil, Gemcitabine)				x		
Alkylating/platinum agents (cyclophosphamide, cisplatin, carboplatin)	x			x		
Radiation	x	x	x	x	x	
Vaccines					x	x

Table 1.1: Summary of conventional therapies effects on the immune system

CHAPTER 2: PACLITAXEL INDUCES MICRONUCLEATION AND ACTIVATES PRO-INFLAMMATORY CGAS/STING SIGNALING IN TRIPLE NEGATIVE BREAST CANCER

Work in this chapter was submitted for revision to *Molecular Cancer Therapeutics*

Paclitaxel induces micronucleation and activates pro-inflammatory cGAS/STING signaling in triple negative breast cancer

Yang Hu, Baraa K. Manasrah, Stephanie M. McGregor, Robert F. Lera, Roshan X. Norman, John B. Tucker, Christina M. Scribano, Rachel E. Yan, Mouhita Humayan, Kari B. Wisinski, Amye J. Tevaarwerk, Ruth M. O'Regan, Lee G. Wilke, Beth A. Weaver, David J Beebe, Ning Jin and Mark E. Burkard

2.1 Abstract

Taxanes remain one of the most effective medical treatments for breast cancer. Recent trials have coupled taxanes with immune checkpoint inhibitors (ICIs) in triple-negative breast cancer (TNBC) patients with promising results. However, the mechanism linking taxanes to immune activation is unclear. To determine if paclitaxel could elicit an antitumoral immune response, we sampled tumor tissues from patients with TNBC receiving weekly paclitaxel (80 mg/m^2) and found increased stromal tumor-infiltrating lymphocytes (sTILs) and micronucleation over baseline in three of six samples. Mechanistically, paclitaxel operates by inducing chromosome missegregation on multipolar spindles during mitosis. Consequently, post-mitotic cells are multinucleated and contain micronuclei, which often activate cyclic GMP-AMP synthase (cGAS) and induce a type I interferon response reliant on the stimulator of interferon genes (STING) pathway. Other microtubule-targeting agents (MTAs), eribulin and vinorelbine, recapitulate this cGAS/STING response and increased the expression of immune checkpoint molecule, programmed death-ligand 1 (PD-L1), in some types of TNBC cells. To test the possibility that MTAs sensitize tumors that express cGAS to ICIs, we identified ten TNBC patients treated with PD-L1 or PD-1, seven of whom also received MTAs. Elevated baseline cGAS expression significantly correlated with treatment response in patients receiving MTAs in combination with ICIs. Our study identifies a mechanism by which MTAs can potentiate an immune response in TNBC. Further, baseline cGAS expression may predict treatment response in therapies combining MTAs and ICIs.

2.2 Introduction

Triple-negative breast cancer (TNBC) is an aggressive breast cancer subtype and taxane-based regimens remain the standard of care. Paclitaxel, which stabilizes polymerized microtubules, is one of the most widely used chemotherapy agents in breast cancers including TNBC (Kellokumpu-Lehtinen et al., 2013; Perez, 1998). In human tumors, it reaches 1-9 μM peak concentration and induces aberrant chromosome segregation, leading to cell death in a portion of daughter cells after mitotic exit (Zasadil et al., 2014b).

The IMpassion130 clinical trial demonstrated an overall survival benefit in patients with PD-L1 positive TNBC receiving PD-L1 inhibitor, atezolizumab, in combination with nab-paclitaxel, compared to patients receiving nab-paclitaxel with placebo (Schmid et al., 2019) and changed the treatment paradigm in patients with metastatic TNBC. A similar clinical trial, KEYNOTE-355 also showed overall survival benefit for patients treated with chemotherapy regimens that included paclitaxel with PD-1 inhibitor, pembrolizumab (Cortes et al., 2020). Although, these clinical trials were not designed to distinguish additive or synergistic drug effects, it remains possible that taxanes and other MTAs can activate the immune system.

Cyclic GMP-AMP synthase (cGAS) is a key component of innate antiviral immunity and induces a pro-inflammatory type I interferon response (J. Wu et al., 2013; L. Sun et al., 2013b). As a cytosolic DNA sensor, cGAS binds to double-stranded DNA (dsDNA) and activates catalysis of 2’3’-cGAMP, a cyclic dinucleotide that further functions to activate stimulator of interferon genes (STING). STING then activates transcription of type I interferons such as interferon-beta (IFN-β). Classically, these interferons can be

secreted to alert both innate and adaptive immune cells to host cells that are infected by dsDNA viruses. cGAS can also be activated by nonspecific sequences including self-DNA from cancer cells. For example, when one or a few chromosomes are erroneously separated from bulk DNA during mitosis, a separate but fragile nuclear envelope forms around the isolated chromosome to create a structure known as a ‘micronucleus’. Such micronuclei are prone to nuclear membrane rupture, exposing the DNA to the cytoplasm (Bartsch et al., 2017; Harding et al., 2017a; Mackenzie et al., 2017a), eliciting cGAS-STING signaling and type I interferon signaling. These interferons can upregulate immune checkpoint molecules such as PD-L1 on cancer cells, providing a rationale for combining MTAs with ICIs (Garcia-Diaz et al., 2017). In addition, both 2’3’-cGAMP and type I interferons recruit and activate M1 macrophages and Batf3 dendritic cells, which can prime effector T-cells for antitumoral cytoxicity (Corrales et al., 2017; Müller et al., 2018, p. 1; Ohkuri et al., 2017). Recently, 2’3’-cGAMP has been reported to be transferred between cells and can modulate and potentially recruit immune cells such as stromal tumor-infiltrating lymphocytes (sTILs), a feature of immune activation that is associated with improved survival in TNBC patients (Carozza et al., 2020; Cordova et al., 2020; Gao et al., 2020).

Here, we investigate a mechanism by which paclitaxel and other MTAs can potentiate ICIs when used in combination and identify a predictive biomarker for these combination therapies in TNBC patients. Paclitaxel and other MTAs trigger a pro-inflammatory immune response via micronuclei generated from aberrant mitosis. Ruptured micronuclei permit cGAS entry, 2’3’-cGAMP production, STING signaling and production of type I interferons in most TNBCs expressing cGAS. Elevated baseline

cGAS expression correlates with treatment response in patients receiving MTAs in combination with ICIs. These findings suggest that cGAS expression can predict patient populations that will have optimal benefit from a combination MTAs and ICIs.

2.3 Results

2.31 Paclitaxel increased tumor-infiltrating lymphocytes in some but not all clinical patient samples

In TNBC, stromal tumor-infiltrating lymphocytes (sTILs) are associated with immune activity and better survival outcomes (Gao et al., 2020). To determine if paclitaxel can be associated with an immune response, we assessed sTILs in six primary breast tumors from treatment-naïve patients with TNBC before paclitaxel and at two time points following initiation of therapy (Figure 1A, B). Day 2 samples were collected 20 hours after the first dose of paclitaxel, when the first wave of mitotic defects can be observed. Day 15 samples were collected 20 hours after the third dose of paclitaxel, which is anticipated to be sufficient for accumulating post-mitotic cellular defects, such as micronuclei. We measured lymphocyte infiltration at each time point. Histologically, there was robust recruitment of sTILs at Day 15 but not at Day 2 in two patient samples, P102 and P103. Similarly, patient sample P113 had increases in sTILs at Day 15, though these increases were modest (Figure 1B). In each case, measurement of TILs from separate cores at the time of biopsy were identical, suggesting little to no variation due to regional tumor sampling (Supplemental Table 1). These data suggest that paclitaxel can induce the recruitment of TILs in some, but not other, TNBC samples,

consistent with other investigations (Demaria et al., 2001). We therefore sought to understand and identify the specific predictors of sTIL recruitment.

Paclitaxel is known to induce mitotic aberrations, which could generate micronuclei. Rupture of micronuclei activates innate immune signaling in certain contexts (Harding et al., 2017a; Mackenzie et al., 2017a). To determine if we can observe increased micronuclei after paclitaxel in human TNBC, we quantified interphase DAPI fragments representing micronuclei, excluding mitotic cells identified by condensed chromosomes and NUMA localization at spindle poles (Figure S1A, Figure 1C). Indeed, the fraction of cells with micronuclei increased at Day 15 compared with the percentage at baseline in three of four samples (Figure S1B), matching the samples that recruited TILs (Figure 1B). We observed a non-significant positive trend of increased micronuclei being associated with increased sTILs in two patient samples (Figure S1C).

Previous studies suggest that cGAS-positive micronuclei are associated with activation of downstream STING pathway. Importantly, activation of the STING pathway with agonists results in sTIL recruitment and has may potentiate immune checkpoint blockade therapies (A. Li et al., 2019). Therefore, we evaluated cGAS recruitment to micronuclei in histological samples from patients on Day 15 (Figure 1C, S1D). We observed a trend towards increased cGAS-positive micronuclei with increased sTILs (Figure S1E), although P118 did not have a sTIL increase despite having cGAS-positive micronuclei, suggesting other modifying factors. Overall, quantitative cGAS expression positively correlated with sTIL recruitment (Figure 1E). These results suggested a signaling pathway that could operate in some tumors to allow microtubule targeting therapy to elicit immune response. Based on these observations in clinical samples, we

hypothesized that cGAS expression and micronucleation may play a role in downstream STING activation, which may potentially promote an immune response. Therefore, we set out to interrogate this hypothesis mechanistically.

2.32 Paclitaxel induces cGAS-positive micronuclei following mitosis on multipolar spindles.

To determine the mechanism by which paclitaxel forms micronuclei, we challenged fluorescently tagged RFP-H2B, GFP-Tubulin MDA-MB-231 TNBC cells with paclitaxel and tracked them through mitosis into the subsequent interphase by live-cell imaging (Figure 2A, Supplemental Videos 1, 2). Cells exposed to clinically relevant doses of paclitaxel are known to form multipolar spindles and divide, sometimes after a delayed mitosis (Zasadil et al., 2014b). In accord with this, we found that most cells complete aberrant cell division on multipolar spindles (Figure 2B). In the subsequent interphase, cells became multinucleated and contained a subset of irregularly sized nuclear fragments, some resembling micronuclei. These findings suggest that mitotic transit on multipolar spindles is sufficient to generate cells with nuclear fragments.

We extended these findings to fixed cell analysis of wild type MDA-MB-231 cells exposed to clinically relevant, 10 nM paclitaxel. Multinucleated cells were frequently observed (68% +/- 6.4) 48 hours after paclitaxel challenge, when compared with controls (1.1% +/- 0.6) (Figure 2C, D). Moreover, a proportion of multinucleated cells had nuclear fragments that stained brightly with cGAS, which far exceeded the untreated controls (Figure 2D). We reasoned that most micronuclei appeared sooner in

cell culture compared to patient samples due to much faster growth rates of cells in culture (Zasadil et al., 2014b).

To determine if this effect is general, we quantified the frequency of cGAS-positive multinucleated cells in cell lines corresponding to distinct molecular subtypes of TNBCs (Figure 2E). Molecular subtypes were determined from previous studies (Lehmann et al., 2011, 2016). Indeed, paclitaxel induced cGAS-positive micronuclei in diverse cell lines, though, importantly, it was absent in MDA-MB-468 and MDA-MB-453 cells, two cell lines that do not express detectable cGAS by immunoblot (Fig. S2C).

Because cGAS recruitment was commonly found on smaller nuclear fragments, we reasoned that fragments with only a small number of chromosomes are most prone to exposure to this nuclear DNA sensor. To test this, we co-stained cells with CREST antibody, which labels centromeres, to mark individual chromosomes (Figure 2F). In untreated cells, we sometimes found cGAS recruitment, most prominently to fragments that lacked CREST foci, suggesting acentric chromosome fragments. However, after treatment, most cGAS-positive micronuclei contained one or two CREST foci, consistent with paclitaxel inducing whole chromosome missegregation. By contrast, we did not find a significant number of cGAS-positive fragments in micronuclei with three or more CREST foci, suggesting that these larger nuclear fragments are less likely to be exposed to cytosolic sensors. This might be due to less lamin B1 being incorporated in smaller micronuclei compared to micronuclei as seen in other studies or faster timing of rupture compared to larger micronuclei (Hatch et al., 2013; Kneissig et al., 2019; S. Liu et al., 2018).

To further characterize the nuclear fragments that contribute to increased cGAS positivity, we categorized each nuclear morphology observed after paclitaxel treatment of TNBC cell lines, resulting in eight distinct phenotypes (Figure S2A). Next, we quantified the nuclear morphologies after paclitaxel exposure in a range of TNBC cell lines with different levels of cGAS expression (Figure S2B-C). Cells with high (MDA-MB-231), intermediate (MDA-MB-436, BT-549, HCC-1806) and low/no cGAS expression (MDA-MB-468, MDA-MB-453) were examined. Cell lines exhibited similar patterns of nuclear phenotypes, with the majority of cells exhibiting a single primary nucleus prior to paclitaxel and multinucleation afterwards. In cells expressing cGAS, the increase in multinucleation was accompanied by an increase in cGAS-positive micronuclei (Figure S2C, D). These results suggest that the formation of cGAS-positive micronuclei is a general effect elicited by treatment with paclitaxel. Similarly, nanomolar concentrations of additional MTAs, vinorelbine and eribulin, also induced cGAS-positive micronucleation at a similar magnitude as that induced by paclitaxel in MDA-MB-231 cells (Figure S2E, F). Given the strikingly similar nuclear phenotype, these results support the conclusion that nanomolar concentrations of MTAs can generally yield micronuclei, and recruit cGAS if it is expressed.

Although these findings suggested a clinically important mechanism of immune activation, we considered alternative explanations. We found cGAS puncta are not simply a consequence of generally increased expression, as judged by unchanged cGAS levels after 4-days exposure to paclitaxel (Figure S3A). We ruled out nonspecific staining with two additional antibodies targeting distinct regions of cGAS, which also stained micronuclei (Figure S3B). Further, we generated biallelic knockout mutants of

cGAS in MDA-MB-231 cells using CRISPR-Cas9 and validated clones by immunoblot, TA cloning and 2’3’-cGAMP production after radiation-induced stimulation (Figures S3C-E). As expected, cGAS-positive puncta were abrogated in cGAS-null MDA-MB-231 cells before or after paclitaxel (Figure S3F). These results provide strong evidence that the observed signals are specific to cGAS. To ensure that the mechanism is consistent with previous studies, we assessed the integrity of the nuclear envelope of micronuclei for rupture, which is known to precede cGAS recruitment to micronuclei in other contexts (Bartsch et al., 2017; Harding et al., 2017a; Mackenzie et al., 2017a). As expected, paclitaxel-induced cGAS-positive micronuclei have reduced levels of nuclear envelope and intranuclear proteins (Figure S3G, H) (S. Liu et al., 2018). Taken together, our findings demonstrate that MTA treatment in TNBC cell lines causes multipolar cell divisions, producing daughter cells with micronuclei containing defective nuclear membranes, which can recruit cGAS.

2.33 Paclitaxel activates cGAS signaling in triple-negative breast cancer cell lines.

cGAS preferentially binds to double stranded DNA (dsDNA) to activate synthesis of STING-substrate, 2’3’-cGAMP (L. Sun et al., 2013b; J. Wu et al., 2013). To interrogate the pathway, we evaluated if the appearance of cGAS-positive micronuclei corresponded with activation of cGAS activity after paclitaxel exposure. To test this, wild type and cGAS knockout MDA-MB-231 cells were exposed to 10 nM paclitaxel over four days and assessed for 2’3’-cGAMP levels. Consistent with activation, paclitaxel increased 2’3’-cGAMP, which peaked after two days in wild type cells, but remained undetectable in cGAS-knockout cells, as expected (Figure 3A). Further, STING

activation, as measured by phosphorylation of downstream proteins TBK1, IRF3, p65, and STAT1, increased after paclitaxel exposure in wild type MDA-MB-231 cells (Figure 3B, S4A). Importantly, paclitaxel failed to induce STING activation after cGAS knockout in MDA-MB-231 cells and also cGAS knockdown in another TNBC cell line, MDA-MB-436, suggesting that STING is specifically activated by upstream cGAS and that this effect is not cell line dependent (Figure 3C, D). In addition, sh-RNA mediated cGAS and STING knockdown also showed decreased upregulation of interferon-stimulated genes after paclitaxel in MDA-MB-231 cells (Figure S4B, C). Increases in 2'3'-cGAMP synthesis also follow in the accumulation of cGAS-positive micronuclei, rather than total micronuclei, which does not increase after Day 1 (see Figure 2D). These results demonstrate that paclitaxel activates cGAS-STING signaling in TNBC cells, and this is associated with the appearance of cGAS-positive micronuclei.

Although MDA-MB-231 cells express abundant cGAS, they are inconsistent in their ability to synthesize type I interferons (Bakhoum et al., 2018; Lohard et al., 2020). In our study, we did not detect IFN-β secretion by MDA-MB-231 after paclitaxel despite activation of the cGAS-STING pathway (Figure 3E). By contrast, MDA-MB-436 cells have an intact type I interferon pathway (Feng et al., 2020; Parkes et al., 2017; Z. Wang, Sun, et al., 2019). Therefore, we also measured IFN-β protein in MDA-MB-436 cells, which readily form cGAS-positive multinucleated cells after paclitaxel (Figure S2D). After five days of 10 nM paclitaxel, we detected increased IFN-β protein in the supernatant (Figure 3F). Importantly, this effect was dependent on cGAS as we observed an attenuation of IFN-β production with siRNA-mediated cGAS knockdown.

Collectively, our data show that paclitaxel activates the STING pathway, and induces synthesis of 2'3'-cGAMP and IFN-β, in a cGAS-dependent manner.

2.34 Paclitaxel induces cGAS-dependent soluble factors that induce M1 polarization.

Following cGAS activation in the setting of self-DNA exposure, cells can initiate a signaling cascade that results in the production of 2'3'-cGAMP, inflammatory cytokines, chemokines and IFN-β (L. Sun et al., 2013b). These soluble factors are secreted and maintained through autocrine and paracrine loops (Hopfner & Hornung, 2020; Lohard et al., 2020). Among immune cells, macrophages have functional plasticity and can be reprogrammed to either an M1 or M2 phenotype in response to environmental cues (S. X. Liu et al., 2020). Macrophage polarization is influenced by IRF/STAT signaling pathways; exposure to lipopolysaccharides and interferon-gamma (IFN-γ) can polarize macrophages to a pro-inflammatory M1 phenotype, resulting in antitumoral activity (Genard et al., 2017). Conversely, exposure to IL-4 and IL-13 can polarize these cells to an anti-inflammatory M2 phenotype in favor of immune suppression, resulting in tumor growth.

We began our investigation with THP-1 derived macrophages as a model because of their accessibility and high reproducibility compared to primary macrophages. Following well-established protocols (Chang, 2009; Genin et al., 2015), THP-1 monocytes were differentiated into M0 macrophages using phorbol myristate acetate (PMA) . M0 macrophages were then incubated with paclitaxel-conditioned media from MDA-MB-231 cells. After incubation, macrophage polarization was assessed by RT-qPCR for M1 and M2 markers (Figure S5A). We first assessed the ability of paclitaxel to

directly polarize macrophages to an M1 phenotype given previous reports that paclitaxel has this effect in a mouse breast cancer model (Wanderley et al., 2018). Importantly, direct exposure of macrophages to 10 nM paclitaxel for four days only minimally upregulated pro-inflammatory chemokines associated with M1 polarization (Figure S5B). By contrast, paclitaxel-conditioned media from MDA-MB-231 cells induced M1 polarization, which is attenuated by cGAS knockout in MDA-MB-231 cells (Figure S5C, D). This finding indicates the release of immunostimulatory factors into conditioned media after paclitaxel is dependent on cGAS. As a complementary approach, we performed 2D co-culture using transwell plates of wild type or cGAS knockout MDA-MB-231 cells with THP-1 in the presence and absence of paclitaxel (Figure S5E). We observed increased M1 polarization of THP-1 cells co-cultured with MDA-MB-231 cells following paclitaxel treatment that was downregulated after cGAS knockout (Figure S5F, G). Importantly, co-culture and incubation with conditioned media polarize THP-1 macrophages to an M1 phenotype to a greater extent than direct treatment with paclitaxel. These data suggest that paclitaxel induces MDA-MB-231 cells to secrete soluble factors, in a cGAS-dependent manner, that exhibit paracrine effects on THP-1 macrophages to elicit an M1 phenotype.

Since THP-1 cells are immortalized and derived from a patient with acute monocytic leukemia, they have differences in gene expression, protein secretion and cellular morphology compared to primary blood-derived human macrophages at baseline and after polarization (Tedesco et al., 2018). To more closely mimic normal human physiology, we incubated M0 macrophages from blood-derived human monocytes in conditioned media from MDA-MB-231 previously treated with and without paclitaxel to

assess for polarization. MDA-MB-231 cells are known to polarize blood-derived human monocytes to an M2 macrophage phenotype with a striking morphological changes with an elongated shape (Hollmén et al., 2015). Therefore, we took advantage of this known phenotype and measured for a known M1 marker, CD80, and the greatest length of the cell after exposure to conditioned media.

Three healthy volunteers contributed monocytes, which were then differentiated into M0 monocytes and separately incubated with conditioned media from MDA-MB-231 parental and cGAS knockout cell lines. Conditioned media were either obtained from MDA-MB-231 previously untreated or treated with two days of 10nM paclitaxel before washing off and replacing with fresh media (Figure 4A). We also polarized M0 macrophages to an M1 phenotype to assess the validity of our CD80 marker (Figure S5H). For all conditions, following three days incubation with conditioned media, blood-derived human macrophages were assessed for M1 polarization. We quantified immunofluorescence images for maximum length of macrophage on bright field images and total CD80 immunofluorescence (Figure 4B). In accordance with previous studies, conditioned media from MDA-MB-231 cells polarized macrophages to a pro-tumoral M2 phenotype, characterized by an elongated shape and decreased CD80 expression (Figure 4C, D). By contrast, conditioned media from paclitaxel-treated MDA-MB-231 maintained round morphology and increased CD80 expression. Importantly, these levels were different from baseline M0 macrophages, suggesting paclitaxel-treated MDA-MB-231 can re-educate M2 macrophages to an M1 phenotype.

As expected, we found that conditioned media from paclitaxel-treated cGAS knockout MDA-MB-231 did not affect polarization of macrophages, illustrating that this

signaling pathway is needed for this effect to occur (Figure 4C, D). CD80 is not known to be affected by cGAS, so we were surprised to see increased expression in the cGAS knockout. However, we do not think this expression is indicative of M1 polarization because the length of cGAS KO cells did not increase compared to parental MDA-MB-231. Potentially, CD80 is regulated by cGAS through some unknown mechanism. Since cGAS-STING activation results in production of 2'3'-cGAMP and IFN-β in some cell lines, we tested if these compounds could induce M1 polarization when exogenously added to conditioned media from cGAS knockout MDA-MB-231 cells. Previous studies suggest that both 2'3'-cGAMP and IFN-β have the capacity to polarize macrophages to an M1 phenotype (Cordova et al., 2020; Downey et al., 2014, 2014; Müller et al., 2018). In concordance, our data suggest that both 2'3'-cGAMP and IFN-β can partly rescue M1 polarization in MDA-MB-231 cGAS knockout cells. Since MDA-MB-231 do not secrete noticeable IFN-β (Figure 3E), we suspect that endogenously produced 2'3'-cGAMP may at least partly be responsible for polarizing macrophages to an M1 phenotype as a result of paclitaxel exposure.

2.35 Microtubule-targeting agents increase surface PD-L1 expression in TNBC.

PD-L1 is an immune checkpoint marker whose expression on tumors can prevent T-cell activation and its expression can be upregulated by type I interferons (Bazhin et al., 2018, p. 1; Garcia-Diaz et al., 2017, p. 1; Juneja et al., 2017, p. 1; Z. Wang, Sun, et al., 2019, p. 1). PD-L1 blockade not only allows activated T-cells to kill tumor cells expressing PD-L1 but may also promote T-cell priming by dendritic cells, which is important for generating an adaptive immune response (Curiel et al., 2003).

Interestingly, T-cell priming may depend on cGAS expression (H. Wang et al., 2017). Therefore, cGAS activation is a possible intermediary in the efficacy of ICIs and the need for them (Bazhin et al., 2018; Garcia-Diaz et al., 2017; Liang et al., 2018; H. Wang et al., 2017; Yum et al., 2020). PD-L1 mRNA expression increases after 20 hours of 30 nM paclitaxel in murine 4T1 and CT26 cancer cell lines (J. Zhang et al., 2018); however, this report did not examine protein expression and surface localization. Therefore, we tested whether these findings extend to human cancer cell lines with prolonged paclitaxel exposure, and whether cGAS was necessary for this effect. For this purpose, we selected two cell lines: MDA-MB-436 cells which have a robust type I interferon response, and MDA-MB-231 cells which do not. As expected, nanomolar paclitaxel upregulated total PD-L1 expression in MDA-MB-436 cells and this effect was dependent on cGAS, as siRNA-mediated depletion of cGAS blocked this effect (Figure 5A). Since only surface rather than intracellular PD-L1 binds to immune cell receptors, we also assessed surface PD-L1 expression on MDA-MB-436 cells (Figure 5B). As expected, paclitaxel significantly upregulated surface PD-L1 in a cGAS-dependent manner, recapitulating our immunoblot results (Figure 5C). By contrast, MDA-MB-231 cells did not exhibit increased total or surface PD-L1 after paclitaxel (Figure S6A-C), due to a lackluster type I interferon response and/or high baseline PD-L1 expression. Interestingly, other MTAs such as vinorelbine and eribulin increased PD-L1 to a greater degree than paclitaxel in MDA-MB-436 cells (Figure 5D). Our results illustrate upregulation of PD-L1 by MTAs in a cGAS-dependent manner, particularly in cell lines with intact IFN-β signaling. These findings are consistent with other studies that have

associated exposure of cells to type I interferons including IFN-β with tumor cell PD-L1 upregulation (Bazhin et al., 2018, p. 1; Garcia-Diaz et al., 2017, p. 1; Liang et al., 2018).

2.36 Some triple negative breast cancer patients with high levels of tumor cGAS have durable responses on combination therapy.

While multiple cancer types may express and activate cGAS, these effects vary greatly (E. K. Curran et al., 2014; Deng et al., 2014; Schadt et al., 2019; Wang-Bishop et al., 2020; Woo et al., 2014). The average cGAS is highest in the hormone-receptor negative subtypes and reaches the highest levels in a small fraction of TNBC tumors (Figure S7A). We reasoned that if the cGAS-STING pathway mediates immune activation after paclitaxel, patients with higher cGAS expression could mount the most robust immune response after treatment. Consistent with this idea, relapse-free survival (RFS) after adjuvant taxane-based chemotherapy was superior with high cGAS expression, though no such effect was found in the absence of chemotherapy (Figure S7B). Interestingly, in hormone receptor-positive breast cancers, there was also a significant positive correlation between cGAS and RFS (Figure S7C). STING is activated by 2’3’-cGAMP, the product of cGAS activity. Unlike cGAS, STING exhibited similar distribution across all breast cancer subtypes (Figure S7D) and did not correlate with RFS in chemotherapy-treated patients (Figure S7E-F). These findings support the idea that cGAS expression, but not STING, varies among TNBC subtypes and could mediate therapeutic response.

Our study so far suggests that paclitaxel can directly activate a cGAS-mediated immune response. To test if cGAS expression could predict response to combined MTAs and ICIs, we obtained pre-treatment FFPE slides from ten metastatic TNBC

patients who were subsequently treated with an ICI with or without MTAs. Quantitative immunofluorescence illustrated variable cGAS levels in tumor specimens (Figures 6A, B). Staining specificity was validated with paraffin-embedded cell pellets from MDA-MB-231 cells which express cGAS and HEK-293T cells, which do not (Figure 6A, C). We found highest cGAS expression in P109, P811, P888, and P169 (Figure 6B). Among these, three of six patients had progression free survival exceeding 20 months after initiation of therapy, a durable response that greatly exceeds the average for triple-negative breast cancer. By contrast, patients with tumors expressing lower levels of cGAS had disease progression several months after initiation of therapy (Figure 6D). To evaluate this quantitatively, we evaluated Spearman correlation of cGAS intensity and progression-free survival, finding these statistically correlated (Figure 6E). Interestingly, P811 remained an outlier with high expression of cGAS and rapid progression, suggesting that additional variables are at play, such as the use of a PD-L1 inhibitor with this subject versus a PD-1 inhibitor with the others. In any case, these data strongly support the idea that basal cGAS expression can help identify patients most likely to benefit from combined MTAs with ICI.

Based on our mechanistic findings and clinical validation data in patient tumor specimens, MTAs may activate an immune response in cells and tumors expressing cGAS. Our results suggest that cGAS expression could help select patients for combined MTAs and ICIs with a strong underlying mechanistic rationale.

2.4 Discussion

In this study, we found that paclitaxel and other MTAs activate the cGAS-STING pathway and then explored the possibility of cGAS as a potential biomarker for combined MTAs and ICIs. We employed clinically relevant levels of paclitaxel in cell culture to assess micronuclei formation and subsequent cGAS recruitment and activation in TNBCs. At these concentrations, human cells complete mitosis on multipolar spindles (Figure 2A-B, Supplemental Videos 1,2), an effect that is markedly distinct from the mitotic arrest elicited by exposure to micromolar concentrations of paclitaxel (Gascoigne & Taylor, 2009; Zasadil et al., 2014b).

Tumor cells act as a sink that concentrates intracellular levels of paclitaxel 67- to over 1000-fold relative to the extracellular concentration (Derry et al., 1995; Jordan et al., 1993, 1996; Zasadil et al., 2014b). Intratumoral paclitaxel levels accumulate to only 1-9 μM in human breast cancer (Zasadil et al., 2014b). Therefore, cell culture paclitaxel concentrations between 5 nM and 50 nM, depending on cell type, best recapitulate physiologic intratumoral levels, contrasting with a number of prior preclinical studies that use 10- to 100-times higher concentrations. Therefore, we expect our mechanistic findings in cell culture using these pharmacologically relevant concentrations reflect the effects of paclitaxel in humans, and further use clinical samples as a touchstone to verify concordance.

Previous work discovered that recruitment of cGAS to mitotic chromosomes modifies the timing of slippage and cell death in cells exposed to 500 nM paclitaxel (Zierhut et al., 2019b). This resultant mitotic arrest permits cell death during mitosis in a cGAS-dependent manner. However, at low-nanomolar paclitaxel, we did not observe appreciable differences in cell death between wild type and cGAS knockout MDA-MB-

231 cells, suggesting that the cGAS effect on mitotic timing does not play a major role in triple-negative breast cancer at pharmacologically achieved concentrations. Further, we do not anticipate a major immunological effect of STING-based signaling during mitosis, given that this cell-cycle phase is short lived and during which chromatin is condensed and transcriptionally silent. For these reasons, we conclude that the crucial cGAS signaling events elicited by paclitaxel are post-mitotic.

Given that division on multipolar spindles directly results in multinucleated cells with micronuclei, we and others hypothesized that cGAS activation resulting from ruptured micronuclei is a major mechanism for paclitaxel-mediated immune activation (Mitchison et al., 2017b). cGAS activates IFN-β synthesis, which is associated with increased TIL recruitment and better patient outcomes (Doherty et al., 2017). The product of cGAS activation, 2’3’-cGAMP, has also been found to modulate immune cells in the tumor microenvironment through tumor-host interactions that include NK cells, macrophages, CD4+ T-cells and dendritic cells (Corrales et al., 2015; Marcus et al., 2018; Ohkuri et al., 2018). We make the distinction between acute and chronic STING activation as the latter can result in immunosuppression. We hypothesize paclitaxel treatment in the short term to result in acute rather than chronic activation of STING, which may result in antitumoral immunity through interferon-mediated pathways. In the context of chronic STING activation, both cancer and host immune cells are hypothesized to upregulate an unfolded protein response through autophagy-ER stress programs, which can drive tumorigenesis and immunosuppression (Bakhoum et al., 2018; Kwon & Bakhoum, 2020).

Antitumoral immunity induced cGAS-STING activation can be further boosted by ICIs in multiple cancer types (A. Li et al., 2019; H. Wang et al., 2017; Yum et al., 2019). Compared with local delivery of radiation or injected STING agonists, paclitaxel has the advantage of systemic administration, allowing it to reach cancer cells at virtually any site, including all metastatic—and micrometastatic—sites of disease. Therefore, the ability of paclitaxel to activate cGAS is highly suitable for treating or preventing metastatic breast cancer in tumors with high cGAS expression. Interestingly, other genotoxic agents such as PARP inhibitors and anthracyclines have been investigated to activate the cGAS-STING pathway and may potentially similarly synergize with ICIs to induce antitumoral immunity (Pantelidou et al., 2019; Z. Wang, Chen, et al., 2019a). These agents also can cause DNA damage and replication stress, which may drive a robust cGAS-STING activation, resulting in greater tumor immunity.

Here, we focused solely on the cGAS DNA sensor. While there are other cytosolic DNA sensors, cGAS is the only indispensable candidate capable of mediating an IFN-β response to self-DNA (Gray et al., 2016; X.-D. Li et al., 2013; Vance, 2016). Other DNA sensors, including AIM2, DAI, IFI16, and DDX41 are unlikely to contribute to paclitaxel-induced IFN-β synthesis. AIM2 is a dsDNA sensor that can indirectly activate type I interferons but is not found in breast cancer cell lines and requires co-stimulation with IFN-γ, which is not known to be upregulated by paclitaxel (He et al., 2018). DAI/ZBP1 and IFI16 can directly activate STING but are expressed at low levels in breast cancer cell lines and tumors (Fujiuchi et al., 2004; Gu et al., 2009). On the contrary, DDX41 is a DNA sensor expressed in many cancers and can activate STING in vitro; however, such activation through this sensor is questionable *in vivo* (E. Curran et al., 2017, p. 41).

LRRFIP1 activates IRF3 signaling through □-catenin phosphorylation, and while the protein is expressed in breast cancers, this pathway appears to induce very little IFN-β synthesis, suggesting that it is only contributes little, if at all, to paclitaxel-mediated IFN-β signaling (P. Yang et al., 2010). While these prior studies cannot rule out minor roles of other sensors, our cGAS knockout and knockdown data strongly support the idea that cGAS is the major DNA sensor involved in paclitaxel-mediated effects on IFN-β.

We recognize that cGAS expression alone may not be sufficient to predict immunotherapy response for TNBC after paclitaxel. Immunotherapy response is influenced by many factors that regulate the immune system such as the presence of detectable neoantigens, and its suppression by the presence of PD-1/PD-L1, regulatory T cells and myeloid-derived suppressor cells (MSDC) among others (Vicari et al., 2009; M. Wang et al., 2017). Paclitaxel may modulate some of these other factors, including inhibiting MDSC and regulatory T-cell populations while increasing PD-1/PD-L1 expression (Peng et al., 2015; Sevko et al., 2013). While we did not investigate the effects of PD-1/PD-L1 blockade on other immune cells, PD-1 blockade on tumor-associated M2 macrophages can directly reactivate phagocytosis and tumor immunity and may contribute to increased immunity rather than just reactivation of cytotoxic T-cells (Gordon et al., 2017).

In some instances, paclitaxel may induce PD-L1 expression through interferons as a feedback system to prevent the immune system from mounting antitumoral immune response, which may be overcome with immune checkpoint inhibition. By contrast, PD-L1 can also be constitutively expressed in some cancers, which may indicate an already immunosuppressed environment that may not benefit from checkpoint inhibitors alone

(Kythreotou et al., 2018, p. 1). Therefore, as a biomarker, cGAS may be more advantageous than PD-L1 because it may be difficult to uncouple inducible versus chronic PD-L1 expression from a patient pre-treatment biopsy (Hao et al., 2019).

While we focused on cGAS activation in TNBC cells, paclitaxel might also directly activate cGAS/STING in tumor-extrinsic host cells. For example, paclitaxel has contributes to reprograming M2 macrophages to an M1 phenotype (Wanderley et al., 2018). In addition, there different components of the cGAS/STING pathway can polarize macrophages to an M1 phenotype. For example, 2'3'-cGAMP secreted by tumors may polarize M2 macrophages to an M1 phenotype (Downey et al., 2014; Müller et al., 2018, p. 1). Thus, we recognize that paclitaxel could modulate immunity in myriad ways, in addition to activating cGAS, complicating its mechanistic interactions with immunotherapy. Further, TNBCs are a highly heterogeneous group of cancers and the mechanism delineated here may be limited to cancers with cGAS expression and other characteristics that promote potential paclitaxel-induced immunostimulatory factors.

Our study systematically demonstrates that paclitaxel activates cGAS-STING via micronuclei rupture. Our data show that, in a fraction of patients, paclitaxel increases micronuclei and TILs. Larger confirmatory studies are required to substantiate these observations. Since nanomolar paclitaxel can polarize macrophages toward an M1 phenotype, this interaction may serve as a key link in activating an adaptive immune response. Further, studies have shown that 2'3'-cGAMP itself can recruit an antitumor response by cross-priming and recruiting CD8+ T-cells, and we find that paclitaxel also induces synthesis of this substrate (T. Li et al., 2016). Future studies with larger cohorts will be necessary to determine if cGAS expression can reliably predict efficacy for

combined MTAs and ICIs. Nevertheless, our results can be valuable in interpreting past clinical trials and designing new clinical trials. For example, IMpassion 131 found no improvement in progression free survival benefit with the addition of atezolizumab to paclitaxel in the PD-L1 positive population (Miles et al., 2017). This finding contrasts with the IMpassion 130 results with nab-paclitaxel, yet this difference could potentially be explained if there were a difference in the proportion of subjects with high-cGAS tumors.

In conclusion, paclitaxel and other MTAs, in addition to eliciting cytotoxic death due to multipolar mitosis, also generate micronuclei, associated with cGAS-STING activation in surviving post-mitotic cells. This is associated with polarization of macrophages to an M1 phenotype and may contribute to lymphocyte recruitment found in some TNBC samples after paclitaxel treatment and better survival for patients on combination therapy. Further studies are needed to confirm our findings *in vivo*. However, given the current lack of effective biomarkers in clinical studies, our findings demonstrate the potential value of cGAS expression in predicting response to standard-of-care and experimental treatments with combined MTAs and ICIs in TNBC.

2.5 Materials and Methods:

Cell lines and culture conditions

All cell lines were either directly purchased from ATCC/NCI or were gifted from other research groups. Cell lines gifted from other research groups were validated using polymorphic short tandem repeat loci throughout 2019 through the Small Molecules Screening Facility at UW-Madison. Mycoplasma contamination was regularly monitored using the R&D Systems Mycoprobe Mycoplasma Detection Kit. All cell lines were maintained at 37°C and 5% CO2 in a humidified incubator in growth media supplemented with 10% fetal bovine serum, 100 units/mL penicillin-streptomycin and 1X plasmocin prophylactic. MDA-MB-231, BT-549 and MDA-MB-468 were obtained from NCI. MDA-MB-436 cells were obtained from ATCC. MDA-MB-453, Hs578T and HCC1806 were gifts from Ruth O'Regan. THP-1 was a gift from David Beebe. MDA-MB-231 stably expressing RFP-H2B and GFP-Tubulin was a gift from Beth Weaver. All triple negative breast cancer cell lines were propagated in Dulbecco's Modified Eagle's Medium (DMEM) supplemented with 4.0 mM L-Glutamine, 4500 mg/L glucose and 1X plasmocin prophylactic. THP-1 was propagated in RPMI 1640 medium with 2 mM L-glutamine, 1.5 g/L sodium bicarbonate, 4.5 g/L glucose, 10 mM HEPES, 1.0 mM sodium pyruvate, 1X glutamax and 1X plasmocin prophylactic.

Reagents and antibodies

Reagents used in this study were Paclitaxel/Taxol (Tocris 1097), Phorbol 12-myristate 13-acetate/PMA (Sigma P8139), digitonin (Sigma D141), Cyclic [G(2',5')pA(3',5')p]/2'3'-cGAMP (Invitrogen tlrl-nacga23) and recombinant human IFN-γ (BD Biosciences

554616). The following primary antibodies were obtained from Cell Signaling Technologies: cGAS D1D3G Rabbit mAb #15102 (immunoblot 1:1000 dilution, immunofluorescence 1:200 dilution); STING D2P2F Rabbit mAb # 13647 (immunoblot 1:1000 dilution, immunofluorescence 1:200 dilution); Phospho-IRF-3 (Ser396) (4D4G) Rabbit mAb #4947 (immunoblot 1:1000 dilution); Phospho-Stat1 (Tyr701) (58D6) Rabbit mAb #9167 (immunoblot 1:1000 dilution), Pan-keratin (C11) Mouse mAB #4545 (IHC 1:100 dilution), PD-L1 Extracellular Domain Specific D8T4X Rabbit mAb Alexa Fluore 647 (flow cytometry 1:100). Other primary antibodies used were α tubulin, clone YL1/2 rat monoclonal IgG2a from Millipore Sigma MAB1864 (immunofluorescence 1:2500 dilution); β actin ab6276 from Abcam (immunoblot 1:1000 dilution); human GAPDH 4650S from Developmental Studies Hybridoma Bank (immunoblot 1:1000).

Infrared 800CW and 680LT secondary antibodies were used at 1:10,000 dilution and were obtained from LI-COR. Rabbit and mouse HRP antibodies were used at 1:10,000 dilution and were obtained from Jackson ImmunoResearch. Detection was performed either on an Odyssey infrared imaging system (LI-COR) or on a film developer. For immunofluorescence microscopy, Alexa-488 , Alexa-594 and Alexa-647 coupled secondary antibodies from Jackson ImmunoResearch were used.

Clinical samples

Clinical data and patient samples were de-identified and approved for use by the University of Wisconsin-Madison Institutional Review Board. All patients signed an informed consent for voluntary participation in trials or sample collection. Furthermore,

all authors had completed training for The Health Insurance Portability and Accountability Act of 1996 and Research Ethics and Compliance.

Patient samples from Figure 1 were obtained from clinical trial UW16106 conducted at University of Wisconsin-Madison. Paclitaxel was initiated as standard infusion on days 1, 8, 15 of a 21-day cycle. Patients were continued on paclitaxel 80mg/m^2 for cycles 2-4 prior to surgery. Biopsies were obtained at diagnostic baseline and 20 hours after infusions on days 1 and 15 and preserved in formalin. Samples were then obtained de-identified by study authors for H&E and IHC analysis.

Patient samples from Figure 5 were obtained from clinical trial UW15068 conducted at University of Wisconsin-Madison. Patients were selected based on history of immune checkpoint blockade during the course of their disease with or without either nab-paclitaxel or eribulin.

Quantification criteria for tumor-infiltrating lymphocytes

Tumor-infiltrating lymphocytes were quantified by based on the International TILs Working Group (Salgado et al., 2015). Briefly, TILs are reported for the stromal compartment, where the numerator and denominator denote areas and not individual cells. The denominator represents the area of stroma and numerator represent the percentage of the stromal area occupied by lymphocytes. TILs are evaluated within the borders of the invasive tumor and are excluded outside of the tumor border and around DCIS and normal lobules. Tumor zones with crush artifacts, necrosis, and regressive

hyalinization as well as in the previous core biopsy site are also excluded from the analysis. All mononuclear host immune cells (including lymphocytes and plasma cells) are scored with exclusion of polymorphonuclear leukocytes. At least one section (4–5 μm, magnification ×200–400) per patient is assessed. Biopsies are not preferred but can be used if full sections are not available as in this study. These criteria are designed for TILs assessment in the pre-therapeutic neoadjuvant setting but we have also used them in the neoadjuvant setting since no other criteria exist for evaluation in the neoadjuvant setting. TILs hot spots are excluded with a full assessment of average TILs in the tumor area by the pathologist as the final number being used in this study.

Immunohistochemistry

Tissue cutting and H&E staining were completed by the Translational Research Initiatives in Pathology (TRIP) and Experimental Pathology laboratories at UW-Madison. Optimization of IHC staining for cGAS D1D3G Rabbit mAb #15102 was completed by the TRIP lab and used at 1:100 dilution. Cancer cells were visualized by Pan-keratin (C11) Mouse mAB #4545 and used at 1:100 dilution. DNA was visualized using DAPI at 1μg/mL dilution. Staining for both cGAS and pan-keratin used the immunofluorescence IHC protocol for pan-keratin, which was obtained from Cell Signaling Technology with the following modification. Antigen retrieval was performed in a pressure cooker at 250 Fahrenheit for 5 minutes in pH 6 citric acid buffer with 0.1% Triton-X.

Quantification of cGAS expression is determined by average (mean) cGAS signal intensity of tumor cell clusters. Each tumor cluster was assessed for cGAS by using the

NIS elements ROI auto-detect tool. Tumor clusters from at least 10 random fields were assessed for each patient treatment condition at 600x magnification. Background subtraction was performed using the minus primary antibody negative control.

Time-lapse video microscopy

For live cell imaging, MDA-MB-231 cells stably expressing H2B-RFP and tubulin-GFP were seeded onto glass-bottomed plates. Cells were maintained at 37 °C in DMEM HG media. Prior to imaging, MDA-MB-231 cells were treated with 10nM paclitaxel. Image acquisition of MDA-MB-231 cells undergoing mitosis in either DMSO or paclitaxel was performed every 4 minutes at 20x magnification on a Nikon Eclipse Ti inverted microscope equipped with a 100x/1.4NA (Plan Apo) DIC oil immersion objective, motorized stage (Prior Scientific) and ORCA Flash4.0 V2+ digital sCMOS camera (Hammamatsu). FITC and Cy5 image datasets were both collected, representing tubulin-GFP and H2B-RFP respectively. Analysis focused on time in mitosis and cell fates. Representative live cell images were captured at 60X objective with a Nikon Spinning Disk Confocal Microscope equipped with Yokogawa CSU-W1, 2 Hamamatsu Orca Flash 4 cameras, motorized stage, generation 4 Perfect Focus System and Tokei Hit. This microscope was supplied for use by the UW Optical Image Core. Video montages of single and combined wavelength channels of confocal microscope images were produced using FIJI.

Immunofluorescence microscopy

Cells were seeded on glass coverslips at low density in 24-well plates and allowed to grow until 50% confluence. For cGAS puncta and STING positivity experiments, cells were challenged for 1-4 days with 10nM paclitaxel. Coverslips were washed twice in PBS before being fixed in 4% paraformaldehyde in PHEM buffer for 15 min at room temperature (RT), washed 3 times in PBS, and then blocked for 30 min at RT in 3% bovine serum albumin (BSA) and 0.1% Triton X-100 in PBS (PBSTx+BSA). Primary antibodies were pooled and diluted in PBSTx+BSA. Coverslips were incubated in primary antibodies for 1 h at RT and washed 3 times in PBSTx. Alexa Fluor (Invitrogen) secondary antibodies were pooled and diluted at 1:350 in PBSTx+BSA. Coverslips were incubated in secondary antibodies for 45 min at RT and then washed twice with PBSTx. Coverslips were counterstained with DAPI and mounted on glass slides with Prolong Diamond anti-fade medium (Invitrogen) and allowed to cure overnight.
Image acquisition was performed on a Nikon Eclipse Ti inverted microscope equipped with a 100x/1.4NA (Plan Apo) DIC oil immersion objective, motorized stage (Prior Scientific), and CoolSNAP HQ2 CCD camera (Photometrics). Optical sections were taken at 0.2 μm intervals and, except for extraction experiments, deconvolved using the AQI 3D Deconvolution module in Nikon Elements.

For quantification of cGAS puncta, observer blinding was performed by slide label concealment. cGAS puncta were quantified as positive if immunofluorescence in puncta is above the background signal and there is also an overlaying DAPI signal. At least 250 cells were quantified for each replicate for a total of 3 replicates per treatment condition. Phenotypes observed upon paclitaxel challenge were also quantified. A classification

scheme of 9 categories of DNA organization was employed for this purpose explained in more detail in the micronuclei quantification criteria section. Diffuse and punctate staining of cGAS positivity was also quantified. CREST signals were also quantified in cGAS puncta.

Quantification of cytoplasmic fluorescence intensity was performed using Nikon Elements. Cells were also imaged at 60x magnification with oil immersion and cell diameters were measured using the Nikon NIS Elements software. Images of at least 100 cells were acquired for each condition for paclitaxel. Threshold levels were equally applied to all images to exclude background intensity. cGAS immunofluorescence intensity was qualitatively determined by examining surrounding cell intensities. Sample size was selected for cell biology experiments based on prior experience and biologically significant effect size. For immunofluorescence, the sample size was typically ~100 cells. Three biological replicates were performed each with this sample size.

Data analysis was performed using Prism 8 (GraphPad). Statistical significance was determined using an ordinary one-way ANOVA with Dunnett's multiple comparisons test with a single pooled variance when comparing multiple cell lines against the vector control or a two-tailed, unpaired t-test with Welch's correction when comparing a single cell line with different chemical treatments.

Micronuclei quantification criteria

Micronuclei were qualitatively assessed based on nuclear morphologies present in untreated MDA-MB-231 cells (Figure S2A). Major (M) nuclei have one nucleus and represent the most abundant phenotype seen in the cell population (Figure 2D). The bi-nucleated+ category includes all nuclear morphologies that have two distinct nuclei categorized as follows. Major Minor (MR) have one large and one small nuclei (equivalent to nuclear structure with 3+ CREST puncta). Major Mini (MI) have one large and a qualitatively smaller nuclei (equivalent to nuclear structure with 2 CREST puncta). Major Micro (MC+) have the smallest nuclei (equivalent to nuclear structure with 1 or 0 CREST puncta). Major Micro+ (MC+) have a major, minor and micronucleus. Major Major+ (MM+) have two Major nuclei with or without micronucleus attached. The multinucleated category includes nuclear categories that typically only show up after paclitaxel treatment. These cells have 3 or more nuclei of similar sizes similar to a bunch of grapes. We divided the multinucleated cells into 3-5 MultiN (MN3+) with three to five nuclei and 6+ MultiN (MN6+) with six or more nuclei. This separation was made because paclitaxel at micromolar concentrations is known to arrest cells in mitosis, which can cause slippage, resulting in the formation of many smaller nuclei, typically greater than 6. However, cells that are delayed by mitosis but that still progress through it typically have fewer nuclei being formed even though slippage can still occur.

Nuclear blebbing is defined as protrusions from the nuclear surface in interphase cells with a phenotype that suggests these structures to be connected to the main and we employed several stringent criteria to define micronuclei to exclude blebbing from our analysis. Micronuclei were defined as structures stained by DAPI that are separate from

the main nucleus (if one exists). Micronuclei were also only quantified if they are oval or circular in shape. Z-stacks were employed over the entire height of the cell to ensure that there is no connection between the micronucleus and potentially other surrounding nuclei. For micronuclei overlapping with larger nuclei, changes in chromatin patterns between overlapping structures should exist or nuclear borders must be seen to clearly demarcate the borders of overlapping structures into either an oval or circular shape.

ELISAs for 2'3'-cGAMP and IFN-β

2'3'-cGAMP ELISA Kit (Item No. 501700) was purchased from Cayman Chemicals and used according to manufacturer's instructions. Lysates for the 2'3'-cGAMP ELISA Kit were prepared by mixing 100uL of lysis buffer with previously frozen cell pellets consisting of 1 million cells flash frozen in liquid nitrogen and stored at -80°C.
For MDA-MB-231, Human IFN Beta Construction Kit (Item No. RHF842CK) was used to measure for supernatant IFN-β according to manufacturer's instructions. For other breast cancer cell lines, Human IFN-beta DuoSet ELISA (Item No. DY814-05) was used with DuoSet ELISA Ancillary Reagent Kit 2 (Item No. DY008) to measure supernatant IFN-β according to manufacturer's instructions. For each condition in measuring IFN-β, 50uL of supernatant was harvested from 2mL of total media in each well harboring 500 thousand cells of 6-well plates.

CRISPR-cas9 knockout of cGAS

A polyclonal pool of cGAS -/- null MDA-MB-231 was produced as follows: Wild type MDA-MB-231 were transfected with Cas9-GFP Protein (Item No. CAS9GFPPRO) from

Sigma Aldrich with predesigned Alt-R® CRISPR-Cas9 guide RNA against cGAS from Integrated DNA Technologies. 48 hours after transfection, cells were singly flow sorted for GFP-positive cells into a 96-well plate. Cells were allowed to grow to confluence before passaging into 6-well plates. After growth to ~80% confluence, half of the cells were lysed and blotted for cGAS protein. Colonies that do not express cGAS further underwent TA cloning using the pGEM-T vector from Promega (Item No. A3600) according to manufacturer's instructions. Only clones that expressed out-of-frame indels were kept for experiments.

RNA interference

shcGAS and shSTING plasmids were purchased from Vector Builder. Predesigned MISSION siRNA against cGAS and STING were purchased from Sigma Aldrich. Transfection of siRNA was completed using Lipofectamine 3000 following manufacturer's instructions. Cells were incubated overnight following transfection followed by fresh media change and incubation for another day before being used for experiments.

THP-1 differentiation

THP-1 cells between passage numbers 5 and 10 were grown in RPMI 1640 media to a density of 1-10 x 105. For differentiation to an M0 macrophage phenotype, THP-1 cells incubated with 320nM of PMA diluted in media in 6 well tissue culture plates for 24 hours. Subsequently, cells were washed three times with Hank's Balanced Salt Solution (HBSS) before replacing with 10% FBS supplemented DMEM-High Glucose media. Cells were rested unperturbed for another 24 hours prior to experimentation.

Digitonin permeabilization

Digitonin permeabilization was carried out in a buffer containing 50 mM HEPES (pH 7), 100 mM KCl, 3 mM MgCl2, 0.1 mM DTT, 85 mM sucrose, 1 mM ATP, 0.1 mM GTP and 0.2% (v/v) FBS. 5ug/mL of digitonin was added either in isolation or with 10 μg/mL of 2′3′ cGAMP in permeabilization buffer for 10 min at 37 °C before replacing with fresh DMEM HG media.

Real-time quantitative PCR

cDNA preparation and quantitative PCR. cDNA was prepared as follows. ~ 3 x 106 cells were harvested and resuspended in 1 ml TRIzol (Life Technologies, # 15596018). For RNA extraction, 0.2 ml chloroform was added after incubation on ice for 10 minutes, and samples were thoroughly mixed. Samples were allowed to stand at room temperature for 10 min before centrifugation for 10 min (10,000 g; 4 ºC). The aqueous phase was removed and mixed with an equal volume of isopropanol and centrifuged. The supernatant was removed and the remaining pellet was washed with 75% ethanol and allowed to dry at room temperature. Samples were eluted using 50 μl of nuclease-free water. ~ 300 ng RNA of each sample were used to generate cDNA using the Transcriptor First Strand cDNA Synthesis kit (Roche, # 04 379 012 001) according to the manufacturer's instructions (both Anchored-oligo (dT)18 as well as random hexamer primers were used). 2 μl of each cDNA reaction were used for quantitative PCR with the LiqhtCycler 480 SYBR Green I Master mix (Roche, # 04 707 516 001), carried out on an iCycler (Bio-Rad) equipped with the IQ 5 detection system. The following temperature

program was used: 5 min 95 ºC; 50 x (10 sec 95 ºC; 20 sec “annealing temperature”; 20 sec 72 ºC).

The following primer sequences comprise the Type I interferon response panel with an annealing temperature of 55°C: STAT1 forward: 5’- CAGCTTGACTCAAAATTCCTGGA-3’, reverse: 5’-TGAAGATTACGCTTGCTTTTCCT-3’; STAT2 forward: 5’-GAGCCAGCAACATGAGATTGA-3’, reverse: 5’-GCCTGGATCTTATATCGGAAGCA-3’; IRF3 forward: 5’-AGAGGCTCGTGATGGTCAAG-3’, reverse: 5’-AGGTCCACAGTATTCTCCAGG-3’; IRF9 forward: 5’-GCCCTACAAGGTGTATCAGTTG-3’, reverse: 5’-TGCTGTCGCTTTGATGGTACT-3’; OAS1 forward: 5’-TGTCCAAGGTGGTAAAGGGTG-3’, reverse: 5’-CCGGCGATTTAACTGATCCTG-3’; IFNB1 forward: 5’-ATGACCAACAAGTGTCTCCTCC-3’, reverse: 5’- GGAATCCAAGCAAGTTGTAGCTC-3’.

The following primer sequences comprise the Type I interferon response panel with an annealing temperature of 57°C: IRF7 forward: 5’-CCCAGCAGGTAGCATTCCC-3’ reverse: 5’-GCAGCAGTTCCTCCGTGTAG-3’; OAS2 forward: 5’-ACGTGACATCCTCGATAAAACTG-3’, reverse: 5’-GAACCCATCAAGGGACTTCTG-3’; NLRC5 forward: 5’-ACAGCATCCTTAGACACTCCG-3’, reverse: 5’-CCTTCCCCAAAAGCACGGT-3’; IFI16 forward: 5’- GTTTGCCGCAATGGGTTCC-3’, reverse: 5’-ATCTCCATGTTTCGGTCAGCA-3’; IFI27 forward: 5’-TCTCTGCCCGGTGTTTTTGT-3’, reverse: 5’-TTCCGTGGCATTCCAGAGTC-3’

The following primer sequences comprise the THP-1 macrophage differentiation panel with annealing temperature of 56°C: RPLP0 forward: 5'-GCAGCATCTACAACCCTGAAG-3', reverse: 5'- CACTGGCAACATTGCGGAC-3'; CCL18 forward: 5'-AAAATTGGCCAGGTGCAGTG-3', reverse: 5'-TGAGGTTTCACCATGTTGGC-3'; CXCL10 forward: 5'-GTGGCATTCAAGGAGTACCTC-3', reverse: 5'-TGATGGCCTTCGATTCTGGATT-3'; CXCL11 forward: 5'-AAGCAGGAAAGGTGCATGAC-3', reverse: 5'-AGCTTTGCTGCTCTTCTTGG-3'; MMP9 forward: 5'-TGTACCGCTATGGTTACACTCG-3', reverse: 5'-GGCAGGGACAGTTGCTTCT-3'; IL10 forward: 5'-GACTTTAAGGGTTACCTGGGTTG-3', reverse: 5'-TCACATGCGCCTTGATGTCTG-3'. Readings were normalized to RPLP0.

Immunoblot

For all experiments, cells were challenged with 10nM paclitaxel for 2 or 4 days and cells were lysed and frozen down and stored at −80°C prior to use. Cell pellets were lysed in lysis buffer (50 mM HEPES pH 7.5, 100 mM NaCl, 0.5% NP-40, 10% glycerol) containing phosphatase inhibitors (10 mM sodium pyrophosphate, 5 mM β-glycerophosphate, 50 mM NaF, 0.3 mM Na3VO4), 1mM PMSF, 1x protease inhibitor cocktail (Thermo-Scientific) and 1 mM dithiothreitol. A 25-gauge syringe was used to provide additional mechanical lysis to the cell membrane before incubating lysate on ice for 30 minutes and centrifuging at 15,000 x g speed at 4°C to remove insoluble pellets. Protein concentration was measured using the Bradford assay. Proteins were separated

by SDS-PAGE, transferred to Immobilon PVDF membrane (Millipore), and blocked for 30 min in 0.1% Tween-20 Tris buffered saline ph 7.4 supplemented with either 5% BSA (STING, phospho-IRF3) or 5% milk (cGAS, phospho-STAT1). Membranes were incubated with gentle agitation for 24 hours at 4°C with primary antibodies diluted in either TBST supplemented with 5% BSA or 5% milk, washed 3x with TBST, incubated for 1 h at room temperature in secondary antibodies conjugated to horseradish peroxidase diluted 1:10,000 in TBST supplemented with 5% milk and subsequently in LI-COR secondary antibodies after developing on film. Membranes were washed and developed with luminol/peroxide (Millipore) and visualized with film. Housekeeping proteins GAPDH and actin were developed

All results were obtained from single gels. To simultaneously probe for the protein of interest and the loading marker, the membrane was divided in two after transfer and incubated in separate antibody solutions. When identical-sized proteins prevented membrane division, the membrane was first probed for the protein of interest, stripped in an acidic glycine wash (100 mM glycine pH 2, 500 mM NaCl, 2% SDS), rinsed in deionized H2O, and then reprobed for the loading marker.

Flow cytometry

Flow cytometry was conducted at the Flow Cytometry Laboratory at UW-Madison. Either MDA-MB-231 or MDA-MB-436 were treated with 10nM paclitaxel, eribulin or vinorelbine prior to harvesting and labeling according to the flow cytometry protocol using PD-L1 Extracellular Domain Specific D8T4X Rabbit mAb Alexa Fluore 647 (flow

cytometry 1:100). Cells were labeled with DAPI at 1ug/mL for live-dead staining. Cells were kept on ice before analysis. FCS Express 7 Research Edition was used to make flow plots. Data analysis was performed using Prism 8 (GraphPad).

2.6 Acknowledgements

We thank Zach Morris, Christian Capitini, Shigeki Miyamoto, Aussie Suzuki and Fotis Asimakopoulos for helpful discussions. We thank Kayla Lemmon for assistance in acquiring patient specimens. We thank Andrew Lynch and Rachel Sundstrom of the Burkard research group for feedback on the manuscript. We thank Jim Zacny for proofreading the manuscript. We thank Jiaquan Yu of the Beebe research group for experimental optimization of conditioned media experiments and for providing the THP-1 cell line. We thank Saswati Bhattacharya for providing technical assistance. We thank the Translational Research Initiatives in Pathology laboratory and Experimental Pathology Laboratory at UW-Madison for cutting tissue slides and for optimizing IHC staining.

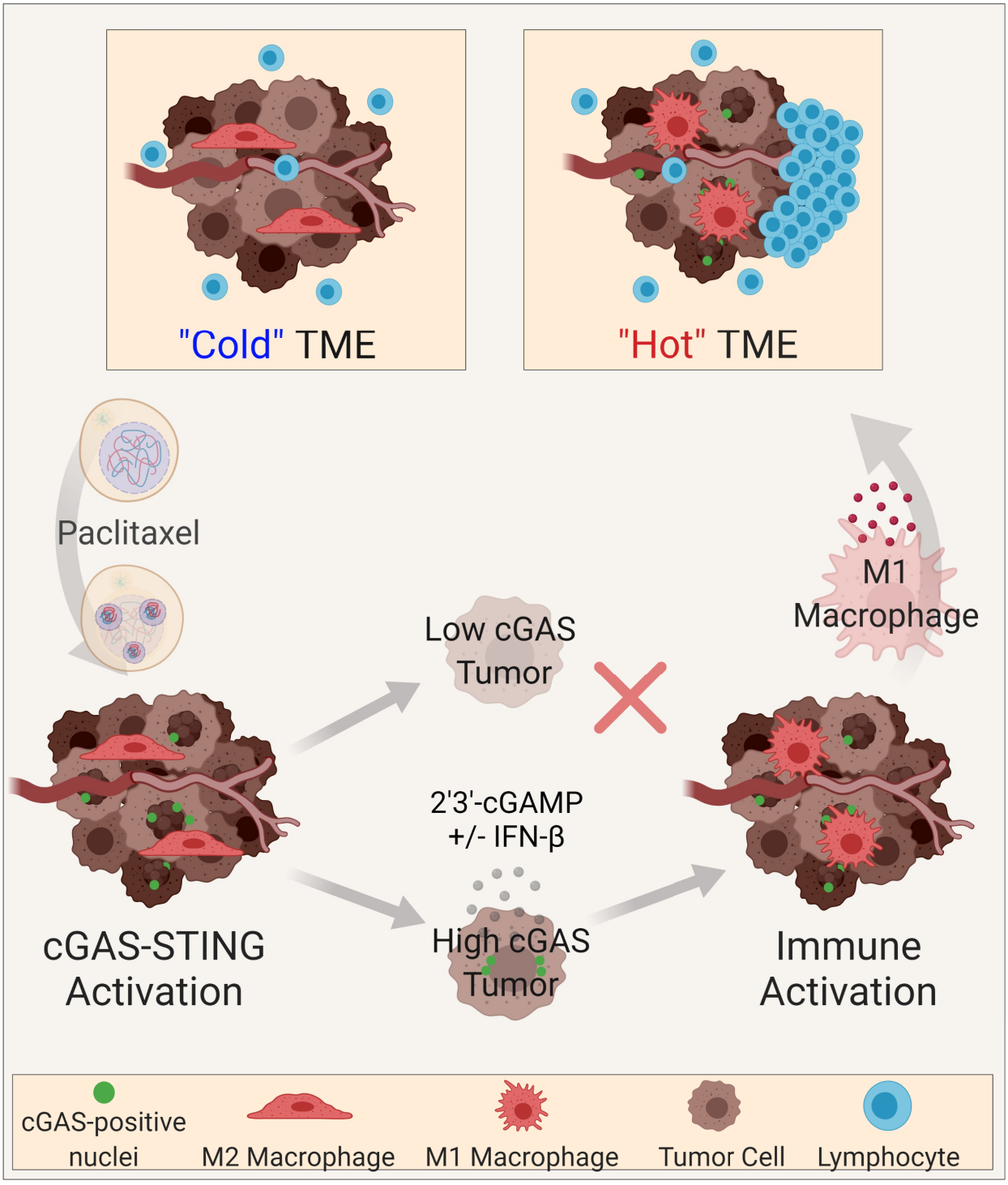
"Cold" TME
"Hot" TME
Paclitaxel
M1
Macrophage
Low cGAS
Tumor
2'3'-cGAMP
+/- IFN-β
cGAS-STING
Activation
High cGAS
Tumor
Immune
Activation
cGAS-positive
nuclei
M2 Macrophage
M1 Macrophage
Tumor Cell
Lymphocyte

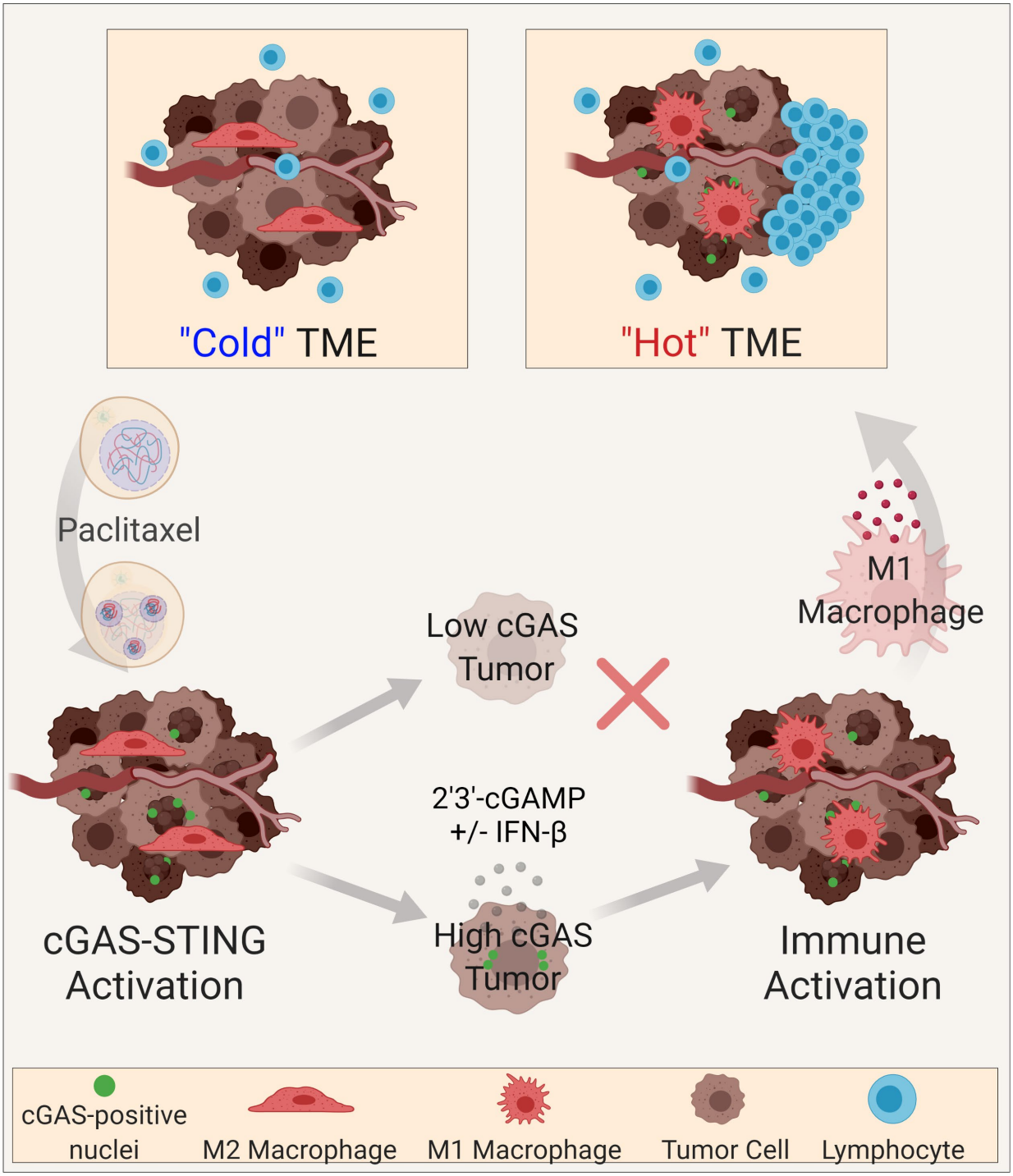

Cover Figure: Putative Mechanism

Figure 1

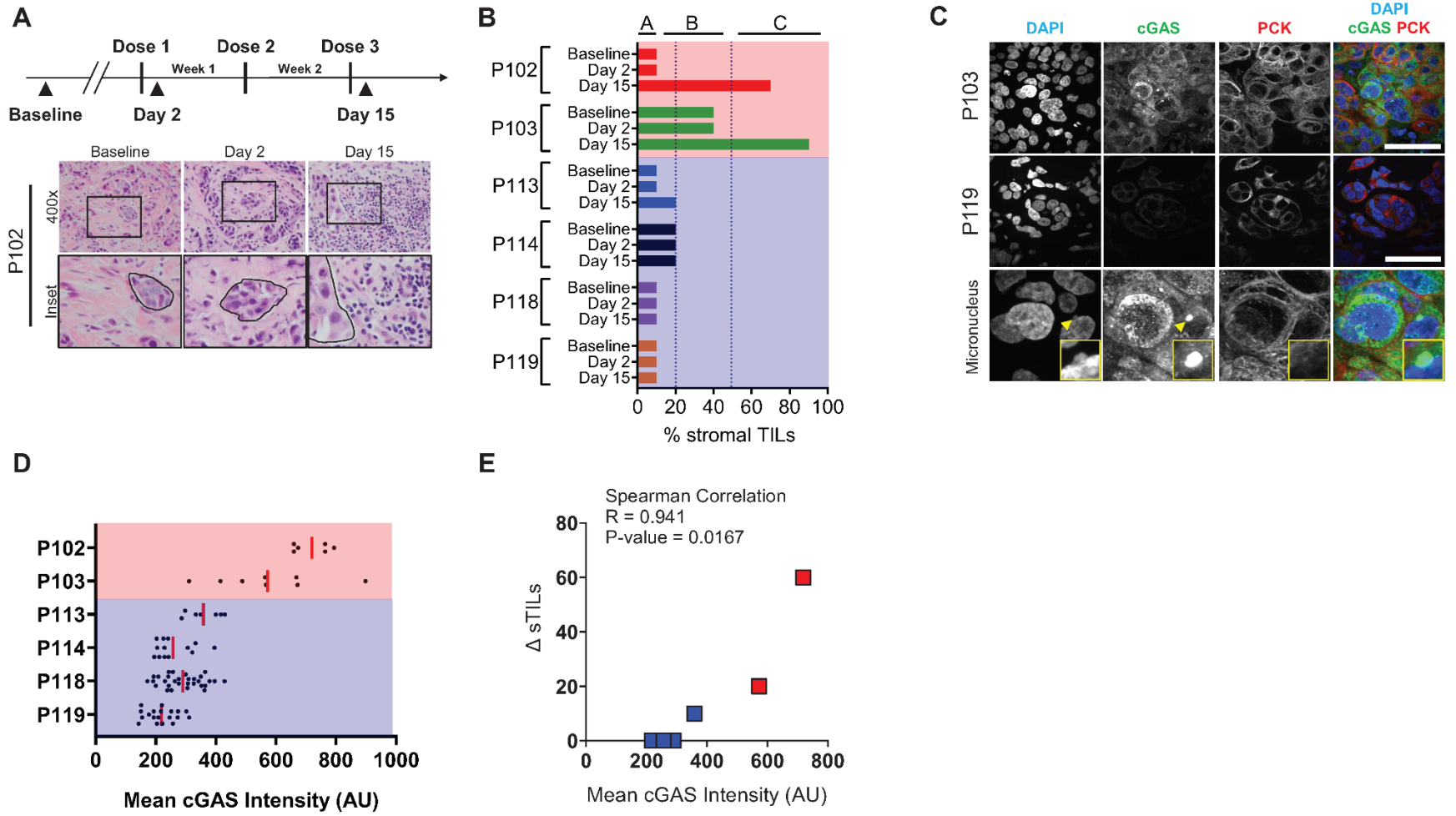
A
Dose 1
Dose 2
Dose 3
Week 1
Week 2
Baseline
Day 2
Day 15
Baseline
Day 2
Day 15
P102
400x
Inset
B
A
B
C
P102
P103
P113
P114
P118
P119
Baseline
Day 2
Day 15
0
20
40
60
80
100
% stromal TILs
C
DAPI
cGAS
PCK
DAPI
cGAS PCK
P103
P119
Micronucleus
D
P102
P103
P113
P114
P118
P119
0
200
400
600
800
1000
Mean cGAS Intensity (AU)
E
Spearman Correlation
R = 0.941
P-value = 0.0167
Δ sTILs
0
20
40
60
80
0
200
400
600
800
Mean cGAS Intensity (AU)

Fig. 1. Some but not all triple-negative breast cancer patients develop tumor-infiltrating lymphocytes following neoadjuvant paclitaxel.

(*A*) Representative hematoxylin and eosin (H&E) images showing increased stromal tumor-infiltrating lymphocytes (sTILs) in one patient P102 after the third dose of 80mg/m^2 neoadjuvant paclitaxel approximately 15 days after the start of therapy. Inset are magnifications with representative tumor outlined in black and stroma surrounding the tumor. Tumor is outlined in black and sTILs are represented by cells with dark, purple nuclei in “Day 15” sample. Original images are at 400x magnification.

(*B*) Dose scheduling of patients with biopsies (P102, P103, P113, P114, P118, P119) undergoing neoadjuvant paclitaxel treatment. Treatment regimen comprises biweekly 80mg/m^2 neoadjuvant paclitaxel for four doses. Quantification of sTILs of patient H&E images by staff pathologist using *International TILs Working Group* criteria. See supporting information for more details.

(*C*) Representative images of tumor cells from patient biopsies of nuclear phenotypes after paclitaxel with staining of DNA (DAPI), cGAS and pan-cytokeratin (PCK). Scale bar, 50μm.

(*D*) Quantification of intratumoral cGAS expression by average (mean) cGAS signal intensity of tumor cell clusters. AU=arbitrary units

(*E*) Spearman correlation of six patients treated with neoadjuvant paclitaxel from (A-D) plotted by change in TILs between “Day 15” and “Baseline”. AU=arbitrary units

Figure 2

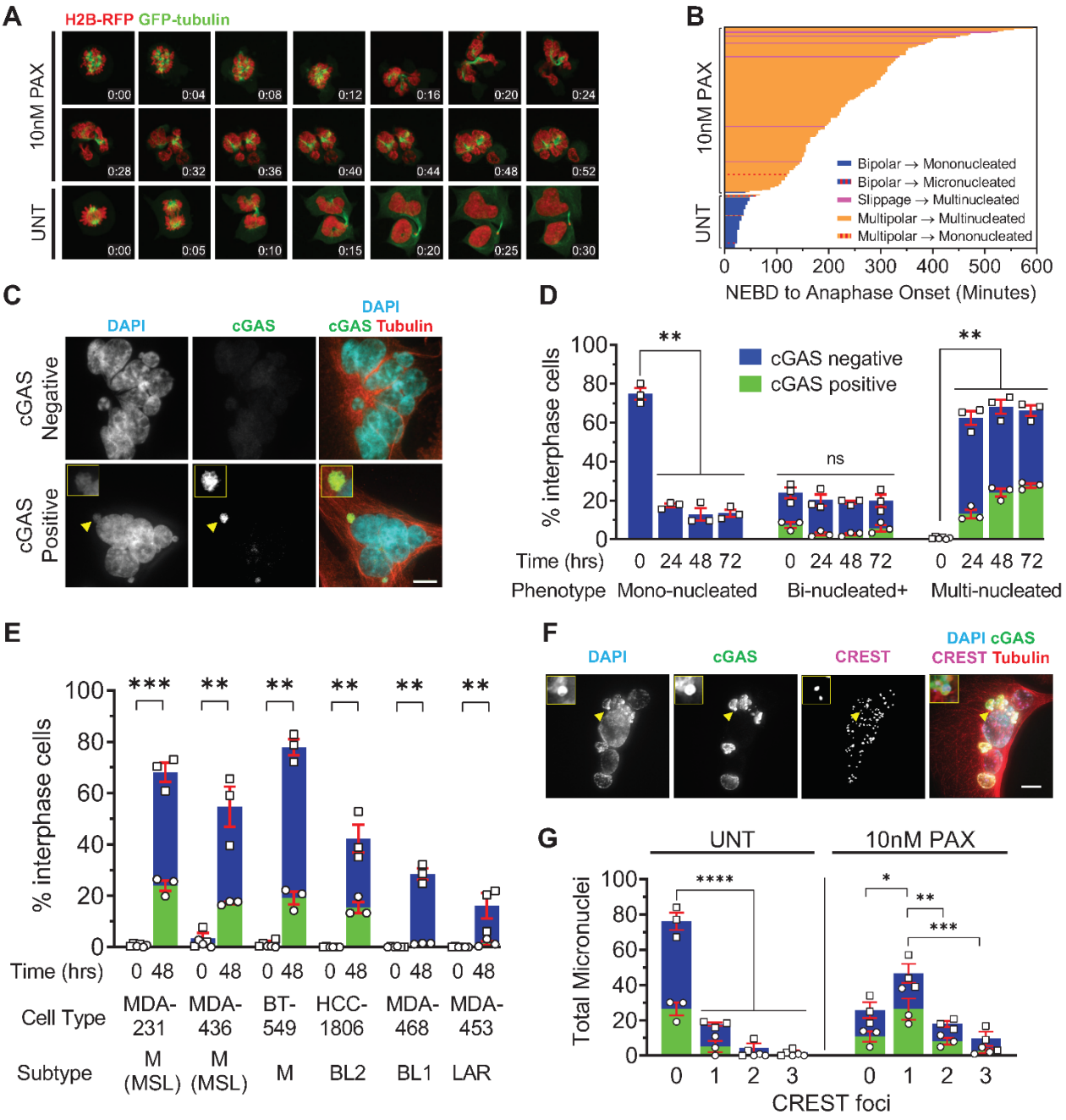
A
H2B-RFP GFP-tubulin
10nM PAX
UNT
0:00
0:04
0:08
0:12
0:16
0:20
0:24
0:28
0:32
0:36
0:40
0:44
0:48
0:52
0:00
0:05
0:10
0:15
0:20
0:25
0:30
B
10nM PAX
UNT
Bipolar → Mononucleated
Bipolar → Micronucleated
Slippage → Multinucleated
Multipolar → Multinucleated
Multipolar → Mononucleated
0
100
200
300
400
500
600
NEBD to Anaphase Onset (Minutes)
C
DAPI
cGAS
DAPI
cGAS Tubulin
cGAS Negative
cGAS Positive
D
% interphase cells
cGAS negative
cGAS positive
**
ns
**
Time (hrs)
0 24 48 72
0 24 48 72
0 24 48 72
Phenotype
Mono-nucleated
Bi-nucleated+
Multi-nucleated
E
% interphase cells
***
**
**
**
**
**
Time (hrs)
0 48
Cell Type
MDA-231
MDA-436
BT-549
HCC-1806
MDA-468
MDA-453
Subtype
M (MSL)
M (MSL)
M
BL2
BL1
LAR
F
DAPI
cGAS
CREST
DAPI cGAS
CREST Tubulin
G
UNT
10nM PAX
Total Micronuclei
****
*
**
***
0 1 2 3
0 1 2 3
CREST foci

Fig. 2. Paclitaxel causes cGAS-positive micronuclei to form in interphase following delayed mitosis on multipolar spindles.

(*A*) Representative images of MDA-MB-231 cells expressing H2B-RFP and tubulin-GFP filmed with 60X objective at 4-min intervals from mitosis to subsequent interphase with no treatment (UNT) or 10 nM paclitaxel (PAX).

(*B*) Quantification of live cell images from (A) for mitotic duration and chromosome segregation defects from Nuclear Envelope Breakdown (NEBD) to anaphase onset and daughter cell interphase nucleus morphology. N=50 cells for UNT and 150 cells for 10nM PAX.

(*C*) Representative images of multinucleated MDA-MB-231 after 10nM paclitaxel with and without cGAS puncta. Scale bar, 10 μm.

(*D*) Quantification of nuclei phenotypes (sum of blue and green bars) and cGAS-positivity (green bar) in MDA-MB-231 interphase cells after 0, 24, 48 and 72 hours of 10nM paclitaxel. N=3 independent experiments comprising ≥250 asynchronous cells per condition. Mean and SEM are plotted. P values are calculated by one-way ANOVA with Tukey-Kramer test (*P < 0.05, **P < 0.01, ***P < 0.001, ns=not significant). See Figure S2A for representative images of nuclei phenotypes.

(*E*) Quantification of micronuclei (sum of blue and green bars) of multinucleated cells of multiple TNBC cell lines after 0 and 48 hours of 10nM paclitaxel N=3 independent experiments comprising ≥250 asynchronous cells per condition. Results for MDA-MB-231 from (D). Mean and SEM are plotted. P-values were calculated by two-tailed, paired Student’s T Test (*P < 0.05, **P < 0.01, ***P < 0.001, ns=not significant). TNBC

subtypes are M=mesenchymal, MSL=mesenchymal stem-like (retired classification), BL1=basal-like 1, BL2=basal-like 2, LAR=luminal androgen receptor.

(*F*) Representative images of multinucleated MDA-MB-231 after 10nM paclitaxel stained for cGAS and CREST. Yellow arrows indicate a cGAS-positive micronucleus with one CREST foci, which is magnified in the top-left inset. Scale bar, 10 μm.

(*G*) Quantification of MDA-MB-231 CREST foci with no treatment (UNT) or after two days of 10nM paclitaxel (10nM PAX) categorized by number of cGAS-positive or cGAS-negative micronuclei. N=3 independent experiments comprising ≥50 asynchronous cells (≥ total 100 micronuclei) per condition. Mean and SEM are plotted. P values were calculated by one-way ANOVA with Tukey-Kramer test (*P < 0.05, **P < 0.01, ***P < 0.001, ns=not significant).

Figure 3

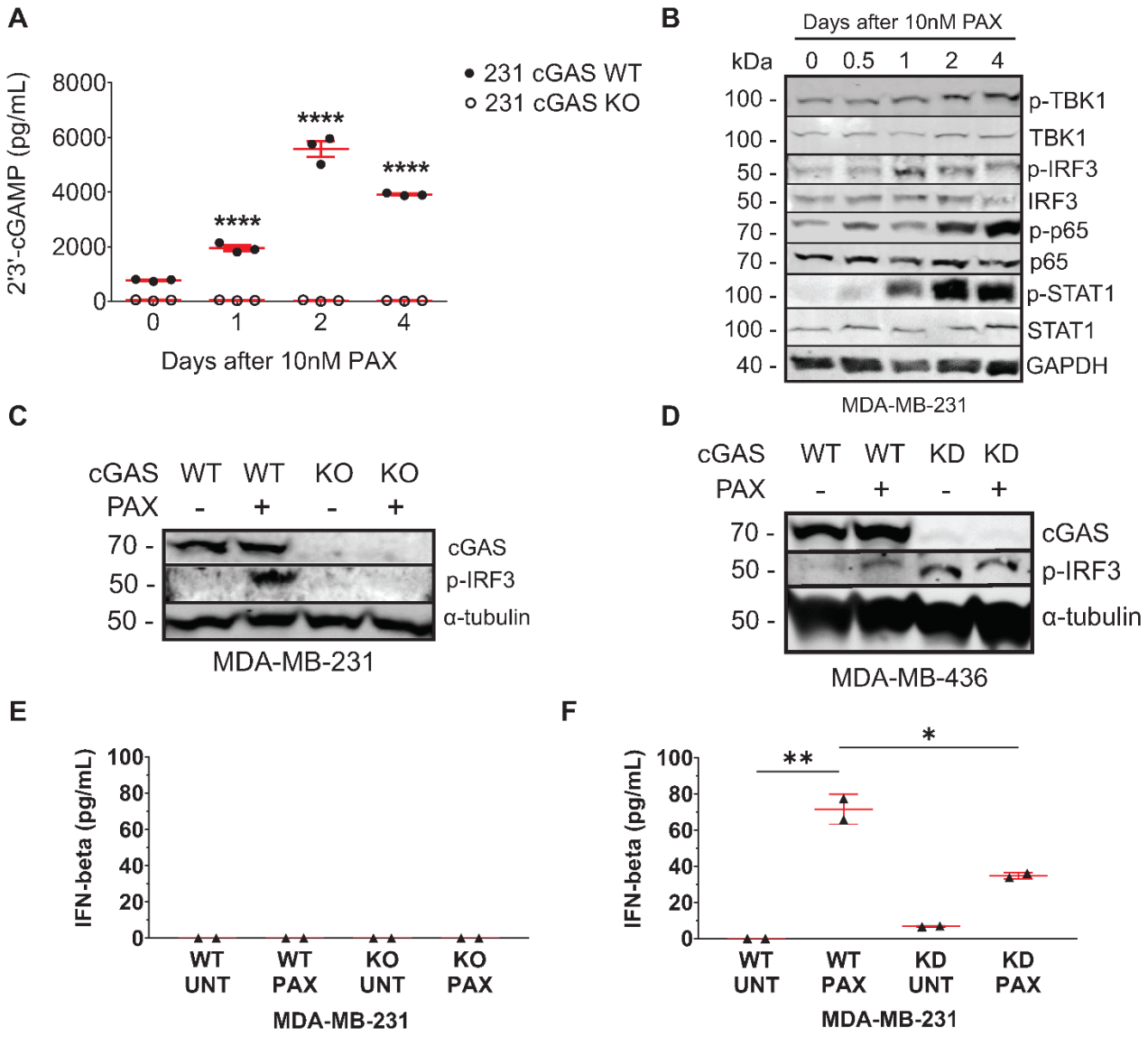

Fig. 3. Paclitaxel activates cGAS signaling in triple-negative breast cancer cell lines.

(*A*) ELISA analysis of 2'3'-cGAMP production in wild type and cGAS knockout MDA-MB-231 four days after exposure to 10nM paclitaxel. N=3 independent experiments. Mean and SEM are plotted. P values were calculated by one-way ANOVA with

Dunnett's test with control as 0 day (*P < 0.05, **P < 0.01, ***P < 0.001, ns=not significant).

(*B*) Representative immunoblot of MDA-MB-231 wild type cells exposed to 10nM paclitaxel after 0, 0.5, 1, 2 and four days probed with phosphoproteins downstream of the STING pathway that increase with activation of the pathway comprising pTBK1, pSTING, pIRF3 and pSTAT1.

(*C*) Representative immunoblot of cGAS, STING and pIRF3 from MDA-MB-231 wild type (WT) and cGAS knockout (KO) cells exposed to 10nM paclitaxel for four days. Alpha tubulin serves as the loading control.

(*D*) Representative immunoblot of cGAS and pIRF3 from MDA-MB-436 wild type (WT) and cGAS knockdown (KD) cells exposed to 10nM paclitaxel for four days. Alpha tubulin serves as the loading control.

(*E*) Interferon-beta measurements of wild type (WT) and cGAS knockout (KO) MDA-MB-231 exposed to no treatment (UNT) or 10nM paclitaxel (PAX) over five days. N=2 independent experiments. Mean and SEM are plotted. P values were calculated by one-way ANOVA with Tukey-Kramer test (*P < 0.05, **P < 0.01, ***P < 0.001, ns=not significant).

(*F*) Interferon-beta measurements of wild type (WT) and si-cGAS knockdown (KD) MDA-MB-436 exposed to no treatment (UNT) or 10nM paclitaxel (PAX) over five days compared. N=2 independent experiments. Mean and SEM are plotted. P values were calculated by one-way ANOVA with Tukey-Kramer test (*P < 0.05, **P < 0.01, ***P < 0.001, ns=not significant).

Figure 4

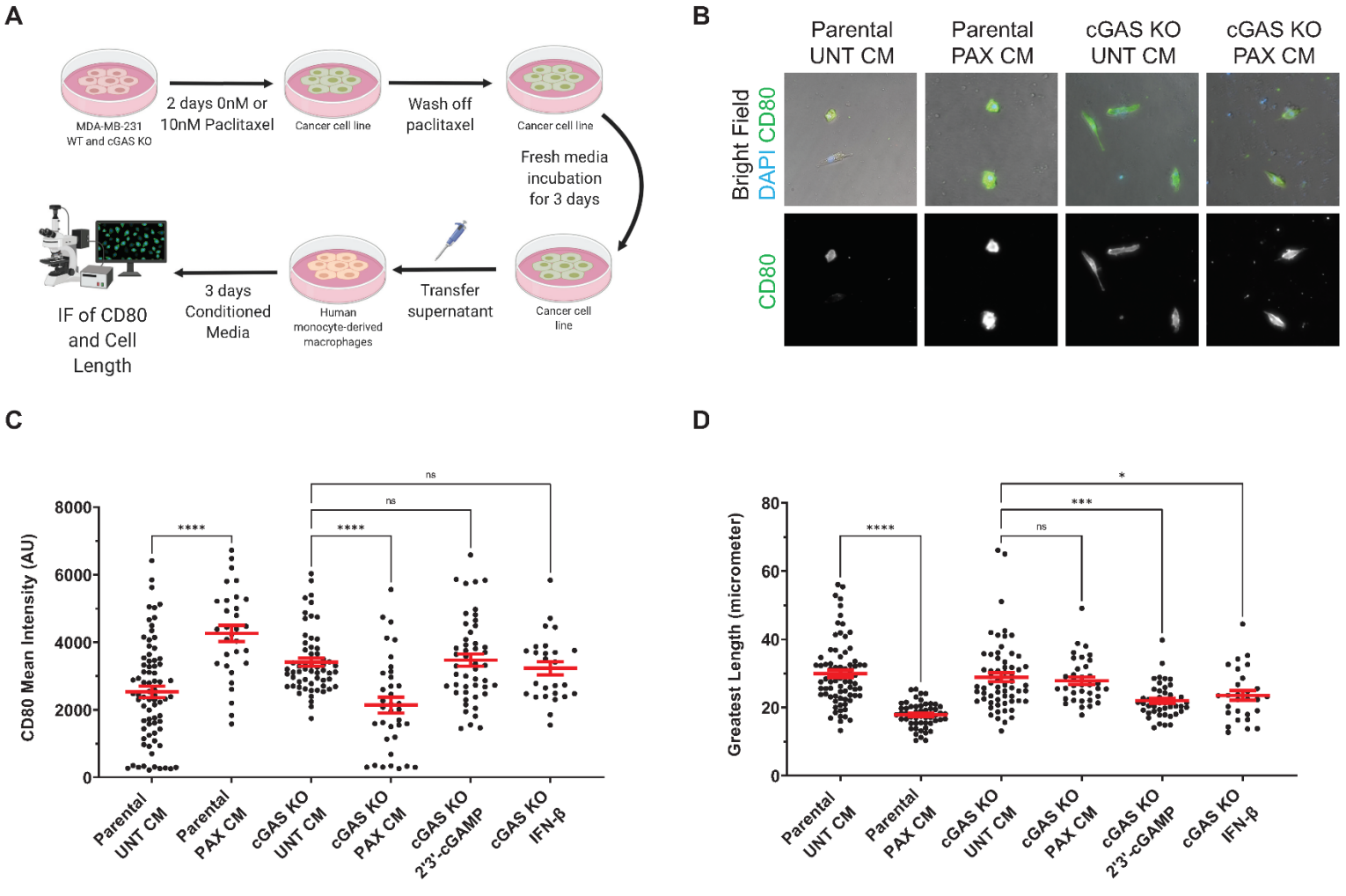
A
MDA-MB-231
WT and cGAS KO
2 days 0nM or
10nM Paclitaxel
Cancer cell line
Wash off
paclitaxel
Cancer cell line
Fresh media
incubation
for 3 days
Cancer cell
line
Transfer
supernatant
Human
monocyte-derived
macrophages
3 days
Conditioned
Media
IF of CD80
and Cell
Length
B
Parental
UNT CM
Parental
PAX CM
cGAS KO
UNT CM
cGAS KO
PAX CM
Bright Field
DAPI CD80
CD80
C
CD80 Mean Intensity (AU)
8000
6000
4000
2000
0
****
****
ns
ns
Parental
UNT CM
Parental
PAX CM
cGAS KO
UNT CM
cGAS KO
PAX CM
cGAS KO
2'3'-cGAMP
cGAS KO
IFN-β
D
Greatest Length (micrometer)
80
60
40
20
0
****
ns
***
*
Parental
UNT CM
Parental
PAX CM
cGAS KO
UNT CM
cGAS KO
PAX CM
cGAS KO
2'3'-cGAMP
cGAS KO
IFN-β

Fig. 4. Paclitaxel causes secretion of cGAS-dependent soluble factors in breast cancer that induce M1 polarization in human macrophages.

(*A*) Schematic of mono-culture conditioned media experiments with human blood-derived macrophages.

(*B*) Representative images of human macrophages expressing CD80 incubated with conditioned media from MDA-MB-231 parental and cGAS knockout cell lines untreated or pre-treated with 10nM paclitaxel.

(*C*) Measurement of CD80 expression on macrophages following conditioned media from parental and cGAS knockout MDA-MB-231 untreated or pre-treated with paclitaxel. N=3 independent experiments. Mean and SEM are plotted. P values were calculated by one-way ANOVA with Tukey-Kramer test (*P < 0.05, **P < 0.01, ***P < 0.001, ns=not significant).

(*D*) Measurement of longest dimension of macrophages following conditioned media from parental and cGAS knockout MDA-MB-231 untreated or pre-treated with paclitaxel. N=3 independent experiments. Mean and SEM are plotted. P values were calculated by one-way ANOVA with Tukey-Kramer test (*P < 0.05, **P < 0.01, ***P < 0.001, ns=not significant).

Figure 5

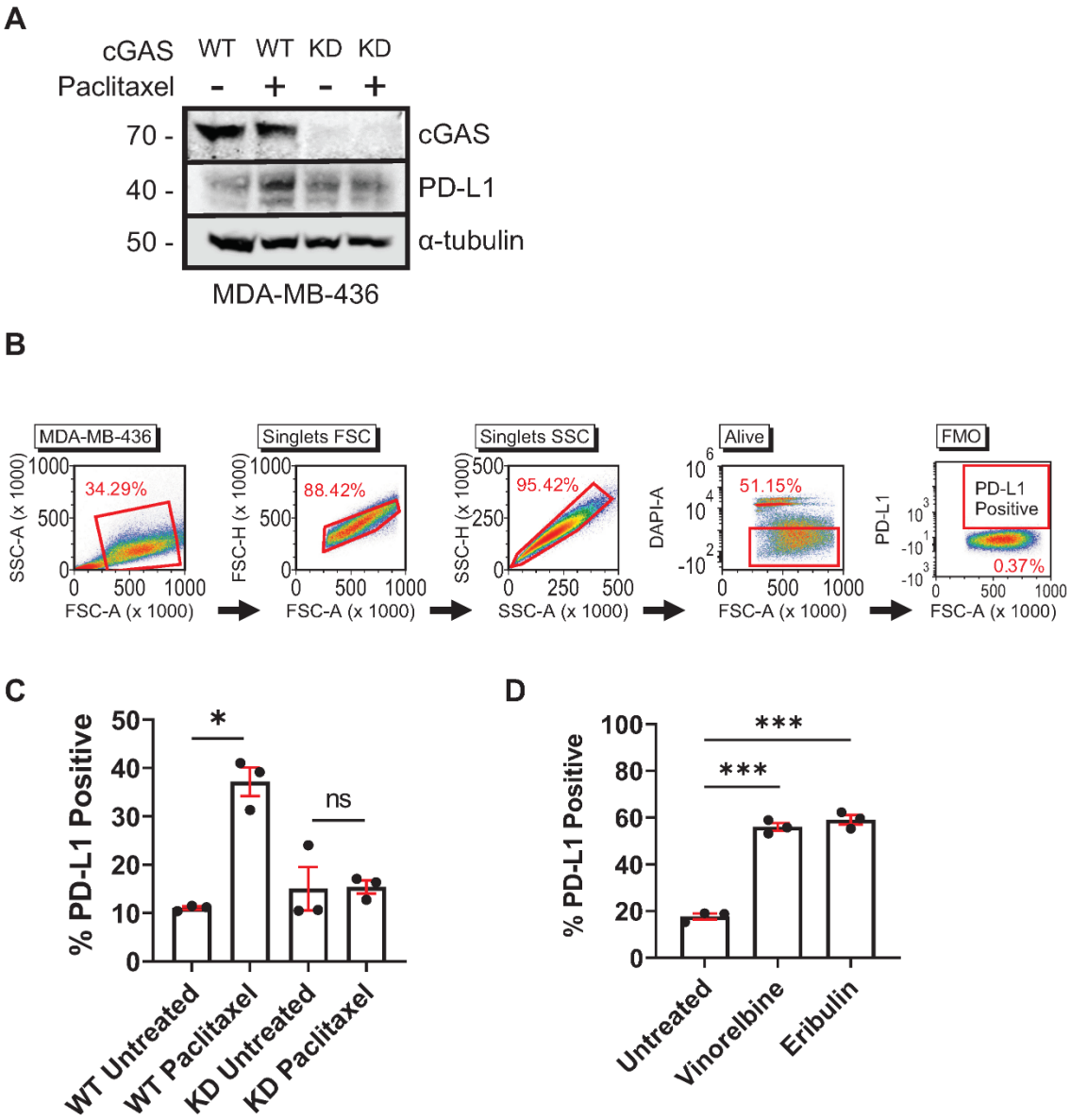

Fig. 5. Nanomolar paclitaxel and other microtubule-targeting agents can increase surface PD-L1 expression in TNBC cell line MDA-MB-436 dependent on cGAS expression.

(*A*) Representative Immunoblot of wild type and cGAS knockout MDA-MB-436 probed for total PD-L1 in MDA-MB-231 cells four days with or without 10nM paclitaxel. Alpha tubulin serves as the loading control.

(*B*) Flow cytometry strategy for PD-L1 expression.

(*C*) Quantification of surface PD-L1 by percent of the live parent population of wild type and si-cGAS MDA-MB-436 cells before and after three days of 10nM paclitaxel. Mean and SEM of n=3 independent biological experiments comprising ≥100,000 events per condition are shown. P values were calculated by one-way ANOVA with Dunnett's test with control as 0 day (*P < 0.05, **P < 0.01, ***P < 0.001, ns=not significant).

(D) Quantification of surface PD-L1 by percent of the live parent population of wild type MDA-MB-436 cells before and after three days of 10nM eribulin and vinorelbine. Mean and SEM of n=3 independent biological experiments comprising ≥100,000 events per condition are shown. P values were calculated by one-way ANOVA with Dunnett's test with control as 0 day (*P < 0.05, **P < 0.01, ***P < 0.001, ns=not significant).

Figure 6

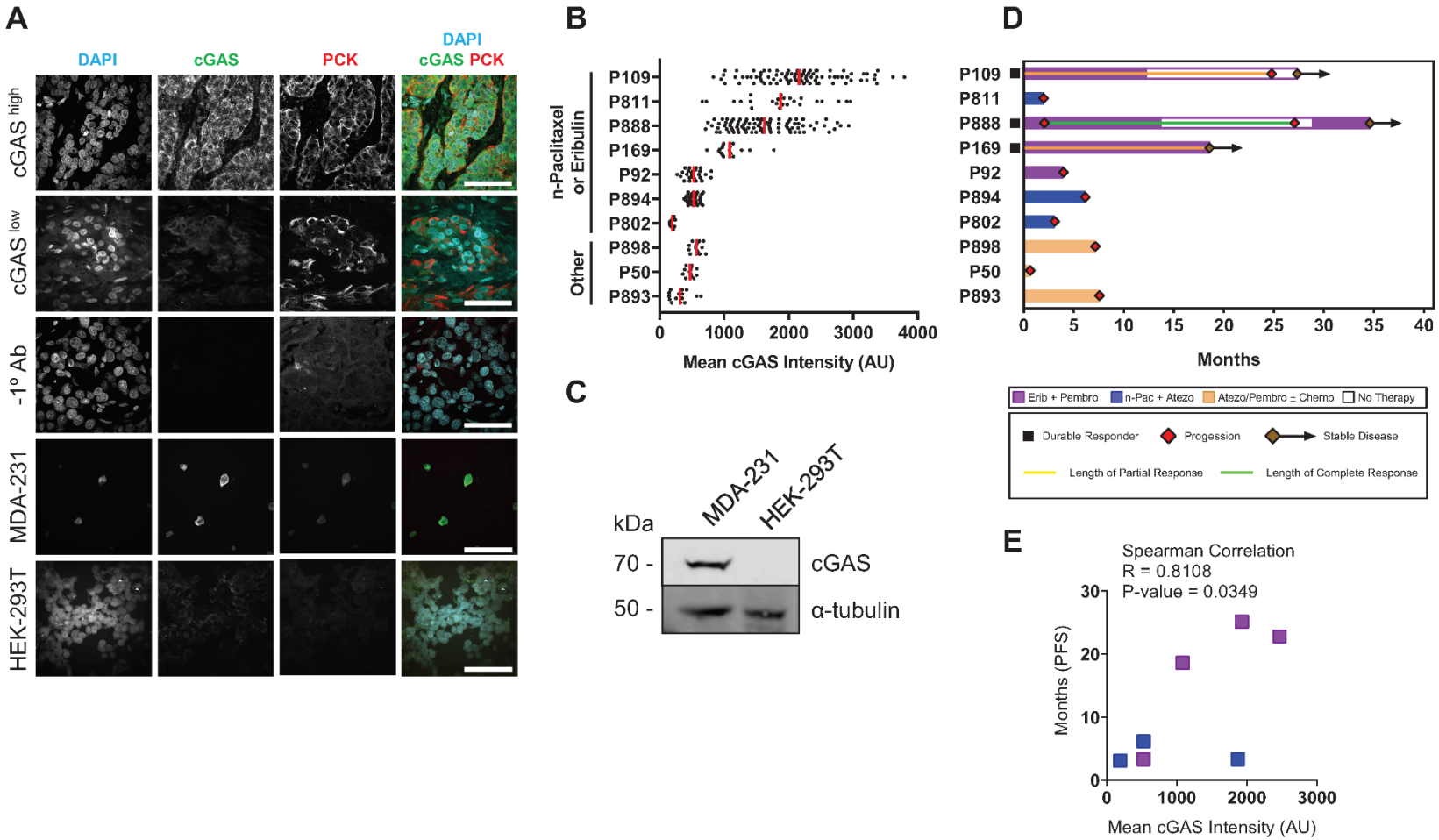
A
DAPI
cGAS
PCK
DAPI cGAS PCK
cGAS high
cGAS low
-1° Ab
MDA-231
HEK-293T
B
n-Paclitaxel or Eribulin
Other
P109
P811
P888
P169
P92
P894
P802
P898
P50
P893
0
1000
2000
3000
4000
Mean cGAS Intensity (AU)
C
kDa
MDA-231
HEK-293T
70 -
50 -
cGAS
α-tubulin
D
0
5
10
15
20
25
30
35
40
Months
Erib + Pembro
n-Pac + Atezo
Atezo/Pembro ± Chemo
No Therapy
Durable Responder
Progession
Stable Disease
Length of Partial Response
Length of Complete Response
E
Spearman Correlation
R = 0.8108
P-value = 0.0349
Months (PFS)
0
10
20
30
0
1000
2000
3000
Mean cGAS Intensity (AU)

Fig. 6. Patients expressing higher levels of cGAS have increased disease control after combined microtubule-targeting agents and PD-1/PD-L1 inhibitors.

(A) Representative images of patient tumors from diagnostic biopsies with DNA (DAPI), cGAS and pan-cytokeratin (PCK) staining. Positive control for cGAS is derived from paraffin-embedded MDA-MB-231 cell pellet stained simultaneously with patient samples under same protocol. Negative control for cGAS is derived from HEK293T cell pellet. Scale bar, 50 μm.

(*B*) Quantification of intratumoral cGAS expression by average (mean) cGAS signal intensity of tumor cell clusters. AU=arbitrary units

(*C*) Immunoblot of cGAS in MDA-MB-231 and HEK293T, which serve as positive and negative controls for cGAS staining.

(*D*) Swimmer's plot showing progression free survival of patients in months after combination therapy of paclitaxel and atezolizumab (PD-L1) or eribulin and pembrolizumab (PD-1) stratified from top to bottom by high to low cGAS expression. Legend indicates treatment regimen (top) and response status (bottom). Top legend color coding also applies to (*E*) for patient treatments.

(*E*) Spearman correlation of seven patients treated with both microtubule and immune checkpoint inhibitors from (B-C) plotted by mean cGAS intensity against progression free survival in months. This analysis excludes three patients without microtubule inhibitor treatment. AU = Arbitrary Units

Supplemental Figure S1

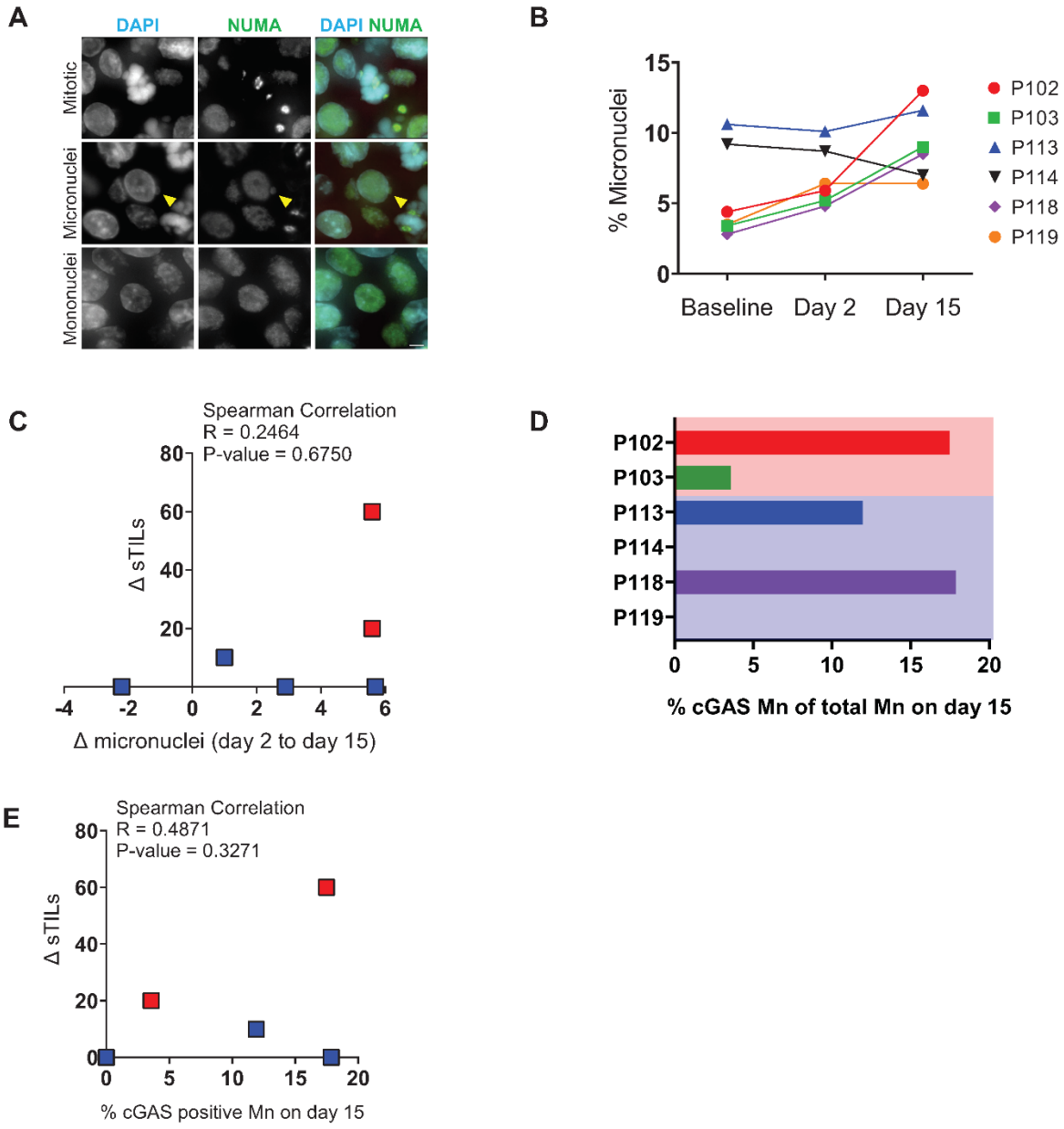

Fig. S1. cGAS-positive micronuclei are present in patient samples after paclitaxel. **(*A*)** Representative images of tumor cells from patient biopsies of nuclear phenotypes after paclitaxel with DAPI (DNA), NUMA (mitotic cells) and pan-cytokeratins (tumor cell boundary). Scale bar, 25μm.

(*B*) Quantification of interphase micronuclei of tumor cells from patient biopsies, N=600-2000 cells collected from at least 10 random fields for all patient treatment conditions. **(*C*)** Scatter plot showing relationship between change in micronuclei and change in TILs between “Day 2” and “Day 15” after neoadjuvant paclitaxel for patients. **(*D*)** Bar graph showing percentage of cGAS-positive micronuclei of total micronuclei on “Day 15” for patients after neoadjuvant paclitaxel. Bars highlighted in red represent patients with increased TILs at “Day 15.” Bars highlighted in blue represent patients without increased TILs. **(*E*)** Scatter plot showing relationship between percentage of positive micronuclei and change in TILs between “Day 2” and “Day 15”.

Supplemental Figure S2

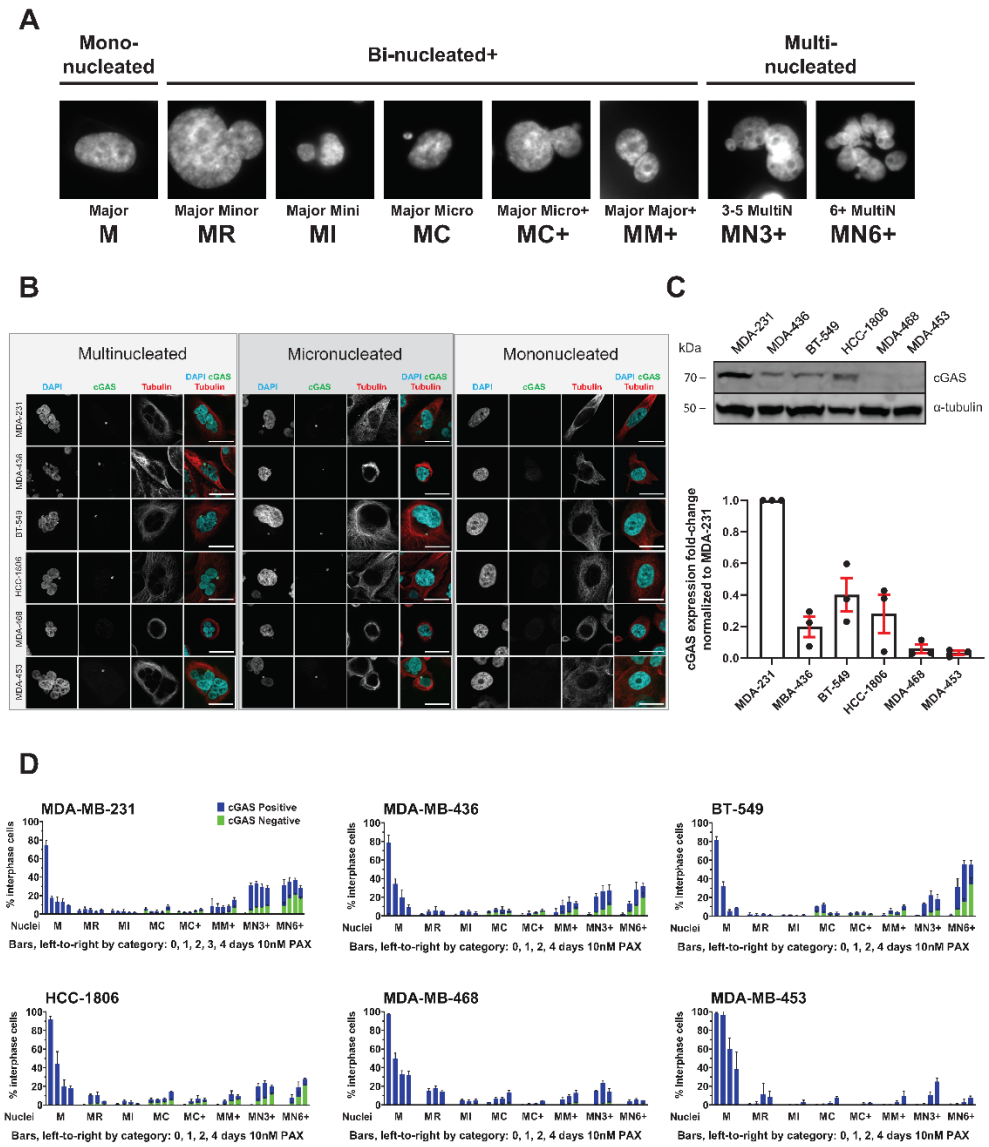

Fig. S2. Nanomolar microtubule-targeting agents such as paclitaxel cause cGAS-positive micronuclei predominantly in multinucleated TNBC cell lines.

(*A*) Representative images of categories of nuclei phenotypes that appear after 10nM paclitaxel exposure of MDA-MB-231. Text above images represent simplified quantification scheme shown in Figure 1D. Detailed quantification scheme shown in text below images was used for Figure S1D.

(*B*) Representative images of multinucleated TNBC cell lines after 10nM paclitaxel, showing cGAS-positive and cGAS-negative micronuclei. Scale bar represents 25 μm.

(*C*) Immunoblot of a panel of TNBC cell lines expressing cGAS protein with quantification of cGAS expression relative to MDA-MB-231 by LI-COR.

(*D*) Quantification of nuclei phenotypes (sum of blue and green bars) and cGAS-positivity (green bar) in TNBC interphase cell lines after 0, 1, 2 and 4 days of 10nM paclitaxel (PAX). Mean and SEM of n=3 independent biological experiments comprising ≥250 cells per condition and replicate are shown.

(*E*) Representative images of MDA-MB-231 cells treated with 10nM paclitaxel, 10nM vinorelbine or 10nM eribulin and stained for cGAS.

(*F*) Quantification of micronucleation and cGAS/STING cells in MDA-MB-231 treated with multiple treatment modalities indicates spindle-targeting treatments lead to highest rates of cGAS localization. Experiments done in triplicate (n=3) with ≥250 cells counted per experiment.

Supplemental Figure S3

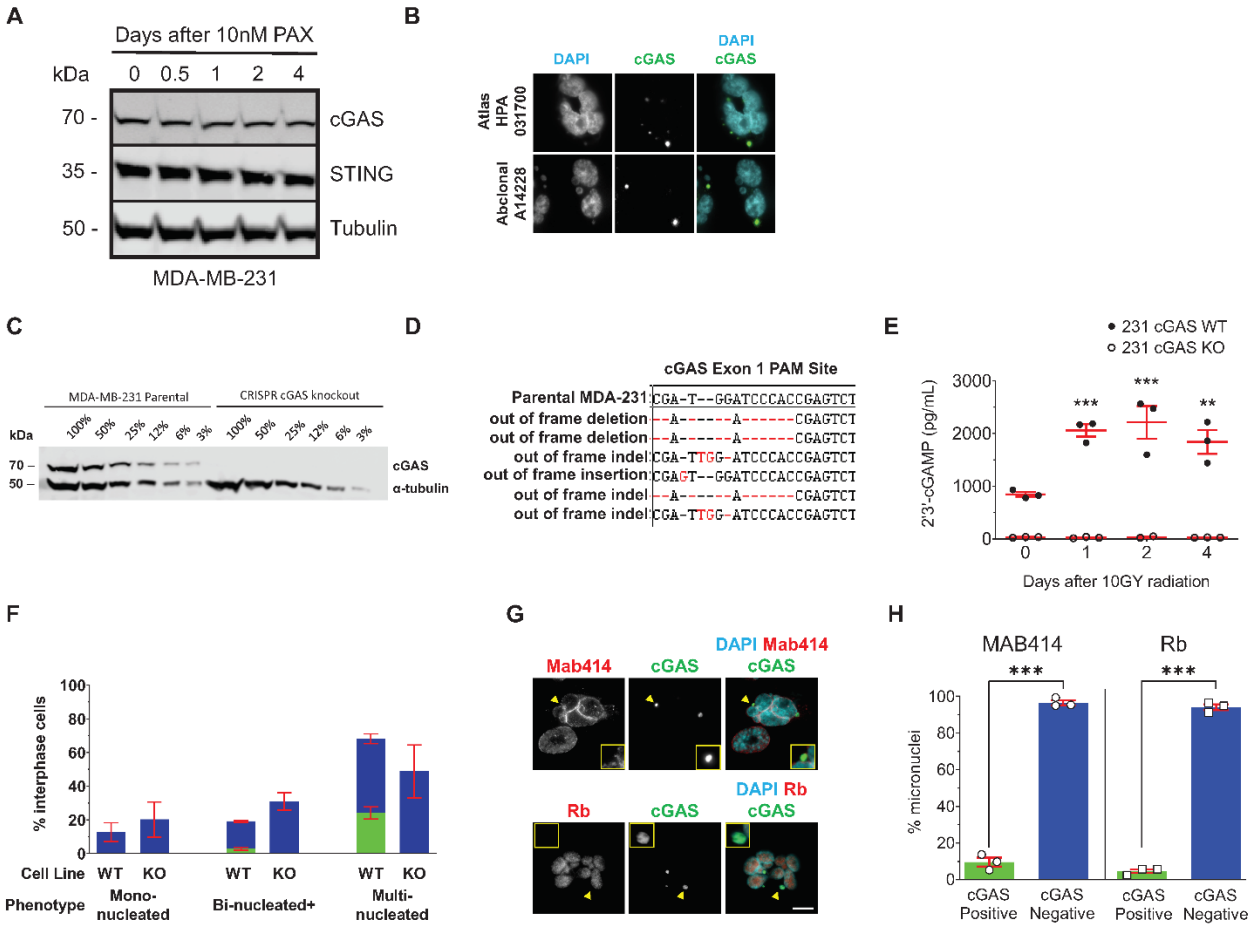

Fig. S3. cGAS is concentrated in interphase micronuclei with envelope defects after paclitaxel.

(***A***) Immunoblot of cGAS expression at 0, 4, 6 and 8 days after 10nM paclitaxel in MDA-MB-231 cells.

(***B***) Representative images of MDA-MB-231 cells exposed to 2 days paclitaxel showing cGAS-positive micronuclei stained with antibodies targeting different epitopes of cGAS protein. Scale bar represents 10μm.

(***C***) Quantification of nuclei phenotypes in MDA-MB-231 after paclitaxel for two antibodies targeting different epitopes of cGAS. See methods for more information.

(***D***) Representative immunoblot of cGAS expression in MDA-MB-231 and CRISPR-Cas9 mediated cGAS knockout.

(***E***) TA cloning of region surrounding the PAM site of cGAS gene. Image shows Sanger sequence reads of unaltered wild type cGAS DNA sequences above with cGAS knockout DNA sequences below of MDA-MB-231. Each sequence represents an individual allele of one cGAS knockout clone.

(***F***) ELISA analysis of 2'3'-cGAMP production in wild type (231 cGAS +/+) and cGAS knockout (231 cGAS -/-) MDA-MB-231 4 days after exposure to 10gy radiation. Mean and SEM of n=3 independent biological experiments are shown. P values were calculated by one-way ANOVA with Dunnett's test with control as 0 day (*P < 0.05, **P < 0.01, ***P < 0.001, ns=not significant).

(***G***) Quantification of nuclei phenotypes (sum of blue and green bars) and cGAS-positivity (green bar) in MDA-MB-231 interphase cells after 2 days of 10nM paclitaxel in wild type and cGAS knockout MDA-MB-231 using a monoclonal antibody against cGAS. N=3 independent experiments comprising ≥250 cells per condition and replicate. Mean and SEM of n=3 independent biological experiments are shown.

(***H***) Representative images of MDA-MB-231 cells stained for cGAS, Mab414, and Rb. Scale bar represents 10 μm.

(***I***) Quantification of Mab414 and Rb in micronuclei after 2 days of 10 nM paclitaxel. N=3 independent experiments comprising ≥50 cells per condition and replicate. Mean and SEM of n=3 independent biological experiments are shown. P values were calculated by two-tailed, paired Student's T test (*P < 0.05, **P < 0.01, ***P < 0.001, ns=not significant).

Supplemental Figure S4

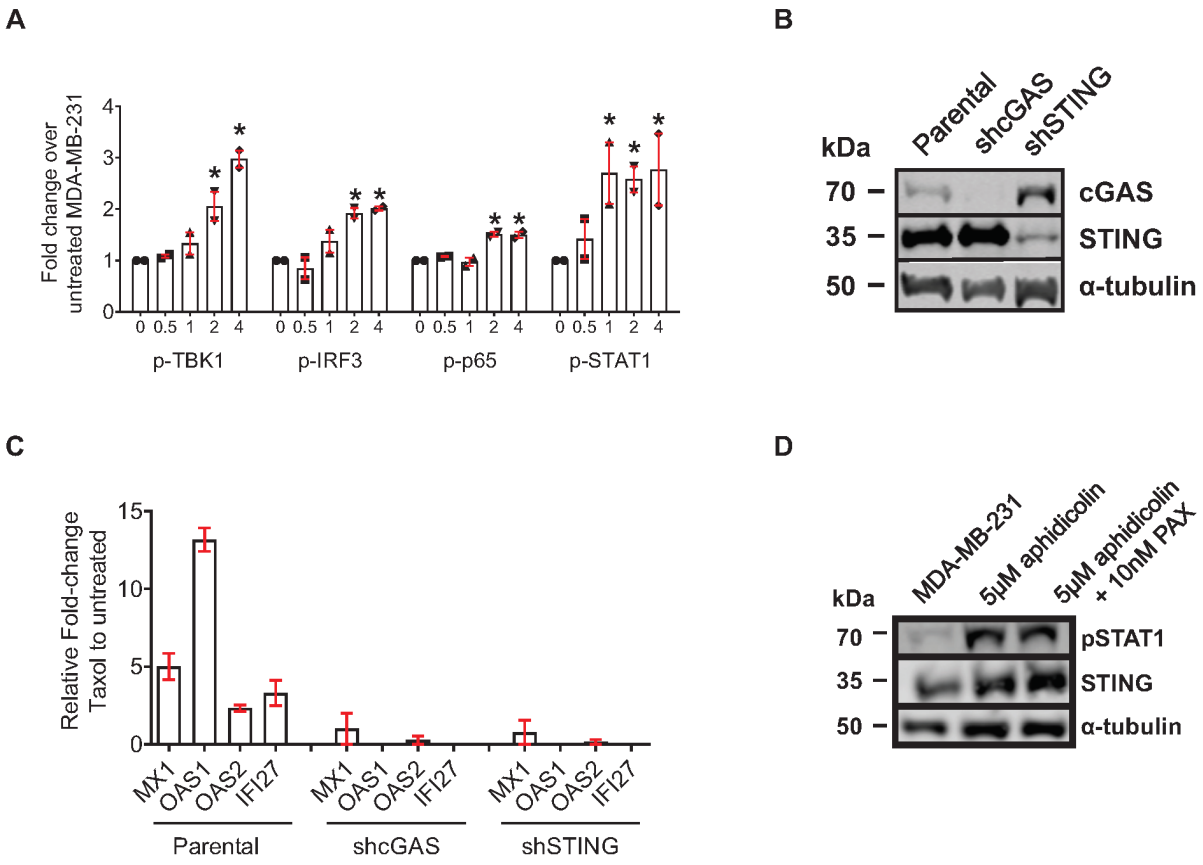

Fig. S4. Paclitaxel activates STING pathway in MDA-MB-231 but not in interphase.

(*A*) Quantification of signal intensity of Immunoblot by LICOR for Figure 3B. Red error bars represent SEM of n=3 independent experiments. P values were calculated by one-way ANOVA with Dunnett's test with comparisons based on control "0 Day" (*P < 0.05).

(*B*) Immunoblot of MDA-MB-231 parental, shcGAS and shSTING cell lines for cGAS and STING expression. Alpha-tubulin used as a loading control.

(*C*) Measurement of interferon-stimulated genes, *MX1, OAS1, OAS2, IFI27*, by RT-qPCR for MDA-MB-231 parental, shcGAS and shSTING cell lines.

(***D***) Immunoblot of MDA-MB-231 for pSTING and STING expression after aphidicolin with and without paclitaxel. Alpha-tubulin used as a loading control.

Supplemental Figure S5

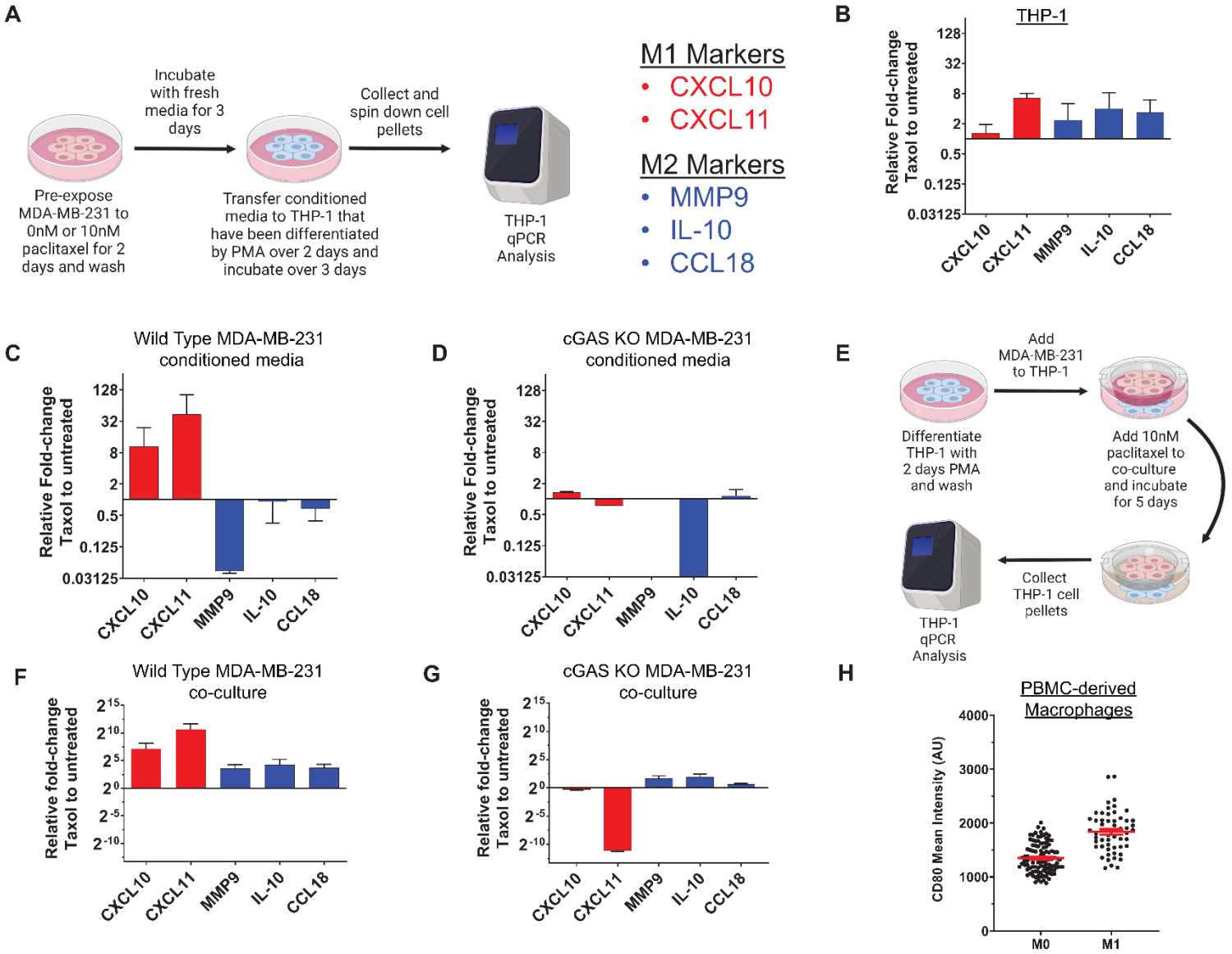

Fig. S5. THP-1 macrophages exhibit M1 polarization after exposure to conditioned media from or co-culture with MDA-MB-231 after paclitaxel.

(***A***) Schematic of mono-culture conditioned media experiments with list of M1 and M2 genes used in experiments.

(***B***) Measurement of M1/M2 gene panel of THP-1 macrophages following 4 days incubation in 10nM paclitaxel. N=2 biological experiments.

(***C***) Measurement of M1/M2 gene panel of THP-1 macrophages following 3 days incubation in 3 days conditioned media from wild type MDA-MB-231 with and without exposure to 2 days 10nM paclitaxel. N=3 biological experiments.

(***D***) Measurement of M1/M2 gene panel of THP-1 macrophages following 3 days incubation in 3 days conditioned media from cGAS knockout MDA-MB-231 with and without exposure to 2 days 10nM paclitaxel. N=3 biological experiments.

(***E***) Schematic of co-culture experiments.

(***F***) Measurement of M1/M2 gene panel of co-cultured THP-1 with wild type MDA-MB-231 with and without 5 days 10nM paclitaxel. N=2 biological experiments.

(***G***) Measurement of M1/M2 gene panel of co-cultured THP-1 with cGAS knockout MDA-MB-231 with and without 5 days 10nM paclitaxel. N=2 biological experiments.

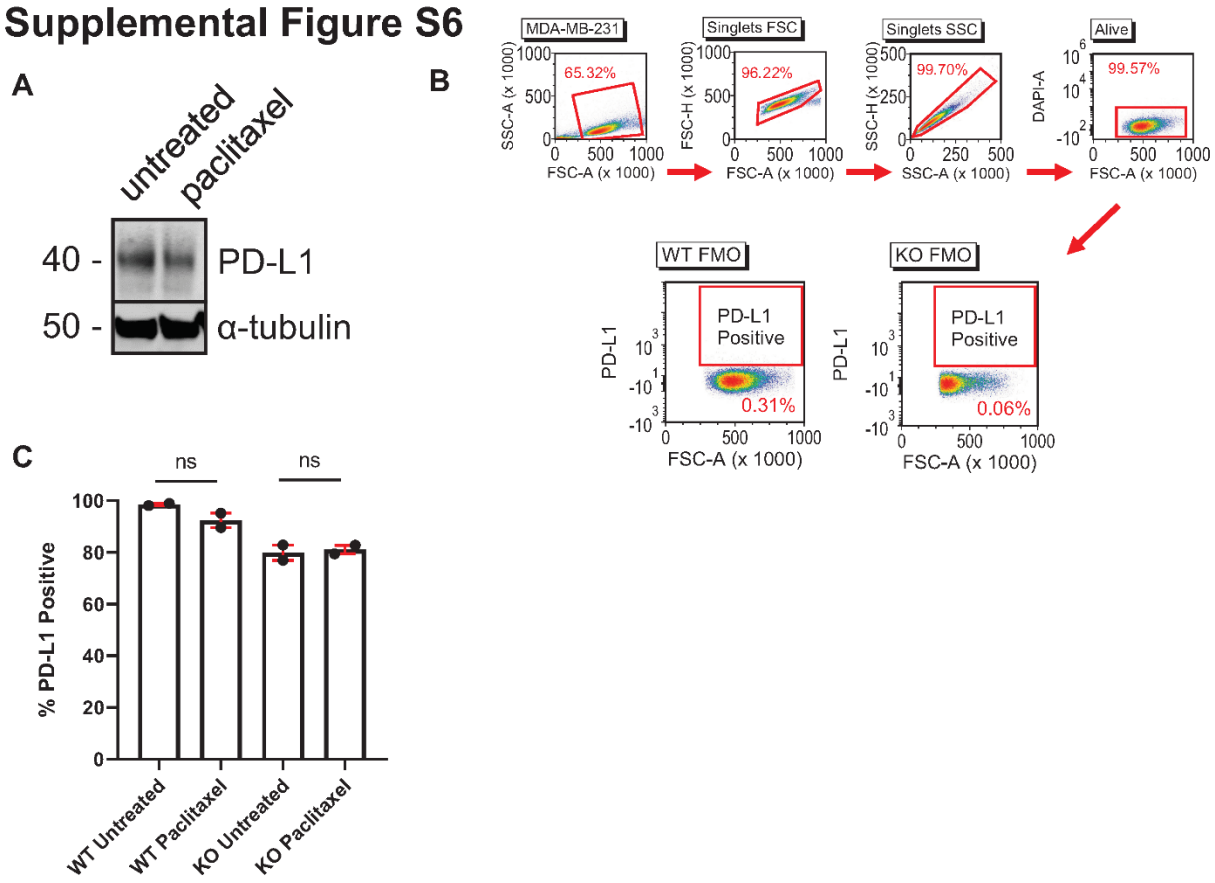

Fig. S6. Expression of PD-L1 is not modulated by nanomolar paclitaxel at the protein level.

(*A*) Representative Immunoblot of wild type MDA-MB-231 probed for total PD-L1 in MDA-MB-231 cells 4 days with or without 10nM paclitaxel. Alpha tubulin serves as the loading control.

(*B*) Flow cytometry gating strategy. MDA-MB-231 were first gated on a forward scatter (FSC)/side scatter (SSC) plot and then further gated by FSC-H and SSC-H to isolate single cells. These were then gated for live cells and then gated for the surface PD-L1 population. Fluorescence minus one (FMO) wild type and cGAS knockout MDA-MB-231 were used to determine the gate parameters for cells positive for surface PD-L1. Data

were analyzed using FCS Express 7 Research Edition software, and population frequencies expressed as percent of the live parent population.

(*C*) Quantification of surface PD-L1 by percent of the live parent population of wild type and cGAS knockout MDA-MB-231 cells before and after 3 days of 10nM paclitaxel. Mean and SEM of n=2 independent biological experiments comprising ≥100,000 events per co+ndition are shown. P values were calculated by one-way ANOVA with Tukey-Kramer test (*P < 0.05, **P < 0.01, ***P < 0.001, ns=not significant).

Supplemental Figure S7

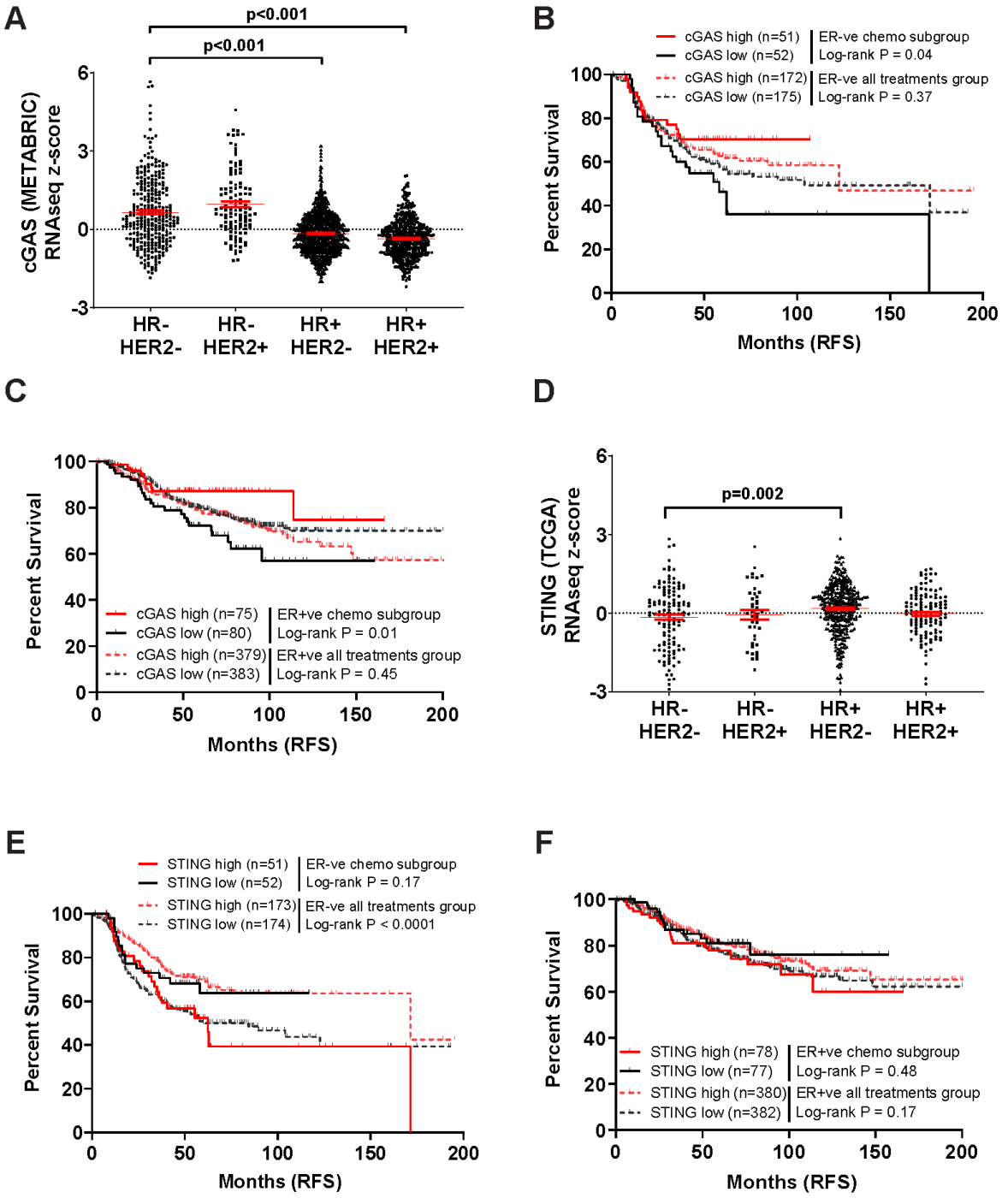

Fig. S7. cGAS expression positively correlates with progression-free survival in patients treated with chemotherapy.

(*A*) cGAS mRNA expression z-scores from breast cancer patients of METABRIC cohort categorized by subtype. A statistically significant difference (p=0.02) between HR-/HER2+ and HR-/HER2- exist. Mean and SD of individual data points are shown. P values were calculated by one-way ANOVA with Tukey-Kramer test (*P < 0.05, **P < 0.01, ***P < 0.001, ns=not significant).

(*B*) Relapse-free survival curves of ER-ve breast cancer patients stratified by cGAS mRNA expression for all treatments and system chemotherapy (taxane, anthracycline, cytoxan) only groups (cutoff: median).

(*C*) Relapse-free survival curves of ER+ve breast cancer patients stratified by cGAS mRNA expression for all treatments and chemotherapy only groups (cutoff: median).

(*D*) STING mRNA expression z-scores from breast cancer patients of TCGA cohort categorized by subtype. Mean and SD of individual data points are shown. P values were calculated by one-way ANOVA with Tukey-Kramer test (*P < 0.05, **P < 0.01, ***P < 0.001, ns=not significant).

(*E*) Relapse-free survival curves of ER-ve breast cancer patients stratified by STING mRNA expression for all treatments and system chemotherapy (taxane, anthracycline, cytoxan) only groups (cutoff: median).

(*F*) Relapse free-survival curves of ER+ve breast cancer patients stratified by STING mRNA expression for all treatments and chemotherapy only groups (cutoff: median).

CHAPTER 3: CONCLUSIONS AND FUTURE DIRECTIONS

This thesis began with a chapter on the review of the different mechanisms by which conventional therapies such as chemotherapy and radiation can activate immune signaling mechanisms. This was proceeded by a chapter examining paclitaxel activating cGAS-STING signaling to induce micronucleation and M1 macrophage polarization. We were most interested in focusing on cGAS/STING signaling over other cytosolic DNA sensors because previous literature suggested that cGAS/STING signaling is most important for activating both 2'3'-cGAMP and IFN-β production, which we believe induced M1 macrophage polarization. While other cytosolic nucleic acid sensors can also activate IFN-β signaling, we did not find ample evidence for their activation in breast cancer by paclitaxel. There is, however, some evidence for cGAS to be activated by paclitaxel signaling in breast cancer (Lohard et al., 2020; Zierhut et al., 2019a). One study did demonstrate paclitaxel to potentially serve as a TLR-4 agonist and to activate IFN-β signaling through toll-like receptor signaling, which is separate from cGAS signaling (Wanderley et al., 2018). However, that study used micromolar concentrations of paclitaxel, which is much higher than clinically relevant concentrations of paclitaxel used in our study. At lower concentrations, we did not find paclitaxel to function as a TLR4 agonist (Chapter 2, Figure S4D).

The first chapter of this thesis examined the current literature regarding mechanistic processes of conventional chemotherapies with the end goal of determining whether there is evidence for effective activation of an immune response from use of these cytotoxic therapies. While it is accepted that chemotherapies can reduce immune cell populations, recent work has suggested that the picture is more complex. For example,

in the second chapter of this thesis we examined how clinically relevant low dose paclitaxel can promote innate immune signaling by tumor cells through the cGAS/STING pathway. Past studies examined high dose paclitaxel, which would arrest cells in mitosis and directly kill them. Whether or not mitotic arrest by high dose paclitaxel can trigger a more robust immune response is not known since these drugs nonspecifically kill rapidly dividing host cells including host immune cells and would exert significant toxicity. In fact, leukopenia is a common side effect of paclitaxel.

However, it is still important to consider dosing and timing of these therapies, which can also affect optimal pathway activation. This is seen to be the case for radiation, which also activates cGAS/STING pathway. For instance, B16 and B78 melanoma cell lines achieved maximal IFNB1 gene upregulation 7 days after irradiation (Jagodinsky et al., 2021). Similarly, a single high dose of radiation results in dsDNA degradation in human cell lines by exonuclease Trex1, which dampens IFNB1 expression; however, the same dose spread over multiple days increases IFNB1 (Vanpouille-Box et al., 2017). Similar studies involving dosing and timing of conventional chemotherapies in the lab and clinical settings would be useful to test this hypothesis.

The second chapter of this thesis examined the role of paclitaxel in activating cGAS/STING to recruit an immune response. While this chapter did not include *in vivo* work, some clinical samples were examined for cGAS expression. There are few biomarkers that can predict response to combination therapies, so it was interesting to see a positive correlation between both tumor-infiltrating lymphocytes and progression free survival for combination therapy of microtubule-targeting agents and immune checkpoint inhibition.

Future studies will benefit from looking at this correlation with a larger clinical cohort of patients on neoadjuvant therapies. This analysis may be completed with currently available datasets from completed clinical trials that have combined paclitaxel with immune checkpoint inhibitors for which either bulk RNA sequencing was performed, or for which tissues are available and can be obtained for IHC analysis. Data from these trials can then be evaluated for cGAS expression by IHC or RNA sequencing. Otherwise, similar clinical trials may be designed either prospectively or retrospectively to analyze the utility of cGAS expression in predicting the effectiveness of combination therapy in patients. More importantly, syngeneic mouse studies evaluating the efficacy of combination therapy in mice implanted with either parental or cGAS-deficient tumors would help to confirm if cGAS expression is required for activation of the immune system and can predict response to combination therapy. In these studies, IHC and flow cytometry can be employed to evaluate changes in immune cell populations and tumor growth over the course of combination therapy in tumors expressing or deficient in cGAS. Macrophage polarization can also be assessed by these same methods in these tissues. In addition, primary cell cultures and organoids may provide further evidence for cGAS-STING activation after paclitaxel.

The appendices of this thesis present work suggesting the activation of cGAS-STING signaling may also be associated with chromosomal instability (CIN) in both breast cancer and leukemia in concordance with previous work (Bakhoum et al., 2018). This is hypothesized to be due to CIN causing micronuclei formation, which can rupture and activate cGAS-STING signaling. Further work will help to clarify the extent of

constitutive activation of cGAS-STING and its impact on immune signaling in breast cancers is warranted as some breast cancers do exhibit CIN (Watkins et al., 2020).

In addition, CIN has been hypothesized to cause seemingly contradictory outcomes of tumorigenesis and immune activation (Bakhoum et al., 2018; Santaguida et al., 2017). Studies suggest that the chronicity of cGAS/STING activation can influence the downstream outcomes and would be worthwhile to study from a therapeutic standpoint. For instance, CIN from underlying cancers can potentially result in chronic activation of cGAS-STING, which may blunt further activation of this signaling pathway, resulting in an immunosuppressive tumor microenvironment (Bakhoum & Cantley, 2018). Therefore, aside from validating the clinical significance of cGAS/STING in activating immunity in patients, an important question would be to evaluate the significance of constitutive cGAS/STING signaling in tumors with a high baseline level of ruptured micronuclei in affecting combination therapy response. More careful investigation of the specific factors underlying inflammation and how it results in tumorigenesis versus immune activation would be important. One way to do this would be to induce CIN or cGAS/STING activation in cell lines or organisms and then to conduct a global transcriptomic or proteomic screen for pathways that are activated or de-activated.

One advantage of using chemotherapy to activate cGAS-STING signaling over targeted STING agonists is that the response can be somewhat targeted to tumor cells with chemotherapy, which tends to be more effective in quickly dividing cells. Potentially, using chemotherapy to activate cGAS-STING would result in a more targeted immune response against tumors over normal cells, which may also be non-specifically targeted by STING agonists. One disadvantage of chemotherapy,

particularly paclitaxel, is that it does not generate neoantigens to help activate an immune response. Therefore, cGAS-STING signaling may be more effective in cancers with a high tumor mutation burden and with neoantigens that can be targeted by the immune system. Potentially, chemotherapy-induced cGAS-STING activation might be useful in future studies that use cancer vaccines to help recruit an immune response.

In conclusion, this thesis focused on how paclitaxel can activate cGAS-STING signaling to polarize macrophages to an M1 phenotype. Due to this mechanism of immune activation, we suggest that cGAS expression may have utility in predicting patient response to combination paclitaxel and checkpoint inhibitor therapy. Similar mechanistic investigations of other chemotherapies may potentially identify biomarkers that can predict combination therapy response and can be worthwhile to pursue.

APPENDIX

Chromosomal instability positively correlates to increased immune cell infiltration in cancer

Yang Hu, Ryan A. Denu, Stephanie M. McGregor, Beth A. Weaver, Mark E. Burkard

Introduction: Chromosomal INstability (CIN) refers to the repeated gain and loss of chromosomes over multiple cell divisions and is a common attribute of many cancers. CIN is caused by errors in mitosis that result in missegregation of entire chromosomes, resulting in karyotypic irregularities that have intrinsic effects on cell survival. Chromosome gain and loss may confer a survival advantage or may cause cell death due to loss of both copies of an essential chromosome. Thus, CIN is a driver of tumor evolution. However, the effect of CIN on immune regulation is controversial. The aim of this study is to explore the relationship of CIN with immune cell infiltration.

Methods: We have conducted pan-cancer gene expression analyses of public cohorts from the METABRIC and TCGA databases using CIBERSORT (Newman et al, Nature Methods, 2015), which applies gene expression data from a list of 547 genes to infer the abundances of immune cell types. Using this method, we evaluated the correlation of CIN with immune cell populations. CIN is estimated by CIN70, a score derived from 70 genes that correlate with total functional aneuploidy in solid tumors. As a complementary approach, we identified 256 patients with Stage I-III breast cancer treated at the UW Carbone Cancer center from 1999-2007. Chromosome number was determined on a cell-by-cell basis using 6 centromeric FISH probes. CIN was measured as the fraction of cells

with non-modal chromosome numbers averaged across the 6 chromosomes. The abundance of stromal tumor-infiltrating lymphocytes (TILs) on H&E slides was determined by a breast pathologist according to the 2014 International TILs Working Group criteria.

Results: CIBERSORT analysis demonstrates statistically significant, positive correlations between CIN70 and immune cells for activated CD4 memory T cells (R-squared=0.11, p-value<0.0001) and M1 macrophages (R-squared=0.11, p-value<0.0001) in the majority of cancer types evaluated. For the cohort of 256 patients with breast cancer, tumors enriched for TILs had significantly higher CIN (0.50 +/- 0.02) compared to tumors with low levels of TILs (0.41 +/- 0.01, p-value=0.002). This result was unaffected by exclusion of highly necrotic tissues, which are known to recruit TILs. Together, these data support the conclusion that CIN tumors have higher levels of immune cell infiltration, although the function of these immune cells remains unclear.

Figures

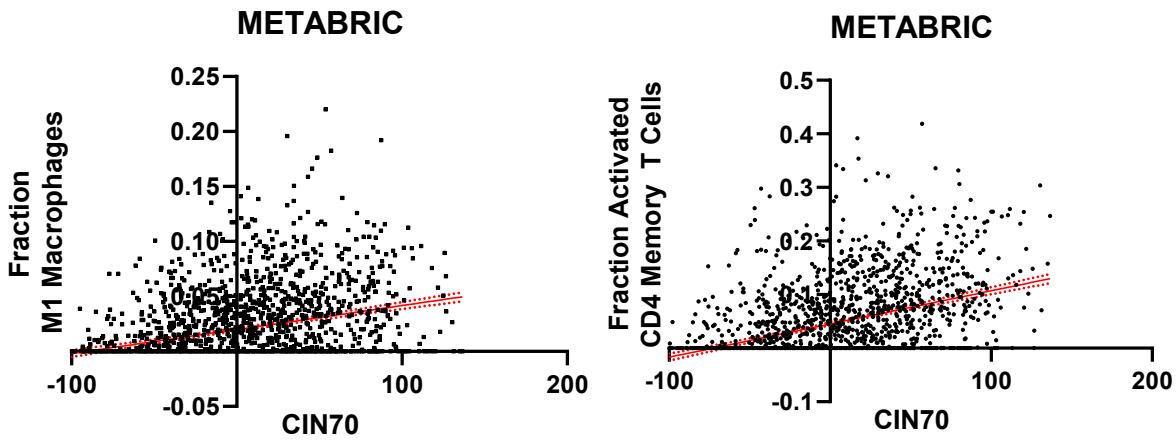

Fig. 1: CIN70 correlates with activated CD4 T-cells and M1 macrophages in the METABRIC cohort. mRNA sequencing data from METABRIC dataset of 2509 primary breast tumors was evaluated for CIN70 gene score on a per-patient basis. CIBERSORT was used to estimate immune cell populations on a per-patient basis. CIN70 was correlated with fraction of activated M1 macrophages and CD4+ memory T-cells. Pearson R (CIN70 vs Activated CD4 Memory T Cells) = 0.4238, P-value < 0.0001. Pearson R (CIN70 vs M1 Macrophages) = 0.3236, P-value < 0.0001.

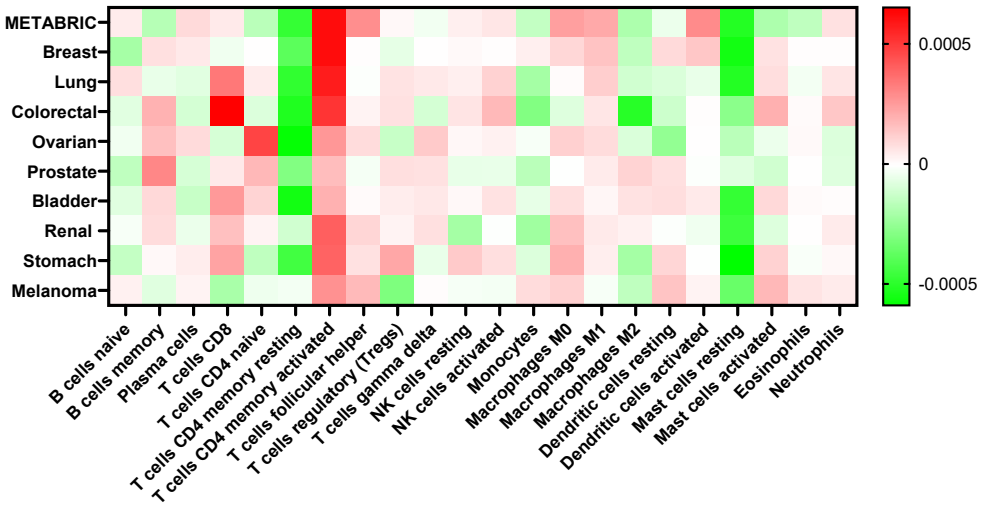
METABRIC
Breast
Lung
Colorectal
Ovarian
Prostate
Bladder
Renal
Stomach
Melanoma
B cells naive
B cells memory
Plasma cells
T cells CD8
T cells CD4 naive
T cells CD4 memory resting
T cells CD4 memory activated
T cells follicular helper
T cells regulatory (Tregs)
T cells gamma delta
NK cells resting
NK cells activated
Monocytes
Macrophages M0
Macrophages M1
Macrophages M2
Dendritic cells resting
Dendritic cells activated
Mast cells resting
Mast cells activated
Eosinophils
Neutrophils
0.0005
0
-0.0005

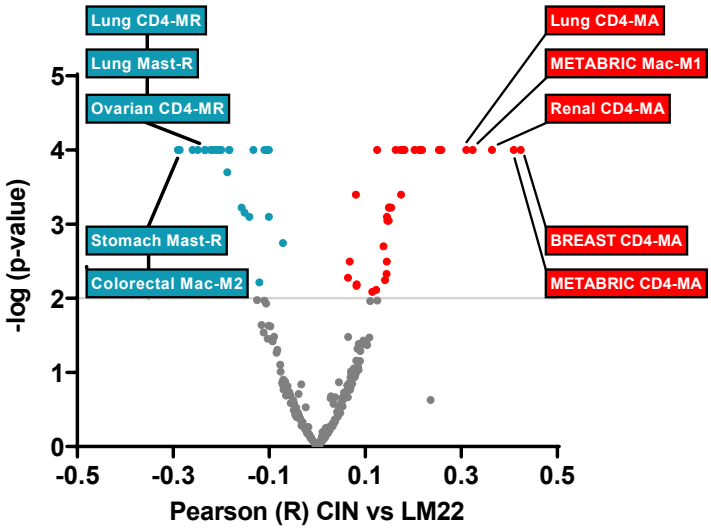
Lung CD4-MR
Lung Mast-R
Ovarian CD4-MR
Stomach Mast-R
Colorectal Mac-M2
Lung CD4-MA
METABRIC Mac-M1
Renal CD4-MA
BREAST CD4-MA
METABRIC CD4-MA
-log (p-value)
Pearson (R) CIN vs LM22

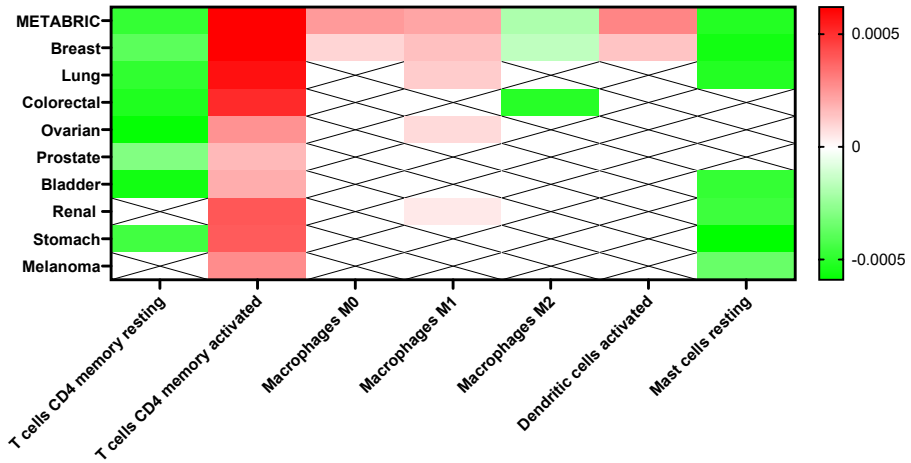
METABRIC
Breast
Lung
Colorectal
Ovarian
Prostate
Bladder
Renal
Stomach
Melanoma
T cells CD4 memory resting
T cells CD4 memory activated
Macrophages M0
Macrophages M1
Macrophages M2
Dendritic cells activated
Mast cells resting
0.0005
0
-0.0005

Fig. 2: Pan-cancer analyses of METABRIC and TCGA mRNA gene expression datasets show CIN70 to correlate with activated CD4 T-cells in pan-cancer. *(Top)* Heat map represents strength of correlations by Pearson R between CIN70 gene score and CIBERSORT-derived immune cell populations using mRNA expression from METABRIC and TCGA datasets. Red boxes indicate positive correlations between CIN70 and indicated immune cell population by cancer database. Green boxes indicate negative correlations. *(Middle)* Volcano plot showing top five most positively (red) and negatively correlated (blue) immune cell populations by CIN70 gene score. *(Bottom)* Statistically significant correlations are in green and red boxes while non-significant correlations are crossed out.

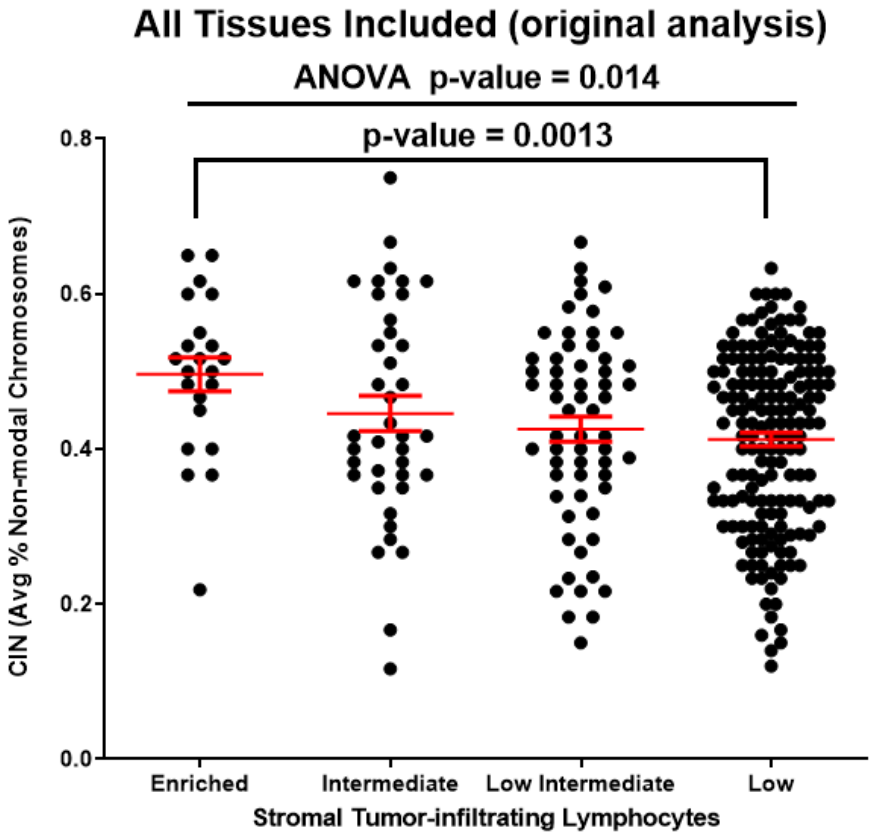

Fig. 3: CIN assessed by 6-chromosome FISH positively correlates with TILs by H&E in clinical samples.

More than 250 primary breast cancer patient biopsies were evaluated by H&E for stromal tumor-infiltrating lymphocytes using the 2014 International TILs Working Group criteria. Samples were also stained for chromosomes 3, 4, 7, 9, 10 and 17 to determine average ploidy for CIN calculations as described in *Choudhary et al. Mol Cancer Ther. 2016*.

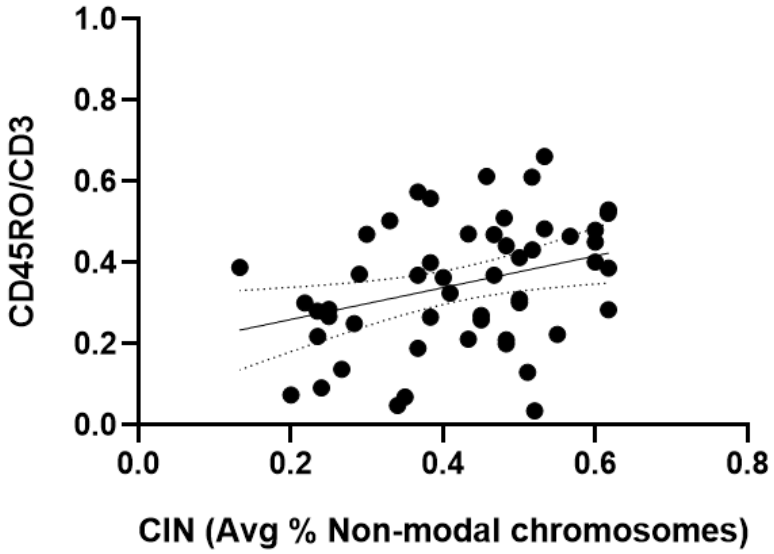

Fig. 4: CIN assessed by 6-chromosome FISH positively correlates with CD4+ T-cells by CD45RO expression in clinical samples.

More than 60 primary breast cancer patient biopsies were evaluated by CD45RO expression by immunofluorescence intensity for CD4+ T-cells and CD3 expression for T-cells. CIN was calculated by 6-chromosome FISH and CD45RO expression was normalized to CD3 expression on a cell-by-cell basis.

Chromosomal instability upregulates interferon in acute myeloid leukemia

Ning Jin, Robert F. Lera, Rachel E. Yan, Fen Guo, Kim Oxendine, Vanessa L. Horner, Yang Hu, Jun Wan, Ryan J. Mattison, Beth A. Weaver, Mark E. Burkard

Abstract: Chromosome instability (CIN) generates genetic and karyotypic diversity that is common in hematological malignancies. Low to moderate levels of CIN are well tolerated and can promote cancer proliferation. However, high levels of CIN are lethal. Thus, CIN may serve both as a prognostic factor to predict clinical outcome and as a predictive biomarker. A retrospective study was performed to evaluate CIN in acute myeloid leukemia (AML). Chromosome mis-segregation frequency was correlated with clinical outcome in bone marrow core biopsy specimens from 17 AML cases. Additionally, we induced chromosome segregation errors in AML cell lines with AZ3146, an inhibitor of the Mps1 mitotic checkpoint kinase, to quantify the phenotypic effects of high CIN. We observed a broad distribution of chromosome mis-segregation frequency in AML bone marrow core specimens. High CIN correlated with complex karyotype in AML, as expected, although there was no clear survival effect. In addition to CIN, experimentally inducing chromosome segregation errors by Mps1 inhibition in AML cell lines causes DNA damage, micronuclei formation, and upregulation of interferon stimulated genes. High levels of CIN appear to be immunostimulatory, suggesting an opportunity to combine mitotic checkpoint inhibitors with immunotherapy in treatment of AML.

REFERENCES

Adams, S., Loi, S., Toppmeyer, D., Cescon, D. W., De Laurentiis, M., Nanda, R., Winer, E. P., Mukai, H., Tamura, K., Armstrong, A., Liu, M. C., Iwata, H., Ryvo, L., Wimberger, P., Rugo, H. S., Tan, A. R., Jia, L., Ding, Y., Karantza, V., & Schmid, P. (2019). Pembrolizumab monotherapy for previously untreated, PD-L1-positive, metastatic triple-negative breast cancer: Cohort B of the phase II KEYNOTE-086 study. *Annals of Oncology: Official Journal of the European Society for Medical Oncology*, *30*(3), 405–411. https://doi.org/10.1093/annonc/mdy518

Ahlmann, M., & Hempel, G. (2016). The effect of cyclophosphamide on the immune system: Implications for clinical cancer therapy. *Cancer Chemotherapy and Pharmacology*, *78*(4), 661–671. https://doi.org/10.1007/s00280-016-3152-1

Alizadeh, D., Trad, M., Hanke, N. T., Larmonier, C. B., Janikashvili, N., Bonnotte, B., Katsanis, E., & Larmonier, N. (2014). Doxorubicin eliminates myeloid-derived suppressor cells and enhances the efficacy of adoptive T-cell transfer in breast cancer. *Cancer Research*, *74*(1), 104–118. https://doi.org/10.1158/0008-5472.CAN-13-1545

Amiel, E., Everts, B., Freitas, T. C., King, I. L., Curtis, J. D., Pearce, E. L., & Pearce, E. J. (2012). Inhibition of mTOR promotes dendritic cell activation and enhances therapeutic autologous vaccination in mice. *Journal of Immunology (Baltimore, Md. : 1950)*, *189*(5), 2151–2158. https://doi.org/10.4049/jimmunol.1103741

An, X., Zhu, Y., Zheng, T., Wang, G., Zhang, M., Li, J., Ji, H., Li, S., Yang, S., Xu, D., Li, Z., Wang, T., He, Y., Zhang, L., Yang, W., Zhao, R., Hao, D., & Li, X. (2019). An Analysis of the Expression and Association with Immune Cell Infiltration of the cGAS/STING Pathway in Pan-Cancer. *Molecular Therapy - Nucleic Acids*, *14*, 80–89. https://doi.org/10.1016/j.omtn.2018.11.003

Anderson, K. G., Stromnes, I. M., & Greenberg, P. D. (2017). Obstacles posed by the tumor microenvironment to T cell activity: A case for synergistic therapies. *Cancer Cell*, *31*(3), 311–325. https://doi.org/10.1016/j.ccell.2017.02.008

Aoto, K., Mimura, K., Okayama, H., Saito, M., Chida, S., Noda, M., Nakajima, T., Saito, K., Abe, N., Ohki, S., Ohtake, T., Takenoshita, S., & Kono, K. (2018). Immunogenic tumor cell death induced by chemotherapy in patients with breast cancer and esophageal squamous cell carcinoma. *Oncology Reports*, *39*(1), 151–159. https://doi.org/10.3892/or.2017.6097

Asbury, C. L. (2017). Anaphase A: Disassembling Microtubules Move Chromosomes toward Spindle Poles. *Biology*, *6*(1). https://doi.org/10.3390/biology6010015

Awwad, M., & North, R. J. (1988). Cyclophosphamide (Cy)-facilitated adoptive immunotherapy of a Cy-resistant tumour. Evidence that Cy permits the expression of

adoptive T-cell mediated immunity by removing suppressor T cells rather than by reducing tumour burden. *Immunology*, *65*(1), 87–92.

Bailly, C., Thuru, X., & Quesnel, B. (2020). Combined cytotoxic chemotherapy and immunotherapy of cancer: Modern times. *NAR Cancer*, *2*(zcaa002). https://doi.org/10.1093/narcan/zcaa002

Bakhoum, S. F., & Cantley, L. C. (2018). The multifaceted role of chromosomal instability in cancer and its microenvironment. *Cell*, *174*(6), 1347–1360. https://doi.org/10.1016/j.cell.2018.08.027

Bakhoum, S. F., Ngo, B., Laughney, A. M., Cavallo, J.-A., Murphy, C. J., Ly, P., Shah, P., Sriram, R. K., Watkins, T. B. K., Taunk, N. K., Duran, M., Pauli, C., Shaw, C., Chadalavada, K., Rajasekhar, V. K., Genovese, G., Venkatesan, S., Birkbak, N. J., McGranahan, N., … Cantley, L. C. (2018). Chromosomal instability drives metastasis through a cytosolic DNA response. *Nature*, *553*(7689), 467–472. https://doi.org/10.1038/nature25432

Bakhoum, S. F., & Swanton, C. (2014). Chromosomal instability, aneuploidy, and cancer. *Frontiers in Oncology*, *4*, 161. https://doi.org/10.3389/fonc.2014.00161

Bartsch, K., Knittler, K., Borowski, C., Rudnik, S., Damme, M., Aden, K., Spehlmann, M. E., Frey, N., Saftig, P., Chalaris, A., & Rabe, B. (2017). Absence of RNase H2 triggers generation of immunogenic micronuclei removed by autophagy. *Human Molecular Genetics*, *26*(20), 3960–3972. https://doi.org/10.1093/hmg/ddx283

Baselga, J., & Albanell, J. (2001). Mechanism of action of anti-HER2 monoclonal antibodies. *Annals of Oncology*, *12*, S35–S41. https://doi.org/10.1093/annonc/12.suppl_1.S35

Baskar, R., Dai, J., Wenlong, N., Yeo, R., & Yeoh, K.-W. (2014). Biological response of cancer cells to radiation treatment. *Frontiers in Molecular Biosciences*, *1*. https://doi.org/10.3389/fmolb.2014.00024

Bazhin, A. V., von Ahn, K., Fritz, J., Werner, J., & Karakhanova, S. (2018). Interferon-α Up-Regulates the Expression of PD-L1 Molecules on Immune Cells Through STAT3 and p38 Signaling. *Frontiers in Immunology*, *9*. https://doi.org/10.3389/fimmu.2018.02129

Beaudouin, J., Gerlich, D., Daigle, N., Eils, R., & Ellenberg, J. (2002). Nuclear Envelope Breakdown Proceeds by Microtubule-Induced Tearing of the Lamina. *Cell*, *108*(1), 83–96. https://doi.org/10.1016/S0092-8674(01)00627-4

Ben-David, U., & Amon, A. (2020). Context is everything: Aneuploidy in cancer. *Nature Reviews Genetics*, *21*(1), 44–62. https://doi.org/10.1038/s41576-019-0171-x

Benedetti, R., Dell'Aversana, C., Giorgio, C., Astorri, R., & Altucci, L. (2017). Breast Cancer Vaccines: New Insights. *Frontiers in Endocrinology*, *8*. https://doi.org/10.3389/fendo.2017.00270

Bharadwaj, R., & Yu, H. (2004). The spindle checkpoint, aneuploidy, and cancer. *Oncogene*, *23*(11), 2016–2027. https://doi.org/10.1038/sj.onc.1207374

Birkbak, N. J., Eklund, A. C., Li, Q., McClelland, S. E., Endesfelder, D., Tan, P., Tan, I. B., Richardson, A. L., Szallasi, Z., & Swanton, C. (2011). Paradoxical relationship between chromosomal instability and survival outcome in cancer. *Cancer Research*, *71*(10), 3447–3452. https://doi.org/10.1158/0008-5472.CAN-10-3667

Boilève, A., Senovilla, L., Vitale, I., Lissa, D., Martins, I., Métivier, D., van den Brink, S., Clevers, H., Galluzzi, L., Castedo, M., & Kroemer, G. (2013). Immunosurveillance against tetraploidization-induced colon tumorigenesis. *Cell Cycle (Georgetown, Tex.)*, *12*(3), 473–479. https://doi.org/10.4161/cc.23369

Bokros, M., & Wang, Y. (2016). Spindle assembly checkpoint silencing and beyond. *Cell Cycle (Georgetown, Tex.)*, *15*(13), 1661–1662. https://doi.org/10.1080/15384101.2016.1176396

Bracci, L., Schiavoni, G., Sistigu, A., & Belardelli, F. (2014). Immune-based mechanisms of cytotoxic chemotherapy: Implications for the design of novel and rationale-based combined treatments against cancer. *Cell Death and Differentiation*, *21*(1), 15–25. https://doi.org/10.1038/cdd.2013.67

Burkard, M. E., & Weaver, B. A. (2017). Tuning Chromosomal Instability to Optimize Tumor Fitness. *Cancer Discovery*, *7*(2), 134–136. https://doi.org/10.1158/2159-8290.CD-16-1415

Carnevalli, L. S., Sinclair, C., Taylor, M. A., Gutierrez, P. M., Langdon, S., Coenen-Stass, A. M. L., Mooney, L., Hughes, A., Jarvis, L., Staniszewska, A., Crafter, C., Sidders, B., Hardaker, E., Hudson, K., & Barry, S. T. (2018). PI3Kα/δ inhibition promotes anti-tumor immunity through direct enhancement of effector CD8+ T-cell activity. *Journal for ImmunoTherapy of Cancer*, *6*(1), 158. https://doi.org/10.1186/s40425-018-0457-0

Carozza, J. A., Böhnert, V., Nguyen, K. C., Skariah, G., Shaw, K. E., Brown, J. A., Rafat, M., von Eyben, R., Graves, E. E., Glenn, J. S., Smith, M., & Li, L. (2020). Extracellular cGAMP is a cancer-cell-produced immunotransmitter involved in radiation-induced anticancer immunity. *Nature Cancer*, *1*(2), 184–196. https://doi.org/10.1038/s43018-020-0028-4

Chang, Z.-L. (2009). Recent development of the mononuclear phagocyte system: In memory of Metchnikoff and Ehrlich on the 100th Anniversary of the 1908 Nobel Prize in

Physiology or Medicine. *Biology of the Cell*, *101*(12), 709–721. https://doi.org/10.1042/BC20080227

Cheeseman, I. M. (2014). The Kinetochore. *Cold Spring Harbor Perspectives in Biology*, *6*(7). https://doi.org/10.1101/cshperspect.a015826

Chen, M.-T., Sun, H.-F., Zhao, Y., Fu, W.-Y., Yang, L.-P., Gao, S.-P., Li, L.-D., Jiang, H., & Jin, W. (2017). Comparison of patterns and prognosis among distant metastatic breast cancer patients by age groups: A SEER population-based analysis. *Scientific Reports*, *7*(1), 9254. https://doi.org/10.1038/s41598-017-10166-8

Compton, D. A. (2011). Mechanisms of Aneuploidy. *Current Opinion in Cell Biology*, *23*(1), 109–113. https://doi.org/10.1016/j.ceb.2010.08.007

Cooper, G. M. (2000). The Eukaryotic Cell Cycle. *The Cell: A Molecular Approach. 2nd Edition*. https://www.ncbi.nlm.nih.gov/books/NBK9876/

Cordova, A. F., Ritchie, C., Böhnert, V., Mardjuki, R. E., & Li, L. (2020). Murine M1 macrophages are among the direct responders to tumor-derived extracellular cGAMP and their human counterparts use SLC46A2 to import cGAMP. *BioRxiv*, 2020.04.15.043299. https://doi.org/10.1101/2020.04.15.043299

Corrales, L., Glickman, L. H., McWhirter, S. M., Kanne, D. B., Sivick, K. E., Katibah, G. E., Woo, S.-R., Lemmens, E., Banda, T., Leong, J. J., Metchette, K., Dubensky, T. W., & Gajewski, T. F. (2015). Direct Activation of STING in the Tumor Microenvironment Leads to Potent and Systemic Tumor Regression and Immunity. *Cell Reports*, *11*(7), 1018–1030. https://doi.org/10.1016/j.celrep.2015.04.031

Corrales, L., Matson, V., Flood, B., Spranger, S., & Gajewski, T. F. (2017). Innate immune signaling and regulation in cancer immunotherapy. *Cell Research*, *27*(1), 96–108. https://doi.org/10.1038/cr.2016.149

Cortes, J., Cescon, D. W., Rugo, H. S., Nowecki, Z., Im, S.-A., Yusof, M. M., Gallardo, C., Lipatov, O., Barrios, C. H., Holgado, E., Iwata, H., Masuda, N., Otero, M. T., Gokmen, E., Loi, S., Guo, Z., Zhao, J., Aktan, G., Karantza, V., … Frances, V.-A. (2020). Pembrolizumab plus chemotherapy versus placebo plus chemotherapy for previously untreated locally recurrent inoperable or metastatic triple-negative breast cancer (KEYNOTE-355): A randomised, placebo-controlled, double-blind, phase 3 clinical trial. *The Lancet*, *396*(10265), 1817–1828. https://doi.org/10.1016/S0140-6736(20)32531-9

Curiel, T. J., Wei, S., Dong, H., Alvarez, X., Cheng, P., Mottram, P., Krzysiek, R., Knutson, K. L., Daniel, B., Zimmermann, M. C., David, O., Burow, M., Gordon, A., Dhurandhar, N., Myers, L., Berggren, R., Hemminki, A., Alvarez, R. D., Emilie, D., … Zou, W. (2003). Blockade of B7-H1 improves myeloid dendritic cell-mediated antitumor immunity. *Nature Medicine*, *9*(5), 562–567. https://doi.org/10.1038/nm863

Curran, E. K., Chen, X., Corrales, L., & Kline, J. (2014). Activation of the Sting Pathway Enhances Immunity and Improves Survival in a Murine Myeloid Leukemia Model. *Blood*, *124*(21), 3759–3759. https://doi.org/10.1182/blood.V124.21.3759.3759

Curran, E., Mattingly, J., Godley, L., & Kline, J. (2017). Role of Ddx41 in the Stimulator of Interferon Genes (STING) Pathway. *Clinical Lymphoma Myeloma and Leukemia*, *17*, S395. https://doi.org/10.1016/j.clml.2017.07.251

Demaria, S., Volm, M. D., Shapiro, R. L., Yee, H. T., Oratz, R., Formenti, S. C., Muggia, F., & Symmans, W. F. (2001). Development of tumor-infiltrating lymphocytes in breast cancer after neoadjuvant paclitaxel chemotherapy. *Clinical Cancer Research: An Official Journal of the American Association for Cancer Research*, *7*(10), 3025–3030.

Deng, L., Liang, H., Xu, M., Yang, X., Burnette, B., Arina, A., Li, X.-D., Mauceri, H., Beckett, M., Darga, T., Huang, X., Gajewski, T. F., Chen, Z. J., Fu, Y.-X., & Weichselbaum, R. R. (2014). STING-Dependent Cytosolic DNA Sensing Promotes Radiation-Induced Type I Interferon-Dependent Antitumor Immunity in Immunogenic Tumors. *Immunity*, *41*(5), 843–852. https://doi.org/10.1016/j.immuni.2014.10.019

Dent, R., Trudeau, M., Pritchard, K. I., Hanna, W. M., Kahn, H. K., Sawka, C. A., Lickley, L. A., Rawlinson, E., Sun, P., & Narod, S. A. (2007). Triple-Negative Breast Cancer: Clinical Features and Patterns of Recurrence. *Clinical Cancer Research*, *13*(15), 4429–4434. https://doi.org/10.1158/1078-0432.CCR-06-3045

Derry, W. B., Wilson, L., & Jordan, M. A. (1995). Substoichiometric Binding of Taxol Suppresses Microtubule Dynamics. *Biochemistry*, *34*(7), 2203–2211. https://doi.org/10.1021/bi00007a014

Doherty, M. R., Cheon, H., Junk, D. J., Vinayak, S., Varadan, V., Telli, M. L., Ford, J. M., Stark, G. R., & Jackson, M. W. (2017). Interferon-beta represses cancer stem cell properties in triple-negative breast cancer. *Proceedings of the National Academy of Sciences of the United States of America*, *114*(52), 13792–13797. https://doi.org/10.1073/pnas.1713728114

Downey, C. M., Aghaei, M., Schwendener, R. A., & Jirik, F. R. (2014). DMXAA Causes Tumor Site-Specific Vascular Disruption in Murine Non-Small Cell Lung Cancer, and like the Endogenous Non-Canonical Cyclic Dinucleotide STING Agonist, 2′3′-cGAMP, Induces M2 Macrophage Repolarization. *PLOS ONE*, *9*(6), e99988. https://doi.org/10.1371/journal.pone.0099988

Dumont, F. J., Staruch, M. J., Koprak, S. L., Melino, M. R., & Sigal, N. H. (1990). Distinct mechanisms of suppression of murine T cell activation by the related macrolides FK-506 and rapamycin. *The Journal of Immunology*, *144*(1), 251–258.

Emens, L. A. (2018). Breast Cancer Immunotherapy: Facts and Hopes. *Clinical Cancer Research*, *24*(3), 511–520. https://doi.org/10.1158/1078-0432.CCR-16-3001

Emens, L. A., & Middleton, G. (2015). The Interplay of Immunotherapy and Chemotherapy: Harnessing Potential Synergies. *Cancer Immunology Research*, *3*(5), 436–443. https://doi.org/10.1158/2326-6066.CIR-15-0064

Feng, X., Tubbs, A., Zhang, C., Tang, M., Sridharan, S., Wang, C., Jiang, D., Su, D., Zhang, H., Chen, Z., Nie, L., Xiong, Y., Huang, M., Nussenzweig, A., & Chen, J. (2020). ATR inhibition potentiates ionizing radiation-induced interferon response via cytosolic nucleic acid-sensing pathways. *The EMBO Journal*, *39*(14), e104036. https://doi.org/10.15252/embj.2019104036

Fischer, M., Dang, C. V., & DeCaprio, J. A. (2018). Chapter 17—Control of Cell Division. In R. Hoffman, E. J. Benz, L. E. Silberstein, H. E. Heslop, J. I. Weitz, J. Anastasi, M. E. Salama, & S. A. Abutalib (Eds.), *Hematology (Seventh Edition)* (pp. 176–185). Elsevier. https://doi.org/10.1016/B978-0-323-35762-3.00017-2

Foley, E. A., & Kapoor, T. M. (2013). Microtubule attachment and spindle assembly checkpoint signalling at the kinetochore. *Nature Reviews. Molecular Cell Biology*, *14*(1), 25–37. https://doi.org/10.1038/nrm3494

Fu, J., Kanne, D. B., Leong, M., Glickman, L. H., McWhirter, S. M., Lemmens, E., Mechette, K., Leong, J. J., Lauer, P., Liu, W., Sivick, K. E., Zeng, Q., Soares, K. C., Zheng, L., Portnoy, D. A., Woodward, J. J., Pardoll, D. M., Dubensky, T. W., & Kim, Y. (2015). STING agonist formulated cancer vaccines can cure established tumors resistant to PD-1 blockade. *Science Translational Medicine*, *7*(283), 283ra52. https://doi.org/10.1126/scitranslmed.aaa4306

Fucikova, J., Kepp, O., Kasikova, L., Petroni, G., Yamazaki, T., Liu, P., Zhao, L., Spisek, R., Kroemer, G., & Galluzzi, L. (2020). Detection of immunogenic cell death and its relevance for cancer therapy. *Cell Death & Disease*, *11*(11), 1–13. https://doi.org/10.1038/s41419-020-03221-2

Fucikova, J., Kralikova, P., Fialova, A., Brtnicky, T., Rob, L., Bartunkova, J., & Spísek, R. (2011). Human tumor cells killed by anthracyclines induce a tumor-specific immune response. *Cancer Research*, *71*(14), 4821–4833. https://doi.org/10.1158/0008-5472.CAN-11-0950

Fujiuchi, N., Aglipay, J. A., Ohtsuka, T., Maehara, N., Sahin, F., Su, G. H., Lee, S. W., & Ouchi, T. (2004). Requirement of IFI16 for the maximal activation of p53 induced by ionizing radiation. *The Journal of Biological Chemistry*, *279*(19), 20339–20344. https://doi.org/10.1074/jbc.M400344200

Galluzzi, L., Vitale, I., Warren, S., Adjemian, S., Agostinis, P., Martinez, A. B., Chan, T. A., Coukos, G., Demaria, S., Deutsch, E., Draganov, D., Edelson, R. L., Formenti, S. C., Fucikova, J., Gabriele, L., Gaipl, U. S., Gameiro, S. R., Garg, A. D., Golden, E., … Marincola, F. M. (2020). Consensus guidelines for the definition, detection and

interpretation of immunogenic cell death. *Journal for Immunotherapy of Cancer*, *8*(1). https://doi.org/10.1136/jitc-2019-000337

Gao, G., Wang, Z., Qu, X., & Zhang, Z. (2020). Prognostic value of tumor-infiltrating lymphocytes in patients with triple-negative breast cancer: A systematic review and meta-analysis. *BMC Cancer*, *20*. https://doi.org/10.1186/s12885-020-6668-z

Garcia-Diaz, A., Shin, D. S., Moreno, B. H., Saco, J., Escuin-Ordinas, H., Rodriguez, G. A., Zaretsky, J. M., Sun, L., Hugo, W., Wang, X., Parisi, G., Saus, C. P., Torrejon, D. Y., Graeber, T. G., Comin-Anduix, B., Hu-Lieskovan, S., Damoiseaux, R., Lo, R. S., & Ribas, A. (2017). Interferon Receptor Signaling Pathways Regulating PD-L1 and PD-L2 Expression. *Cell Reports*, *19*(6), 1189–1201. https://doi.org/10.1016/j.celrep.2017.04.031

Gascoigne, K. E., & Taylor, S. S. (2009). How do anti-mitotic drugs kill cancer cells? *Journal of Cell Science*, *122*(Pt 15), 2579–2585. https://doi.org/10.1242/jcs.039719

Genard, G., Lucas, S., & Michiels, C. (2017). Reprogramming of Tumor-Associated Macrophages with Anticancer Therapies: Radiotherapy versus Chemo- and Immunotherapies. *Frontiers in Immunology*, *8*, 828. https://doi.org/10.3389/fimmu.2017.00828

Genin, M., Clement, F., Fattaccioli, A., Raes, M., & Michiels, C. (2015). M1 and M2 macrophages derived from THP-1 cells differentially modulate the response of cancer cells to etoposide. *BMC Cancer*, *15*, 577. https://doi.org/10.1186/s12885-015-1546-9

Ghiringhelli, F., Bruchard, M., & Apetoh, L. (2013). Immune effects of 5-fluorouracil. *Oncoimmunology*, *2*(3). https://doi.org/10.4161/onci.23139

Godek, K. M., Kabeche, L., & Compton, D. A. (2015). Regulation of kinetochore–microtubule attachments through homeostatic control during mitosis. *Nature Reviews. Molecular Cell Biology*, *16*(1), 57–64. https://doi.org/10.1038/nrm3916

Goel, S., DeCristo, M. J., Watt, A. C., BrinJones, H., Sceneay, J., Li, B. B., Khan, N., Ubellacker, J. M., Xie, S., Metzger-Filho, O., Hoog, J., Ellis, M. J., Ma, C. X., Ramm, S., Krop, I. E., Winer, E. P., Roberts, T. M., Kim, H.-J., McAllister, S. S., & Zhao, J. J. (2017). CDK4/6 inhibition triggers anti-tumour immunity. *Nature*, *548*(7668), 471–475. https://doi.org/10.1038/nature23465

Gordon, S. R., Maute, R. L., Dulken, B. W., Hutter, G., George, B. M., McCracken, M. N., Gupta, R., Tsai, J. M., Sinha, R., Corey, D., Ring, A. M., Connolly, A. J., & Weissman, I. L. (2017). PD-1 expression by tumour-associated macrophages inhibits phagocytosis and tumour immunity. *Nature*, *545*(7655), 495–499. https://doi.org/10.1038/nature22396

Gray, E. E., Winship, D., Snyder, J. M., Child, S. J., Geballe, A. P., & Stetson, D. B. (2016). The AIM2-like Receptors Are Dispensable for the Interferon Response to Intracellular DNA. *Immunity*, *45*(2), 255–266. https://doi.org/10.1016/j.immuni.2016.06.015

Griguolo, G., Pascual, T., Dieci, M. V., Guarneri, V., & Prat, A. (2019). Interaction of host immunity with HER2-targeted treatment and tumor heterogeneity in HER2-positive breast cancer. *Journal for ImmunoTherapy of Cancer*, *7*(1), 90. https://doi.org/10.1186/s40425-019-0548-6

Grywalska, E., Pasiarski, M., Góźdź, S., & Roliński, J. (2018). Immune-checkpoint inhibitors for combating T-cell dysfunction in cancer. *OncoTargets and Therapy*, *11*, 6505–6524. https://doi.org/10.2147/OTT.S150817

Gu, W., Pan, F., & Singer, R. H. (2009). Blocking beta-catenin binding to the ZBP1 promoter represses ZBP1 expression, leading to increased proliferation and migration of metastatic breast-cancer cells. *Journal of Cell Science*, *122*(Pt 11), 1895–1905. https://doi.org/10.1242/jcs.045278

Gustafson, C. E., Jadhav, R., Cao, W., Qi, Q., Pegram, M., Tian, L., Weyand, C. M., & Goronzy, J. J. (n.d.). Immune cell repertoires in breast cancer patients after adjuvant chemotherapy. *JCI Insight*, *5*(4). https://doi.org/10.1172/jci.insight.134569

Han, Y., Yu, X., Li, S., Tian, Y., & Liu, C. (2020). New Perspectives for Resistance to PARP Inhibitors in Triple-Negative Breast Cancer. *Frontiers in Oncology*, *10*. https://doi.org/10.3389/fonc.2020.578095

Hannesdóttir, L., Tymoszuk, P., Parajuli, N., Wasmer, M.-H., Philipp, S., Daschil, N., Datta, S., Koller, J.-B., Tripp, C. H., Stoitzner, P., Müller-Holzner, E., Wiegers, G. J., Sexl, V., Villunger, A., & Doppler, W. (2013). Lapatinib and doxorubicin enhance the Stat1-dependent antitumor immune response. *European Journal of Immunology*, *43*(10), 2718–2729. https://doi.org/10.1002/eji.201242505

Hao, D., Wang, G., Yang, W., Gong, J., Li, X., Xiao, M., He, L., Wang, L., Li, X., & Di, L. (2019). Reactive versus Constitutive: Reconcile the Controversial Results about the Prognostic Value of PD-L1 Expression in cancer. *International Journal of Biological Sciences*, *15*(9), 1933–1941. https://doi.org/10.7150/ijbs.33297

Harding, S. M., Benci, J. L., Irianto, J., Discher, D. E., Minn, A. J., & Greenberg, R. A. (2017a). Mitotic progression following DNA damage enables pattern recognition within micronuclei. *Nature*, *548*(7668), 466–470. https://doi.org/10.1038/nature23470

Harding, S. M., Benci, J. L., Irianto, J., Discher, D. E., Minn, A. J., & Greenberg, R. A. (2017b). Mitotic progression following DNA damage enables pattern recognition within micronuclei. *Nature*, *548*(7668), 466–470. https://doi.org/10.1038/nature23470

Hartwell, L., Hood, L., Goldberg, M., Reynolds, A., Silver, L., & Veres, R. (2008). *Genetics From Genes to Genomes*. New York: McGraw-Hill.

Hatch, E. M., Fischer, A. H., Deerinck, T. J., & Hetzer, M. W. (2013). Catastrophic Nuclear Envelope Collapse in Cancer Cell Micronuclei. *Cell*, *154*(1), 47–60. https://doi.org/10.1016/j.cell.2013.06.007

Hato, S. V., Khong, A., Vries, I. J. M. de, & Lesterhuis, W. J. (2014). Molecular Pathways: The Immunogenic Effects of Platinum-Based Chemotherapeutics. *Clinical Cancer Research*, *20*(11), 2831–2837. https://doi.org/10.1158/1078-0432.CCR-13-3141

He, Q., Fu, Y., Tian, D., & Yan, W. (2018). The contrasting roles of inflammasomes in cancer. *American Journal of Cancer Research*, *8*(4), 566–583.

Heinemann, V. (2005). Gemcitabine in metastatic breast cancer. *Expert Review of Anticancer Therapy*, *5*(3), 429–443. https://doi.org/10.1586/14737140.5.3.429

Heinhuis, K. M., Ros, W., Kok, M., Steeghs, N., Beijnen, J. H., & Schellens, J. H. M. (2019). Enhancing antitumor response by combining immune checkpoint inhibitors with chemotherapy in solid tumors. *Annals of Oncology*, *30*(2), 219–235. https://doi.org/10.1093/annonc/mdy551

Hervas-Stubbs, S., Perez-Gracia, J. L., Rouzaut, A., Sanmamed, M. F., Le Bon, A., & Melero, I. (2011). Direct effects of type I interferons on cells of the immune system. *Clinical Cancer Research: An Official Journal of the American Association for Cancer Research*, *17*(9), 2619–2627. https://doi.org/10.1158/1078-0432.CCR-10-1114

Holland, A. J., & Cleveland, D. W. (2009). Boveri revisited: Chromosomal instability, aneuploidy and tumorigenesis. *Nature Reviews. Molecular Cell Biology*, *10*(7), 478–487. https://doi.org/10.1038/nrm2718

Hollmén, M., Roudnicky, F., Karaman, S., & Detmar, M. (2015). Characterization of macrophage—Cancer cell crosstalk in estrogen receptor positive and triple-negative breast cancer. *Scientific Reports*, *5*. https://doi.org/10.1038/srep09188

Hong, S.-H., Yoon, I.-H., Kim, Y.-H., Yang, S.-H., Park, M.-J., Nam, H.-Y., Kim, B., Kim, Y., Park, C.-S., & Park, C.-G. (2010). High-dose cyclophosphamide-mediated anti-tumor effects by the superior expansion of CD44high cells after their selective depletion. *Immunobiology*, *215*(3), 182–193. https://doi.org/10.1016/j.imbio.2009.01.010

Hopfner, K.-P., & Hornung, V. (2020). Molecular mechanisms and cellular functions of cGAS–STING signalling. *Nature Reviews Molecular Cell Biology*, *21*(9), 501–521. https://doi.org/10.1038/s41580-020-0244-x

Hori, T., Amano, M., Suzuki, A., Backer, C. B., Welburn, J. P., Dong, Y., McEwen, B. F., Shang, W.-H., Suzuki, E., Okawa, K., Cheeseman, I. M., & Fukagawa, T. (2008). CCAN

makes multiple contacts with centromeric DNA to provide distinct pathways to the outer kinetochore. *Cell*, *135*(6), 1039–1052. https://doi.org/10.1016/j.cell.2008.10.019

Hori, T., Shang, W.-H., Takeuchi, K., & Fukagawa, T. (2013). The CCAN recruits CENP-A to the centromere and forms the structural core for kinetochore assembly. *The Journal of Cell Biology*, *200*(1), 45–60. https://doi.org/10.1083/jcb.201210106

Hornig, N. C. D., Knowles, P. P., McDonald, N. Q., & Uhlmann, F. (2002). The dual mechanism of separase regulation by securin. *Current Biology: CB*, *12*(12), 973–982. https://doi.org/10.1016/s0960-9822(02)00847-3

Horvat, T. Z., Adel, N. G., Dang, T.-O., Momtaz, P., Postow, M. A., Callahan, M. K., Carvajal, R. D., Dickson, M. A., D'Angelo, S. P., Woo, K. M., Panageas, K. S., Wolchok, J. D., & Chapman, P. B. (2015). Immune-Related Adverse Events, Need for Systemic Immunosuppression, and Effects on Survival and Time to Treatment Failure in Patients With Melanoma Treated With Ipilimumab at Memorial Sloan Kettering Cancer Center. *Journal of Clinical Oncology*, *33*(28), 3193–3198. https://doi.org/10.1200/JCO.2015.60.8448

Houssami, N., Macaskill, P., von Minckwitz, G., Marinovich, M. L., & Mamounas, E. (2012). Meta-analysis of the association of breast cancer subtype and pathologic complete response to neoadjuvant chemotherapy. *European Journal of Cancer*, *48*(18), 3342–3354. https://doi.org/10.1016/j.ejca.2012.05.023

Howell, B. J., McEwen, B. F., Canman, J. C., Hoffman, D. B., Farrar, E. M., Rieder, C. L., & Salmon, E. D. (2001). Cytoplasmic dynein/dynactin drives kinetochore protein transport to the spindle poles and has a role in mitotic spindle checkpoint inactivation. *The Journal of Cell Biology*, *155*(7), 1159–1172. https://doi.org/10.1083/jcb.200105093

Hu, Z. I., Ho, A. Y., & McArthur, H. L. (2017). Combined Radiation Therapy and Immune Checkpoint Blockade Therapy for Breast Cancer. *International Journal of Radiation Oncology*Biology*Physics*, *99*(1), 153–164. https://doi.org/10.1016/j.ijrobp.2017.05.029

Hughes, E., Scurr, M., Campbell, E., Jones, E., Godkin, A., & Gallimore, A. (2018). T-cell modulation by cyclophosphamide for tumour therapy. *Immunology*, *154*(1), 62–68. https://doi.org/10.1111/imm.12913

Imai, H., Dansako, H., Ueda, Y., Satoh, S., & Kato, N. (2018). Daunorubicin, a topoisomerase II poison, suppresses viral production of hepatitis B virus by inducing cGAS-dependent innate immune response. *Biochemical and Biophysical Research Communications*, *504*(4), 672–678. https://doi.org/10.1016/j.bbrc.2018.08.195

Israels, E. D., & Israels, L. G. (2000). The Cell Cycle. *The Oncologist*, *5*(6), 510–513. https://doi.org/10.1634/theoncologist.5-6-510

Italiani, P., & Boraschi, D. (2014). From Monocytes to M1/M2 Macrophages: Phenotypical vs. Functional Differentiation. *Frontiers in Immunology*, *5*. https://doi.org/10.3389/fimmu.2014.00514

Izawa, D., & Pines, J. (2015). The mitotic checkpoint complex binds a second CDC20 to inhibit active APC/C. *Nature*, *517*(7536), 631–634. https://doi.org/10.1038/nature13911

Jager, N. A., Wallis de Vries, B. M., Hillebrands, J.-L., Harlaar, N. J., Tio, R. A., Slart, R. H. J. A., van Dam, G. M., Boersma, H. H., Zeebregts, C. J., & Westra, J. (2016). Distribution of Matrix Metalloproteinases in Human Atherosclerotic Carotid Plaques and Their Production by Smooth Muscle Cells and Macrophage Subsets. *Molecular Imaging and Biology*, *18*, 283–291. https://doi.org/10.1007/s11307-015-0882-0

Jagodinsky, J. C., Jin, W. J., Bates, A. M., Hernandez, R., Grudzinski, J. J., Marsh, I. R., Chakravarty, I., Arthur, I. S., Zangl, L. M., Brown, R. J., Nystuen, E. J., Emma, S. E., Kerr, C., Carlson, P. M., Sriramaneni, R. N., Engle, J. W., Aluicio-Sarduy, E., Barnhart, T. E., Le, T., … Morris, Z. S. (2021). Temporal analysis of type 1 interferon activation in tumor cells following external beam radiotherapy or targeted radionuclide therapy. *Theranostics*, *11*(13), 6120–6137. https://doi.org/10.7150/thno.54881

Ji, Z., Gao, H., Jia, L., Li, B., & Yu, H. (2017). A sequential multi-target Mps1 phosphorylation cascade promotes spindle checkpoint signaling. *ELife*, *6*, e22513. https://doi.org/10.7554/eLife.22513

Jiang, M., Gu, D., Dai, J., Huang, Q., & Tian, L. (2020). Dark Side of Cytotoxic Therapy: Chemoradiation-Induced Cell Death and Tumor Repopulation. *Trends in Cancer*, *6*(5), 419–431. https://doi.org/10.1016/j.trecan.2020.01.018

Jordan, M. A., Toso, R. J., Thrower, D., & Wilson, L. (1993). Mechanism of mitotic block and inhibition of cell proliferation by taxol at low concentrations. *Proceedings of the National Academy of Sciences of the United States of America*, *90*(20), 9552–9556. https://doi.org/10.1073/pnas.90.20.9552

Jordan, M. A., Wendell, K., Gardiner, S., Derry, W. B., Copp, H., & Wilson, L. (1996). Mitotic block induced in HeLa cells by low concentrations of paclitaxel (Taxol) results in abnormal mitotic exit and apoptotic cell death. *Cancer Research*, *56*(4), 816–825.

Juneja, V. R., McGuire, K. A., Manguso, R. T., LaFleur, M. W., Collins, N., Haining, W. N., Freeman, G. J., & Sharpe, A. H. (2017). PD-L1 on tumor cells is sufficient for immune evasion in immunogenic tumors and inhibits CD8 T cell cytotoxicity. *The Journal of Experimental Medicine*, *214*(4), 895–904. https://doi.org/10.1084/jem.20160801

Kalos, M., & June, C. H. (2013). Adoptive T cell Transfer for Cancer Immunotherapy in the Era of Synthetic Biology. *Immunity*, *39*(1). https://doi.org/10.1016/j.immuni.2013.07.002

Kapoor, T. M., Lampson, M. A., Hergert, P., Cameron, L., Cimini, D., Salmon, E. D., McEwen, B. F., & Khodjakov, A. (2006). Chromosomes Can Congress to the Metaphase Plate Before Biorientation. *Science (New York, N.Y.)*, *311*(5759), 388–391. https://doi.org/10.1126/science.1122142

Kellokumpu-Lehtinen, P., Tuunanen, T., Asola, R., Elomaa, L., Heikkinen, M., Kokko, R., Järvenpää, R., Lehtinen, I., Maiche, A., Kaleva-Kerola, J., Huusko, M., Möykkynen, K., & Ala-Luhtala, T. (2013). Weekly paclitaxel—An effective treatment for advanced breast cancer. *Anticancer Research*, *33*(6), 2623–2627.

Kim, C., Wang, X.-D., & Yu, Y. (2020). PARP1 inhibitors trigger innate immunity via PARP1 trapping-induced DNA damage response. *ELife*, *9*, e60637. https://doi.org/10.7554/eLife.60637

Kneissig, M., Keuper, K., de Pagter, M. S., van Roosmalen, M. J., Martin, J., Otto, H., Passerini, V., Campos Sparr, A., Renkens, I., Kropveld, F., Vasudevan, A., Sheltzer, J. M., Kloosterman, W. P., & Storchova, Z. (2019). Micronuclei-based model system reveals functional consequences of chromothripsis in human cells. *ELife*, *8*, e50292. https://doi.org/10.7554/eLife.50292

Knouse, K. A., Wu, J., Whittaker, C. A., & Amon, A. (2014). Single cell sequencing reveals low levels of aneuploidy across mammalian tissues. *Proceedings of the National Academy of Sciences of the United States of America*, *111*(37), 13409–13414. https://doi.org/10.1073/pnas.1415287111

Krishnamurti, U., & Silverman, J. F. (2014). HER2 in Breast Cancer: A Review and Update. *Advances in Anatomic Pathology*, *21*(2), 100–107. https://doi.org/10.1097/PAP.0000000000000015

Kwon, J., & Bakhoum, S. F. (2020). The cytosolic DNA-sensing cGAS-STING pathway in cancer. *Cancer Discovery*, *10*(1), 26–39. https://doi.org/10.1158/2159-8290.CD-19-0761

Kythreotou, A., Siddique, A., Mauri, F. A., Bower, M., & Pinato, D. J. (2018). Pd-L1. *Journal of Clinical Pathology*, *71*(3), 189–194. https://doi.org/10.1136/jclinpath-2017-204853

Ladoire, S., Enot, D., Andre, F., Zitvogel, L., & Kroemer, G. (2016). Immunogenic cell death-related biomarkers: Impact on the survival of breast cancer patients after adjuvant chemotherapy. *Oncoimmunology*, *5*(2), e1082706. https://doi.org/10.1080/2162402X.2015.1082706

Langdon, S., Hughes, A., Taylor, M. A., Kuczynski, E. A., Mele, D. A., Delpuech, O., Jarvis, L., Staniszewska, A., Cosulich, S., Carnevalli, L. S., & Sinclair, C. (2018). Combination of dual mTORC1/2 inhibition and immune-checkpoint blockade potentiates

anti-tumour immunity. *Oncoimmunology*, *7*(8). https://doi.org/10.1080/2162402X.2018.1458810

Lee, A. J. X., Endesfelder, D., Rowan, A. J., Walther, A., Birkbak, N. J., Futreal, P. A., Downward, J., Szallasi, Z., Tomlinson, I. P. M., Kschischo, M., & Swanton, C. (2011). Chromosomal Instability Confers Intrinsic Multi-Drug Resistance. *Cancer Research*, *71*(5), 1858–1870. https://doi.org/10.1158/0008-5472.CAN-10-3604

Lehmann, B. D., Bauer, J. A., Chen, X., Sanders, M. E., Chakravarthy, A. B., Shyr, Y., & Pietenpol, J. A. (2011). Identification of human triple-negative breast cancer subtypes and preclinical models for selection of targeted therapies. *The Journal of Clinical Investigation*, *121*(7), 2750–2767. https://doi.org/10.1172/JCI45014

Lehmann, B. D., Jovanović, B., Chen, X., Estrada, M. V., Johnson, K. N., Shyr, Y., Moses, H. L., Sanders, M. E., & Pietenpol, J. A. (2016). Refinement of Triple-Negative Breast Cancer Molecular Subtypes: Implications for Neoadjuvant Chemotherapy Selection. *PLOS ONE*, *11*(6), e0157368. https://doi.org/10.1371/journal.pone.0157368

Lhuillier, C., Rudqvist, N.-P., Yamazaki, T., Zhang, T., Charpentier, M., Galluzzi, L., Dephoure, N., Clement, C. C., Santambrogio, L., Zhou, X. K., Formenti, S. C., & Demaria, S. (2021). Radiotherapy-exposed CD8+ and CD4+ neoantigens enhance tumor control. *The Journal of Clinical Investigation*, *131*(5). https://doi.org/10.1172/JCI138740

Li, A., Yi, M., Qin, S., Song, Y., Chu, Q., & Wu, K. (2019). Activating cGAS-STING pathway for the optimal effect of cancer immunotherapy. *Journal of Hematology & Oncology*, *12*(1), 35. https://doi.org/10.1186/s13045-019-0721-x

Li, T., Cheng, H., Yuan, H., Xu, Q., Shu, C., Zhang, Y., Xu, P., Tan, J., Rui, Y., Li, P., & Tan, X. (2016). Antitumor Activity of cGAMP via Stimulation of cGAS-cGAMP-STING-IRF3 Mediated Innate Immune Response. *Scientific Reports*, *6*(1), 19049. https://doi.org/10.1038/srep19049

Li, X.-D., Wu, J., Gao, D., Wang, H., Sun, L., & Chen, Z. J. (2013). Pivotal roles of cGAS-cGAMP signaling in antiviral defense and immune adjuvant effects. *Science (New York, N.Y.)*, *341*(6152), 1390–1394. https://doi.org/10.1126/science.1244040

Lian, A. T. Y., & Chircop, M. (2016). Mitosis in Animal Cells. In R. A. Bradshaw & P. D. Stahl (Eds.), *Encyclopedia of Cell Biology* (pp. 478–493). Academic Press. https://doi.org/10.1016/B978-0-12-394447-4.30064-5

Liang, Y., Tang, H., Guo, J., Qiu, X., Yang, Z., Ren, Z., Sun, Z., Bian, Y., Xu, L., Xu, H., Shen, J., Han, Y., Dong, H., Peng, H., & Fu, Y.-X. (2018). Targeting IFNα to tumor by anti-PD-L1 creates feedforward antitumor responses to overcome checkpoint blockade resistance. *Nature Communications*, *9*(1), 4586. https://doi.org/10.1038/s41467-018-06890-y

Liu, P., Jaffar, J., Hellstrom, I., & Hellstrom, K. E. (2010). Administration of cyclophosphamide changes the immune profile of tumor-bearing mice. *Journal of Immunotherapy (Hagerstown, Md. : 1997)*, *33*(1), 53–59. https://doi.org/10.1097/CJI.0b013e3181b56af4

Liu, S., Cai, X., Wu, J., Cong, Q., Chen, X., Li, T., Du, F., Ren, J., Wu, Y.-T., Grishin, N. V., & Chen, Z. J. (2015). Phosphorylation of innate immune adaptor proteins MAVS, STING, and TRIF induces IRF3 activation. *Science*, *347*(6227), aaa2630. https://doi.org/10.1126/science.aaa2630

Liu, S., Kwon, M., Mannino, M., Yang, N., Renda, F., Khodjakov, A., & Pellman, D. (2018). Nuclear envelope assembly defects link mitotic errors to chromothripsis. *Nature*, *561*(7724), 551–555. https://doi.org/10.1038/s41586-018-0534-z

Liu, S. X., Gustafson, H. H., Jackson, D. L., Pun, S. H., & Trapnell, C. (2020). Trajectory analysis quantifies transcriptional plasticity during macrophage polarization. *Scientific Reports*, *10*(1), 12273. https://doi.org/10.1038/s41598-020-68766-w

Lohard, S., Bourgeois, N., Maillet, L., Gautier, F., Fétiveau, A., Lasla, H., Nguyen, F., Vuillier, C., Dumont, A., Moreau-Aubry, A., Frapin, M., David, L., Loussouarn, D., Kerdraon, O., Campone, M., Jézéquel, P., Juin, P. P., & Barillé-Nion, S. (2020). STING-dependent paracriny shapes apoptotic priming of breast tumors in response to anti-mitotic treatment. *Nature Communications*, *11*(1), 259. https://doi.org/10.1038/s41467-019-13689-y

Mackenzie, K. J., Carroll, P., Martin, C.-A., Murina, O., Fluteau, A., Simpson, D. J., Olova, N., Sutcliffe, H., Rainger, J. K., Leitch, A., Osborn, R. T., Wheeler, A. P., Nowotny, M., Gilbert, N., Chandra, T., Reijns, M. A. M., & Jackson, A. P. (2017a). CGAS surveillance of micronuclei links genome instability to innate immunity. *Nature*, *548*(7668), 461–465. https://doi.org/10.1038/nature23449

Mackenzie, K. J., Carroll, P., Martin, C.-A., Murina, O., Fluteau, A., Simpson, D. J., Olova, N., Sutcliffe, H., Rainger, J. K., Leitch, A., Osborn, R. T., Wheeler, A. P., Nowotny, M., Gilbert, N., Chandra, T., Reijns, M. A. M., & Jackson, A. P. (2017b). CGAS surveillance of micronuclei links genome instability to innate immunity. *Nature*, *548*(7668), 461–465. https://doi.org/10.1038/nature23449

Maldonado, M., & Kapoor, T. M. (2011). Constitutive Mad1 targeting to kinetochores uncouples checkpoint signalling from chromosome biorientation. *Nature Cell Biology*, *13*(4), 475–482. https://doi.org/10.1038/ncb2223

Marcus, A., Mao, A. J., Lensink-Vasan, M., Wang, L., Vance, R. E., & Raulet, D. H. (2018). Tumor-Derived cGAMP Triggers a STING-Mediated Interferon Response in Non-tumor Cells to Activate the NK Cell Response. *Immunity*, *49*(4), 754-763.e4. https://doi.org/10.1016/j.immuni.2018.09.016

Margolis, S. R., Wilson, S. C., & Vance, R. E. (2017). Evolutionary Origins of cGAS-STING Signaling. *Trends in Immunology*, *38*(10), 733–743. https://doi.org/10.1016/j.it.2017.03.004

Martínez-Balbás, M. A., Dey, A., Rabindran, S. K., Ozato, K., & Wu, C. (1995). Displacement of sequence-specific transcription factors from mitotic chromatin. *Cell*, *83*(1), 29–38. https://doi.org/10.1016/0092-8674(95)90231-7

May, K. M., & Hardwick, K. G. (2006). The spindle checkpoint. *Journal of Cell Science*, *119*(20), 4139–4142. https://doi.org/10.1242/jcs.03165

Mayr, M. I., Hümmer, S., Bormann, J., Grüner, T., Adio, S., Woehlke, G., & Mayer, T. U. (2007). The human kinesin Kif18A is a motile microtubule depolymerase essential for chromosome congression. *Current Biology: CB*, *17*(6), 488–498. https://doi.org/10.1016/j.cub.2007.02.036

McDonnell, A. M., Lesterhuis, W. J., Khong, A., Nowak, A. K., Lake, R. A., Currie, A. J., & Robinson, B. W. S. (2015). Tumor-infiltrating dendritic cells exhibit defective cross-presentation of tumor antigens, but is reversed by chemotherapy. *European Journal of Immunology*, *45*(1), 49–59. https://doi.org/10.1002/eji.201444722

McIntosh, J. R. (2016). Mitosis. *Cold Spring Harbor Perspectives in Biology*, *8*(9). https://doi.org/10.1101/cshperspect.a023218

Miles, D. (2020, September 19). Primary results from IMpassion131, a double-blind placebo-controlled randomized phase III trial of first-line paclitaxel atezolizumab for unresectable locally advanced/metastatic triple-negative breast cancer. *ESMO Virtual Congress 2020. Abstract LBA15.*

Miles, D., Andre, F., Gligorov, J., Verma, S., Xu, B., Cameron, D., Barrios, C. H., Schneeweiss, A., Easton, V., Dolado, I., & O'Shaughnessy, J. (2017). IMpassion131: Phase III study comparing 1L atezolizumab with paclitaxel vs placebo with paclitaxel in treatment-naive patients with inoperable locally advanced or metastatic triple negative breast cancer (mTNBC). *Annals of Oncology*, *28*, v105. https://doi.org/10.1093/annonc/mdx365.080

Mills, C. D., Kincaid, K., Alt, J. M., Heilman, M. J., & Hill, A. M. (2000). M-1/M-2 Macrophages and the Th1/Th2 Paradigm. *The Journal of Immunology*, *164*(12), 6166–6173. https://doi.org/10.4049/jimmunol.164.12.6166

Mitchison, T. J., Pineda, J., Shi, J., & Florian, S. (2017a). Is inflammatory micronucleation the key to a successful anti-mitotic cancer drug? *Open Biology*, *7*(11), 170182. https://doi.org/10.1098/rsob.170182

Mitchison, T. J., Pineda, J., Shi, J., & Florian, S. (2017b). Is inflammatory micronucleation the key to a successful anti-mitotic cancer drug? *Open Biology*, *7*(11), 170182. https://doi.org/10.1098/rsob.170182

Molina, M. A., Codony-Servat, J., Albanell, J., Rojo, F., Arribas, J., & Baselga, J. (2001). Trastuzumab (herceptin), a humanized anti-Her2 receptor monoclonal antibody, inhibits basal and activated Her2 ectodomain cleavage in breast cancer cells. *Cancer Research*, *61*(12), 4744–4749.

Morimoto, Y., Kishida, T., Kotani, S., Takayama, K., & Mazda, O. (2018). Interferon-β signal may up-regulate PD-L1 expression through IRF9-dependent and independent pathways in lung cancer cells. *Biochemical and Biophysical Research Communications*, *507*(1), 330–336. https://doi.org/10.1016/j.bbrc.2018.11.035

Morrison, R., Schleicher, S. M., Sun, Y., Niermann, K. J., Kim, S., Spratt, D. E., Chung, C. H., & Lu, B. (2010). Targeting the Mechanisms of Resistance to Chemotherapy and Radiotherapy with the Cancer Stem Cell Hypothesis. *Journal of Oncology*, *2011*, e941876. https://doi.org/10.1155/2011/941876

Moschella, F., Torelli, G. F., Valentini, M., Urbani, F., Buccione, C., Petrucci, M. T., Natalino, F., Belardelli, F., Foà, R., & Proietti, E. (2013). Cyclophosphamide Induces a Type I Interferon–Associated Sterile Inflammatory Response Signature in Cancer Patients' Blood Cells: Implications for Cancer Chemoimmunotherapy. *Clinical Cancer Research*, *19*(15), 4249–4261. https://doi.org/10.1158/1078-0432.CCR-12-3666

Müller, E., Speth, M., Christopoulos, P. F., Lunde, A., Avdagic, A., Øynebråten, I., & Corthay, A. (2018). Both Type I and Type II Interferons Can Activate Antitumor M1 Macrophages When Combined With TLR Stimulation. *Frontiers in Immunology*, *9*. https://doi.org/10.3389/fimmu.2018.02520

Muntasell, A., Cabo, M., Servitja, S., Tusquets, I., Martínez-García, M., Rovira, A., Rojo, F., Albanell, J., & López-Botet, M. (2017). Interplay between Natural Killer Cells and Anti-HER2 Antibodies: Perspectives for Breast Cancer Immunotherapy. *Frontiers in Immunology*, *8*. https://doi.org/10.3389/fimmu.2017.01544

Murai, J., Huang, S. N., Das, B. B., Renaud, A., Zhang, Y., Doroshow, J. H., Ji, J., Takeda, S., & Pommier, Y. (2012). Differential trapping of PARP1 and PARP2 by clinical PARP inhibitors. *Cancer Research*, *72*(21), 5588–5599. https://doi.org/10.1158/0008-5472.CAN-12-2753

Musacchio, A., & Salmon, E. D. (2007). The spindle-assembly checkpoint in space and time. *Nature Reviews Molecular Cell Biology*, *8*(5), 379–393. https://doi.org/10.1038/nrm2163

Nanda, R., Liu, M. C., Yau, C., Shatsky, R., Pusztai, L., Wallace, A., Chien, A. J., Forero-Torres, A., Ellis, E., Han, H., Clark, A., Albain, K., Boughey, J. C., Jaskowiak, N.

T., Elias, A., Isaacs, C., Kemmer, K., Helsten, T., Majure, M., … Esserman, L. J. (2020). Effect of Pembrolizumab Plus Neoadjuvant Chemotherapy on Pathologic Complete Response in Women With Early-Stage Breast Cancer: An Analysis of the Ongoing Phase 2 Adaptively Randomized I-SPY2 Trial. *JAMA Oncology*, *6*(5), 676–684. https://doi.org/10.1001/jamaoncol.2019.6650

Naour, J. L., Zitvogel, L., Galluzzi, L., Vacchelli, E., & Kroemer, G. (2020). Trial watch: STING agonists in cancer therapy. *OncoImmunology*, *9*(1), 1777624. https://doi.org/10.1080/2162402X.2020.1777624

Noguchi, M., Moriya, F., Koga, N., Matsueda, S., Sasada, T., Yamada, A., Kakuma, T., & Itoh, K. (2016). A randomized phase II clinical trial of personalized peptide vaccination with metronomic low-dose cyclophosphamide in patients with metastatic castration-resistant prostate cancer. *Cancer Immunology, Immunotherapy*, *65*(2), 151–160. https://doi.org/10.1007/s00262-015-1781-6

O'Donnell, J. S., Massi, D., Teng, M. W. L., & Mandala, M. (2018). PI3K-AKT-mTOR inhibition in cancer immunotherapy, redux. *Seminars in Cancer Biology*, *48*, 91–103. https://doi.org/10.1016/j.semcancer.2017.04.015

Ohkuri, T., Kosaka, A., Ishibashi, K., Kumai, T., Hirata, Y., Ohara, K., Nagato, T., Oikawa, K., Aoki, N., Harabuchi, Y., Celis, E., & Kobayashi, H. (2017). Intratumoral administration of cGAMP transiently accumulates potent macrophages for anti-tumor immunity at a mouse tumor site. *Cancer Immunology, Immunotherapy: CII*, *66*(6), 705–716. https://doi.org/10.1007/s00262-017-1975-1

Ohkuri, T., Kosaka, A., Nagato, T., & Kobayashi, H. (2018). Effects of STING stimulation on macrophages: STING agonists polarize into "classically" or "alternatively" activated macrophages? *Human Vaccines & Immunotherapeutics*, *14*(2), 285–287. https://doi.org/10.1080/21645515.2017.1395995

Ohtani, M., Nagai, S., Kondo, S., Mizuno, S., Nakamura, K., Tanabe, M., Takeuchi, T., Matsuda, S., & Koyasu, S. (2008). Mammalian target of rapamycin and glycogen synthase kinase 3 differentially regulate lipopolysaccharide-induced interleukin-12 production in dendritic cells. *Blood*, *112*(3), 635–643. https://doi.org/10.1182/blood-2008-02-137430

Okkenhaug, K., Graupera, M., & Vanhaesebroeck, B. (2016). Targeting PI3K in cancer: Impact on tumor cells, their protective stroma, angiogenesis and immunotherapy. *Cancer Discovery*, *6*(10), 1090–1105. https://doi.org/10.1158/2159-8290.CD-16-0716

Opzoomer, J. W., Sosnowska, D., Anstee, J. E., Spicer, J. F., & Arnold, J. N. (2019). Cytotoxic Chemotherapy as an Immune Stimulus: A Molecular Perspective on Turning Up the Immunological Heat on Cancer. *Frontiers in Immunology*, *10*, 1654. https://doi.org/10.3389/fimmu.2019.01654

Orecchioni, M., Ghosheh, Y., Pramod, A. B., & Ley, K. (2019). Macrophage Polarization: Different Gene Signatures in M1(LPS+) vs. Classically and M2(LPS–) vs. Alternatively Activated Macrophages. *Frontiers in Immunology*, *10*. https://doi.org/10.3389/fimmu.2019.01084

Ossovskaya, V., Koo, I. C., Kaldjian, E. P., Alvares, C., & Sherman, B. M. (2010). Upregulation of Poly (ADP-Ribose) Polymerase-1 (PARP1) in Triple-Negative Breast Cancer and Other Primary Human Tumor Types. *Genes & Cancer*, *1*(8), 812–821. https://doi.org/10.1177/1947601910383418

Pantelidou, C., Sonzogni, O., Taveira, M. D. O., Mehta, A. K., Kothari, A., Wang, D., Visal, T., Li, M. K., Pinto, J., Castrillon, J. A., Cheney, E. M., Bouwman, P., Jonkers, J., Rottenberg, S., Guerriero, J. L., Wulf, G. M., & Shapiro, G. I. (2019). PARP Inhibitor Efficacy Depends on CD8+ T-cell Recruitment via Intratumoral STING Pathway Activation in BRCA-Deficient Models of Triple-Negative Breast Cancer. *Cancer Discovery*, *9*(6), 722–737. https://doi.org/10.1158/2159-8290.CD-18-1218

Parkes, E. E., Walker, S. M., Taggart, L. E., McCabe, N., Knight, L. A., Wilkinson, R., McCloskey, K. D., Buckley, N. E., Savage, K. I., Salto-Tellez, M., McQuaid, S., Harte, M. T., Mullan, P. B., Harkin, D. P., & Kennedy, R. D. (2017). Activation of STING-Dependent Innate Immune Signaling By S-Phase-Specific DNA Damage in Breast Cancer. *Journal of the National Cancer Institute*, *109*(1). https://doi.org/10.1093/jnci/djw199

Pavelka, N., Rancati, G., Zhu, J., Bradford, W. D., Saraf, A., Florens, L., Sanderson, B. W., Hattem, G. L., & Li, R. (2010). Aneuploidy confers quantitative proteome changes and phenotypic variation in budding yeast. *Nature*, *468*(7321), 321–325. https://doi.org/10.1038/nature09529

Peng, J., Hamanishi, J., Matsumura, N., Abiko, K., Murat, K., Baba, T., Yamaguchi, K., Horikawa, N., Hosoe, Y., Murphy, S. K., Konishi, I., & Mandai, M. (2015). Chemotherapy Induces Programmed Cell Death-Ligand 1 Overexpression via the Nuclear Factor-κB to Foster an Immunosuppressive Tumor Microenvironment in Ovarian Cancer. *Cancer Research*, *75*(23), 5034–5045. https://doi.org/10.1158/0008-5472.CAN-14-3098

Penn, I., & Starzl, T. E. (1973). Immunosuppression and Cancer. *Transplantation Proceedings*, *5*(1), 943–947.

Perez, E. A. (1998). Paclitaxel in Breast Cancer. *The Oncologist*, *3*(6), 373–389.

Peyraud, F., & Italiano, A. (2020). Combined PARP Inhibition and Immune Checkpoint Therapy in Solid Tumors. *Cancers*, *12*(6). https://doi.org/10.3390/cancers12061502

Pol, J., Vacchelli, E., Aranda, F., Castoldi, F., Eggermont, A., Cremer, I., Sautès-Fridman, C., Fucikova, J., Galon, J., Spisek, R., Tartour, E., Zitvogel, L., Kroemer, G., & Galluzzi, L. (2015). Trial Watch: Immunogenic cell death inducers for anticancer

chemotherapy. *Oncoimmunology*, *4*(4), e1008866. https://doi.org/10.1080/2162402X.2015.1008866

Pollard, T. D., & O'Shaughnessy, B. (2019). Molecular Mechanism of Cytokinesis. *Annual Review of Biochemistry*, *88*, 661–689. https://doi.org/10.1146/annurev-biochem-062917-012530

Powell, J. D., Pollizzi, K. N., Heikamp, E. B., & Horton, M. R. (2012). Regulation of Immune Responses by mTOR. *Annual Review of Immunology*, *30*(1), 39–68. https://doi.org/10.1146/annurev-immunol-020711-075024

Qiao, R., Weissmann, F., Yamaguchi, M., Brown, N. G., VanderLinden, R., Imre, R., Jarvis, M. A., Brunner, M. R., Davidson, I. F., Litos, G., Haselbach, D., Mechtler, K., Stark, H., Schulman, B. A., & Peters, J.-M. (2016). Mechanism of APC/CCDC20 activation by mitotic phosphorylation. *Proceedings of the National Academy of Sciences of the United States of America*, *113*(19), E2570-2578. https://doi.org/10.1073/pnas.1604929113

Rapoport, B. L., & Anderson, R. (2019). Realizing the Clinical Potential of Immunogenic Cell Death in Cancer Chemotherapy and Radiotherapy. *International Journal of Molecular Sciences*, *20*(4). https://doi.org/10.3390/ijms20040959

Replogle, J. M., Zhou, W., Amaro, A. E., McFarland, J. M., Villalobos-Ortiz, M., Ryan, J., Letai, A., Yilmaz, O., Sheltzer, J., Lippard, S. J., Ben-David, U., & Amon, A. (2020). Aneuploidy increases resistance to chemotherapeutics by antagonizing cell division. *Proceedings of the National Academy of Sciences*, *117*(48), 30566–30576. https://doi.org/10.1073/pnas.2009506117

Rotstein, S., Blomgren, H., Petrini, B., Wasserman, J., & Baral, E. (1985). Long term effects on the immune system following local radiation therapy for breast cancer. I. Cellular composition of the peripheral blood lymphocyte population. *International Journal of Radiation Oncology, Biology, Physics*, *11*(5), 921–925. https://doi.org/10.1016/0360-3016(85)90114-2

Ryan, S. D., Britigan, E. M. C., Zasadil, L. M., Witte, K., Audhya, A., Roopra, A., & Weaver, B. A. (2012). Up-regulation of the mitotic checkpoint component Mad1 causes chromosomal instability and resistance to microtubule poisons. *Proceedings of the National Academy of Sciences of the United States of America*, *109*(33), E2205-2214. https://doi.org/10.1073/pnas.1201911109

Salgado, R., Denkert, C., Demaria, S., Sirtaine, N., Klauschen, F., Pruneri, G., Wienert, S., Van den Eynden, G., Baehner, F. L., Penault-Llorca, F., Perez, E. A., Thompson, E. A., Symmans, W. F., Richardson, A. L., Brock, J., Criscitiello, C., Bailey, H., Ignatiadis, M., Floris, G., … Loi, S. (2015). The evaluation of tumor-infiltrating lymphocytes (TILs) in breast cancer: Recommendations by an International TILs Working Group 2014. *Annals of Oncology*, *26*(2), 259–271. https://doi.org/10.1093/annonc/mdu450

Sánchez-Margalet, V., Barco-Sánchez, A., Vilariño-García, T., Jiménez-Cortegana, C., Pérez-Pérez, A., Henao-Carrasco, F., Virizuela-Echaburu, J. A., Nogales-Fernández, E., Gala, M. C. Á. la, Lobo-Acosta, M. A., Palazón-Carrión, N., Nieto, A., & Cruz-Merino, L. de la. (2019). Circulating regulatory T cells from breast cancer patients in response to neoadjuvant chemotherapy. *Translational Cancer Research*, *8*(1). https://doi.org/10.21037/26532

Sansregret, L., Patterson, J. O., Dewhurst, S., López-García, C., Koch, A., McGranahan, N., Chao, W. C. H., Barry, D. J., Rowan, A., Instrell, R., Horswell, S., Way, M., Howell, M., Singleton, M. R., Medema, R. H., Nurse, P., Petronczki, M., & Swanton, C. (2017). APC/C Dysfunction Limits Excessive Cancer Chromosomal Instability. *Cancer Discovery*, *7*(2), 218–233. https://doi.org/10.1158/2159-8290.CD-16-0645

Sansregret, L., Vanhaesebroeck, B., & Swanton, C. (2018). Determinants and clinical implications of chromosomal instability in cancer. *Nature Reviews Clinical Oncology*, *15*(3), 139–150. https://doi.org/10.1038/nrclinonc.2017.198

Santaguida, S., Richardson, A., Iyer, D. R., M'Saad, O., Zasadil, L., Knouse, K. A., Wong, Y. L., Rhind, N., Desai, A., & Amon, A. (2017). Chromosome Mis-segregation Generates Cell-Cycle-Arrested Cells with Complex Karyotypes that Are Eliminated by the Immune System. *Developmental Cell*, *41*(6), 638-651.e5. https://doi.org/10.1016/j.devcel.2017.05.022

Schadt, L., Sparano, C., Schweiger, N. A., Silina, K., Cecconi, V., Lucchiari, G., Yagita, H., Guggisberg, E., Saba, S., Nascakova, Z., Barchet, W., & van den Broek, M. (2019). Cancer-Cell-Intrinsic cGAS Expression Mediates Tumor Immunogenicity. *Cell Reports*, *29*(5), 1236-1248.e7. https://doi.org/10.1016/j.celrep.2019.09.065

Schmid, P., Adams, S., Rugo, H. S., Schneeweiss, A., Barrios, C. H., Iwata, H., Diéras, V., Hegg, R., Im, S.-A., Shaw Wright, G., Henschel, V., Molinero, L., Chui, S. Y., Funke, R., Husain, A., Winer, E. P., Loi, S., & Emens, L. A. (2018). Atezolizumab and Nab-Paclitaxel in Advanced Triple-Negative Breast Cancer. *New England Journal of Medicine*, *379*(22), 2108–2121. https://doi.org/10.1056/NEJMoa1809615

Schmid, P., Adams, S., Rugo, H. S., Schneeweiss, A., Barrios, C. H., Iwata, H., Dieras, V., Henschel, V., Molinero, L., Chui, S. Y., Husain, A., Winer, E. P., Loi, S., & Emens, L. A. (2019). IMpassion130: Updated overall survival (OS) from a global, randomized, double-blind, placebo-controlled, Phase III study of atezolizumab (atezo) + *nab*-paclitaxel (nP) in previously untreated locally advanced or metastatic triple-negative breast cancer (mTNBC). *Journal of Clinical Oncology*, *37*(15_suppl), 1003–1003. https://doi.org/10.1200/JCO.2019.37.15_suppl.1003

Scholey, J. M., Civelekoglu-Scholey, G., & Brust-Mascher, I. (2016). Anaphase B. *Biology*, *5*(4). https://doi.org/10.3390/biology5040051

Senovilla, L., Vitale, I., Martins, I., Tailler, M., Pailleret, C., Michaud, M., Galluzzi, L., Adjemian, S., Kepp, O., Niso-Santano, M., Shen, S., Mariño, G., Criollo, A., Boilève, A., Job, B., Ladoire, S., Ghiringhelli, F., Sistigu, A., Yamazaki, T., … Kroemer, G. (2012). An immunosurveillance mechanism controls cancer cell ploidy. *Science (New York, N.Y.)*, *337*(6102), 1678–1684. https://doi.org/10.1126/science.1224922

Sevko, A., Michels, T., Vrohlings, M., Umansky, L., Beckhove, P., Kato, M., Shurin, G. V., Shurin, M. R., & Umansky, V. (2013). Antitumor effect of paclitaxel is mediated by inhibition of myeloid-derived suppressor cells and chronic inflammation in the spontaneous melanoma model. *Journal of Immunology (Baltimore, Md.: 1950)*, *190*(5), 2464–2471. https://doi.org/10.4049/jimmunol.1202781

Sheltzer, J. M., Blank, H. M., Pfau, S. J., Tange, Y., George, B. M., Humpton, T. J., Brito, I. L., Hiraoka, Y., Niwa, O., & Amon, A. (2011). Aneuploidy drives genomic instability in yeast. *Science (New York, N.Y.)*, *333*(6045), 1026–1030. https://doi.org/10.1126/science.1206412

Shen, J., Zhao, W., Ju, Z., Wang, L., Peng, Y., Labrie, M., Yap, T. A., Mills, G. B., & Peng, G. (2019). PARPi Triggers the STING-Dependent Immune Response and Enhances the Therapeutic Efficacy of Immune Checkpoint Blockade Independent of BRCAness. *Cancer Research*, *79*(2), 311–319. https://doi.org/10.1158/0008-5472.CAN-18-1003

Sherr, C. J., & Bartek, J. (2017). Cell Cycle–Targeted Cancer Therapies. *Annual Review of Cancer Biology*, *1*(1), 41–57. https://doi.org/10.1146/annurev-cancerbio-040716-075628

Stover, D. G., Coloff, J. L., Barry, W. T., Brugge, J. S., Winer, E. P., & Selfors, L. M. (2016). The Role of Proliferation in Determining Response to Neoadjuvant Chemotherapy in Breast Cancer: A Gene Expression–Based Meta-Analysis. *Clinical Cancer Research*, *22*(24), 6039–6050. https://doi.org/10.1158/1078-0432.CCR-16-0471

Sun, L., Wu, J., Du, F., Chen, X., & Chen, Z. J. (2013a). Cyclic GMP-AMP synthase is a cytosolic DNA sensor that activates the type I interferon pathway. *Science (New York, N.Y.)*, *339*(6121), 786–791. https://doi.org/10.1126/science.1232458

Sun, L., Wu, J., Du, F., Chen, X., & Chen, Z. J. (2013b). Cyclic GMP-AMP synthase is a cytosolic DNA sensor that activates the type I interferon pathway. *Science (New York, N.Y.)*, *339*(6121), 786–791. https://doi.org/10.1126/science.1232458

Sun, S.-Y. (2020). Searching for the real function of mTOR signaling in the regulation of PD-L1 expression. *Translational Oncology*, *13*(12), 100847. https://doi.org/10.1016/j.tranon.2020.100847

Sung, H., Ferlay, J., Siegel, R. L., Laversanne, M., Soerjomataram, I., Jemal, A., & Bray, F. (2020). Global cancer statistics 2020: GLOBOCAN estimates of incidence and

mortality worldwide for 36 cancers in 185 countries. *CA: A Cancer Journal for Clinicians*. https://doi.org/10.3322/caac.21660

Takeuchi, A., Eto, M., Yamada, H., Tatsugami, K., Naito, S., & Yoshikai, Y. (2012). A reduction of recipient regulatory T cells by cyclophosphamide contributes to an anti-tumor effect of nonmyeloablative allogeneic stem cell transplantation in mice. *International Journal of Cancer*, *130*(2), 365–376. https://doi.org/10.1002/ijc.26009

Tan, C. H., Gasic, I., Huber-Reggi, S. P., Dudka, D., Barisic, M., Maiato, H., & Meraldi, P. (2015). The equatorial position of the metaphase plate ensures symmetric cell divisions. *ELife*, *4*. https://doi.org/10.7554/eLife.05124

Tedesco, S., De Majo, F., Kim, J., Trenti, A., Trevisi, L., Fadini, G. P., Bolego, C., Zandstra, P. W., Cignarella, A., & Vitiello, L. (2018). Convenience versus Biological Significance: Are PMA-Differentiated THP-1 Cells a Reliable Substitute for Blood-Derived Macrophages When Studying in Vitro Polarization? *Frontiers in Pharmacology*, *9*. https://doi.org/10.3389/fphar.2018.00071

Tesniere, A., Schlemmer, F., Boige, V., Kepp, O., Martins, I., Ghiringhelli, F., Aymeric, L., Michaud, M., Apetoh, L., Barault, L., Mendiboure, J., Pignon, J.-P., Jooste, V., van Endert, P., Ducreux, M., Zitvogel, L., Piard, F., & Kroemer, G. (2010). Immunogenic death of colon cancer cells treated with oxaliplatin. *Oncogene*, *29*(4), 482–491. https://doi.org/10.1038/onc.2009.356

Thill, M., & Schmidt, M. (2018). Management of adverse events during cyclin-dependent kinase 4/6 (CDK4/6) inhibitor-based treatment in breast cancer. *Therapeutic Advances in Medical Oncology*, *10*, 1758835918793326. https://doi.org/10.1177/1758835918793326

Tokumaru, Y., Joyce, D., & Takabe, K. (2020). Current status and limitations of immunotherapy for breast cancer. *Surgery*, *167*(3), 628–630. https://doi.org/10.1016/j.surg.2019.09.018

Tripathi, R., Modur, V., Senovilla, L., Kroemer, G., & Komurov, K. (2019). Suppression of tumor antigen presentation during aneuploid tumor evolution contributes to immune evasion. *Oncoimmunology*, *8*(11), 1657374. https://doi.org/10.1080/2162402X.2019.1657374

Vance, R. E. (2016). Cytosolic DNA Sensing: The Field Narrows. *Immunity*, *45*(2), 227–228. https://doi.org/10.1016/j.immuni.2016.08.006

Vanpouille-Box, C., Alard, A., Aryankalayil, M. J., Sarfraz, Y., Diamond, J. M., Schneider, R. J., Inghirami, G., Coleman, C. N., Formenti, S. C., & Demaria, S. (2017). DNA exonuclease Trex1 regulates radiotherapy-induced tumour immunogenicity. *Nature Communications*, *8*(1), 15618. https://doi.org/10.1038/ncomms15618

Varma, D., & Salmon, E. D. (2012). The KMN protein network – chief conductors of the kinetochore orchestra. *Journal of Cell Science*, *125*(24), 5927–5936. https://doi.org/10.1242/jcs.093724

Venkatesh, P., & Kasi, A. (2020). Anthracyclines. In *StatPearls*. StatPearls Publishing. http://www.ncbi.nlm.nih.gov/books/NBK538187/

Vicari, A. P., Luu, R., Zhang, N., Patel, S., Makinen, S. R., Hanson, D. C., Weeratna, R. D., & Krieg, A. M. (2009). Paclitaxel reduces regulatory T cell numbers and inhibitory function and enhances the anti-tumor effects of the TLR9 agonist PF-3512676 in the mouse. *Cancer Immunology, Immunotherapy: CII*, *58*(4), 615–628. https://doi.org/10.1007/s00262-008-0586-2

Vikas, P., Borcherding, N., & Zhang, W. (2018). The clinical promise of immunotherapy in triple-negative breast cancer. *Cancer Management and Research*, *10*, 6823–6833. https://doi.org/10.2147/CMAR.S185176

Vincent, J., Mignot, G., Chalmin, F., Ladoire, S., Bruchard, M., Chevriaux, A., Martin, F., Apetoh, L., Rébé, C., & Ghiringhelli, F. (2010). 5-Fluorouracil selectively kills tumor-associated myeloid-derived suppressor cells resulting in enhanced T cell-dependent antitumor immunity. *Cancer Research*, *70*(8), 3052–3061. https://doi.org/10.1158/0008-5472.CAN-09-3690

Walle, T., Martinez Monge, R., Cerwenka, A., Ajona, D., Melero, I., & Lecanda, F. (2018). Radiation effects on antitumor immune responses: Current perspectives and challenges. *Therapeutic Advances in Medical Oncology*, *10*. https://doi.org/10.1177/1758834017742575

Wanderley, C. W., Colon, D. F., Luiz, J. P. M., Oliveira, F. F., Viacava, P. R., Leite, C. A., Pereira, J. A., Silva, C. M., Silva, C. R., Silva, R. L., Speck-Hernandez, C. A., Mota, J. M., Alves-Filho, J. C., Lima-Júnior, R. C., Cunha, T. M., & Cunha, F. Q. (2018). Paclitaxel reduces tumor growth by reprogramming tumor-associated macrophages to an M1- profile in a TLR4-dependent manner. *Cancer Research*, canres.3480.2017. https://doi.org/10.1158/0008-5472.CAN-17-3480

Wang, H., Hu, S., Chen, X., Shi, H., Chen, C., Sun, L., & Chen, Z. J. (2017). CGAS is essential for the antitumor effect of immune checkpoint blockade. *Proceedings of the National Academy of Sciences*, *114*(7), 1637–1642. https://doi.org/10.1073/pnas.1621363114

Wang, M., Zhang, C., Song, Y., Wang, Z., Wang, Y., Luo, F., Xu, Y., Zhao, Y., Wu, Z., & Xu, Y. (2017). Mechanism of immune evasion in breast cancer. *OncoTargets and Therapy*, *10*, 1561–1573. https://doi.org/10.2147/OTT.S126424

Wang, Z., Chen, J., Hu, J., Zhang, H., Xu, F., He, W., Wang, X., Li, M., Lu, W., Zeng, G., Zhou, P., Huang, P., Chen, S., Li, W., Xia, L., & Xia, X. (2019a). CGAS/STING axis

mediates a topoisomerase II inhibitor–induced tumor immunogenicity. *The Journal of Clinical Investigation*, *129*(11), 4850–4862. https://doi.org/10.1172/JCI127471

Wang, Z., Chen, J., Hu, J., Zhang, H., Xu, F., He, W., Wang, X., Li, M., Lu, W., Zeng, G., Zhou, P., Huang, P., Chen, S., Li, W., Xia, L.-P., & Xia, X. (2019b). CGAS/STING axis mediates a topoisomerase II inhibitor-induced tumor immunogenicity. *The Journal of Clinical Investigation*, *129*(11), 4850–4862. https://doi.org/10.1172/JCI127471

Wang, Z., Sun, K., Xiao, Y., Feng, B., Mikule, K., Ma, X., Feng, N., Vellano, C. P., Federico, L., Marszalek, J. R., Mills, G. B., Hanke, J., Ramaswamy, S., & Wang, J. (2019). Niraparib activates interferon signaling and potentiates anti-PD-1 antibody efficacy in tumor models. *Scientific Reports*, *9*(1), 1853. https://doi.org/10.1038/s41598-019-38534-6

Wang, Z., Till, B., & Gao, Q. (2017). Chemotherapeutic agent-mediated elimination of myeloid-derived suppressor cells. *Oncoimmunology*, *6*(7). https://doi.org/10.1080/2162402X.2017.1331807

Wang-Bishop, L., Wehbe, M., Shae, D., James, J., Hacker, B. C., Garland, K., Chistov, P. P., Rafat, M., Balko, J. M., & Wilson, J. T. (2020). Potent STING activation stimulates immunogenic cell death to enhance antitumor immunity in neuroblastoma. *Journal for ImmunoTherapy of Cancer*, *8*(1), e000282. https://doi.org/10.1136/jitc-2019-000282

Watkins, T. B. K., Lim, E. L., Petkovic, M., Elizalde, S., Birkbak, N. J., Wilson, G. A., Moore, D. A., Grönroos, E., Rowan, A., Dewhurst, S. M., Demeulemeester, J., Dentro, S. C., Horswell, S., Au, L., Haase, K., Escudero, M., Rosenthal, R., Bakir, M. A., Xu, H., … Swanton, C. (2020). Pervasive chromosomal instability and karyotype order in tumour evolution. *Nature*, *587*(7832), 126–132. https://doi.org/10.1038/s41586-020-2698-6

Weaver, B. A. (2014). How Taxol/paclitaxel kills cancer cells. *Molecular Biology of the Cell*, *25*(18), 2677–2681. https://doi.org/10.1091/mbc.E14-04-0916

Weaver, B. A., & Cleveland, D. W. (2006). Does aneuploidy cause cancer? *Current Opinion in Cell Biology*, *18*(6), 658–667. https://doi.org/10.1016/j.ceb.2006.10.002

Weaver, B. A., & Cleveland, D. W. (2008). The aneuploidy paradox in cell growth and tumorigenesis. *Cancer Cell*, *14*(6), 431–433. https://doi.org/10.1016/j.ccr.2008.11.011

Weichhart, T., Costantino, G., Poglitsch, M., Rosner, M., Zeyda, M., Stuhlmeier, K. M., Kolbe, T., Stulnig, T. M., Hörl, W. H., Hengstschläger, M., Müller, M., & Säemann, M. D. (2008). The TSC-mTOR Signaling Pathway Regulates the Innate Inflammatory Response. *Immunity*, *29*(4), 565–577. https://doi.org/10.1016/j.immuni.2008.08.012

Westhorpe, F. G., Tighe, A., Lara-Gonzalez, P., & Taylor, S. S. (2011). P31comet-mediated extraction of Mad2 from the MCC promotes efficient mitotic exit. *Journal of Cell Science*, *124*(Pt 22), 3905–3916. https://doi.org/10.1242/jcs.093286

Woo, S.-R., Fuertes, M. B., Corrales, L., Spranger, S., Furdyna, M. J., Leung, M. Y. K., Duggan, R., Wang, Y., Barber, G. N., Fitzgerald, K. A., Alegre, M.-L., & Gajewski, T. F. (2014). STING-dependent cytosolic DNA sensing mediates innate immune recognition of immunogenic tumors. *Immunity*, *41*(5), 830–842. https://doi.org/10.1016/j.immuni.2014.10.017

Wu, J., Sun, L., Chen, X., Du, F., Shi, H., Chen, C., & Chen, Z. J. (2013). Cyclic GMP-AMP is an endogenous second messenger in innate immune signaling by cytosolic DNA. *Science (New York, N.Y.)*, *339*(6121), 826–830. https://doi.org/10.1126/science.1229963

Wu, Y., Deng, Z., Wang, H., Ma, W., Zhou, C., & Zhang, S. (2016). Repeated cycles of 5-fluorouracil chemotherapy impaired anti-tumor functions of cytotoxic T cells in a CT26 tumor-bearing mouse model. *BMC Immunology*, *17*(1), 29. https://doi.org/10.1186/s12865-016-0167-7

Yamagishi, Y., Yang, C.-H., Tanno, Y., & Watanabe, Y. (2012). MPS1/Mph1 phosphorylates the kinetochore protein KNL1/Spc7 to recruit SAC components. *Nature Cell Biology*, *14*(7), 746–752. https://doi.org/10.1038/ncb2515

Yang, H., Rudge, D. G., Koos, J. D., Vaidialingam, B., Yang, H. J., & Pavletich, N. P. (2013). MTOR kinase structure, mechanism and regulation. *Nature*, *497*(7448), 217–223. https://doi.org/10.1038/nature12122

Yang, P., An, H., Liu, X., Wen, M., Zheng, Y., Rui, Y., & Cao, X. (2010). The cytosolic nucleic acid sensor LRRFIP1 mediates the production of type I interferon via a beta-catenin-dependent pathway. *Nature Immunology*, *11*(6), 487–494. https://doi.org/10.1038/ni.1876

Yona, A. H., Manor, Y. S., Herbst, R. H., Romano, G. H., Mitchell, A., Kupiec, M., Pilpel, Y., & Dahan, O. (2012). Chromosomal duplication is a transient evolutionary solution to stress. *Proceedings of the National Academy of Sciences of the United States of America*, *109*(51), 21010–21015. https://doi.org/10.1073/pnas.1211150109

Yum, S., Li, M., & Chen, Z. J. (2020). Old dogs, new trick: Classic cancer therapies activate cGAS. *Cell Research*, *30*(8), 639–648. https://doi.org/10.1038/s41422-020-0346-1

Yum, S., Li, M., Frankel, A. E., & Chen, Z. J. (2019). Roles of the cGAS-STING Pathway in Cancer Immunosurveillance and Immunotherapy. *Annual Review of Cancer Biology*, *3*(1), 323–344. https://doi.org/10.1146/annurev-cancerbio-030518-055636

Zasadil, L. M., Andersen, K. A., Yeum, D., Rocque, G. B., Wilke, L. G., Tevaarwerk, A. J., Raines, R. T., Burkard, M. E., & Weaver, B. A. (2014a). Cytotoxicity of Paclitaxel in Breast Cancer Is due to Chromosome Missegregation on Multipolar Spindles. *Science Translational Medicine*, *6*(229), 229ra43-229ra43. https://doi.org/10.1126/scitranslmed.3007965

Zasadil, L. M., Andersen, K. A., Yeum, D., Rocque, G. B., Wilke, L. G., Tevaarwerk, A. J., Raines, R. T., Burkard, M. E., & Weaver, B. A. (2014b). Cytotoxicity of paclitaxel in breast cancer is due to chromosome missegregation on multipolar spindles. *Science Translational Medicine*, *6*(229), 229ra43. https://doi.org/10.1126/scitranslmed.3007965

Zhang, G., Kruse, T., López-Méndez, B., Sylvestersen, K. B., Garvanska, D. H., Schopper, S., Nielsen, M. L., & Nilsson, J. (2017). Bub1 positions Mad1 close to KNL1 MELT repeats to promote checkpoint signalling. *Nature Communications*, *8*(1), 15822. https://doi.org/10.1038/ncomms15822

Zhang, J., Bu, X., Wang, H., Zhu, Y., Geng, Y., Nihira, N. T., Tan, Y., Ci, Y., Wu, F., Dai, X., Guo, J., Huang, Y.-H., Fan, C., Ren, S., Sun, Y., Freeman, G. J., Sicinski, P., & Wei, W. (2018). Cyclin D-CDK4 kinase destabilizes PD-L1 via Cul3SPOP to control cancer immune surveillance. *Nature*, *553*(7686), 91–95. https://doi.org/10.1038/nature25015

Zhang, Z., Yu, X., Wang, Z., Wu, P., & Huang, J. (2015). Anthracyclines potentiate anti-tumor immunity: A new opportunity for chemoimmunotherapy. *Cancer Letters*, *369*(2), 331–335. https://doi.org/10.1016/j.canlet.2015.10.002

Zhou, F. (2009). Molecular mechanisms of IFN-gamma to up-regulate MHC class I antigen processing and presentation. *International Reviews of Immunology*, *28*(3–4), 239–260. https://doi.org/10.1080/08830180902978120

Zierhut, C., Yamaguchi, N., Paredes, M., Luo, J.-D., Carroll, T., & Funabiki, H. (2019a). The Cytoplasmic DNA Sensor cGAS Promotes Mitotic Cell Death. *Cell*, *178*(2), 302-315.e23. https://doi.org/10.1016/j.cell.2019.05.035

Zierhut, C., Yamaguchi, N., Paredes, M., Luo, J.-D., Carroll, T., & Funabiki, H. (2019b). The Cytoplasmic DNA Sensor cGAS Promotes Mitotic Cell Death. *Cell*, *178*(2), 302-315.e23. https://doi.org/10.1016/j.cell.2019.05.035